A LOW SIDELOBE NOTCH ANTENNA ARRAY

A Thesis Submitted

in Partial Fulfillment of the Requirements

for the Degree of

Master of Technology

by

Major Arun Sehgal

to the

DEPARTMENT OF ELECTRICAL ENGINEERING

INDIAN INSTITUTE OF TECHNOLOGY, KANPUR

March 1996

EE-1996-M-SEH-LOW

Certificate

It is certified that the work contained in the thesis entitled "**A LOW SIDELOBE NOTCH ANTENNA ARRAY**", by Major Arun Sehgal, has been carried out under my supervision and that this work has not been submitted elsewhere for a degree.

March 1996

Dr. M Sachidananda

Professor

Department of Electrical Engineering

I.I.T. Kanpur

Abstract

This thesis records the efforts made in developing a linear array of notch elements, which was envisaged as one component of a larger 2-D airborne surveillance radar antenna. The specifications of the antenna were arrived at based on the requirements of the airborne antenna which requires a low side lobe level and thin cross section. Thin cross section was one of the major considerations in the design of this antenna, which is to be mounted outside the aircraft with a suitable radome.

Based on the requirements, a notch antenna was selected as the basic radiator. The design approach has been completely experimental and the aim was to demonstrate the feasibility only. The work was carried out under certain constraints, major constraints being the high cost of microwave substrate. A low cost glass epoxy substrate was used for the fabrication, whose loss factor is high resulting in low gain for the antenna. However, the pattern characteristics is not affected by this.

The parameters of a single notch antenna element were finalised first. Several feed structures were tried and finally a shielded microstrip feed line, on glass epoxy substrate was selected. The antenna was fabricated using Aluminium plate to provide high power handling capacity and structural rigidity. The bandwidth obtained was about 500 MHz at 3.2 GHz with a VSWR less than 1.85 in the band.

The mutual coupling evaluation among the elements of the array was done experimentally. The measured mutual coupling was found to be very low (< -20 dB) between adjacent elements. The array excitation coefficients were designed to give a Taylor pattern with -30 dB side lobe level. A 2 meter long array with 32 elements was fabricated. The active impedance computation of the elements was carried out and a corporate feed network designed, in microstrip form, based on this. A combination

of glass epoxy substrate, coaxial cables, and glass epoxy substrate was used for the complete feed network, to reduce the cost.

The array was mechanically constructed in 8 pieces for ease in fabrication, and assembled together to form the array. Near-field measurements were performed on the array since far-field testing facility was not available. With limitations in the testing procedure and precise fabrication of the array, an average side lobe level of -25 dB was achieved, with VSWR at centre frequency of 3.2 GHz being 1.22. With a better feed network and sophisticated fabrication facility it is possible to achieve a side lobe level as low as -35 to -40 dB.

To

My Family

Acknowledgements

I attribute the successful completion of my thesis to my guide,Dr M.Sachidananda, who has been a source of inspiration and whose professional knowledge, posetive approach and easy accessibility have made this study an enjoyable one.

I am deeply indebted to Harish, Apu and Chaitanya who have helped me surmount many a hurdle I faced during my thesis. I also thank my colleague Pradip Paliwal whose encouragement and help was a thing I cherish. Dr A.Biswas was always a source of encouragement for me. I shall remember all of you.

My sincere thanks also go to Department of Electrical Engineering and the Advanced Centre for Electronic Systems for the facilities extended to me and for a cordial working atmosphere.

I take this oppurtunity to express my gratitude to Mr.Tewari and Ram Bahadur of Electrical Department Workshop, Mr.Kole and Dinesh of PCB section and the staff of Central Workshop who helped me in fabrication of the array.

I will be failing in my duty if I fail to convey my gratitude to the Corps of Electrical and Mechanical Engineers who have sent me to this wonderful institute.

Last, but not the least, I lay a major part of my success on the shoulders of my wife and children, without whose kind understanding and support, I would not have achieved this success.

Major Arun Sehgal

Contents

List of Figures

Chapter 1

Introduction

1.1 Introduction

Antennas used in airborne radar applications have certain stringent performance requirements regarding the side lobe level. Because the radar is mounted on a moving platform, the conventional clutter rejection methods do not work and the complexity of the signal processing scheme is enormously increased for an airborne surveillance type radar, especially when it is used in detection of low flying aircraft in the presence of ground clutter. It is a well known fact that the antenna side lobe level has to be less than -35 db for any signal processing scheme of detecting the low flying targets in the presence of ground clutter. This is because the received power can be attributed to that received from the direction of main beam alone, only if the side lobe level is low enough.

A further requirement of airborne antenna is an aerodynamically shaped radome that does not effect the performance of the aircraft. The effect of the radome on the antenna performance also has to be taken into account in the design of the antenna. Many of the smaller antennas are generally mounted in the nose cone or tail with a radome cover conforming to the aerodynamic shape of the aircraft. However, if the

antenna is large, it has to be mounted outside the aircraft body. In such a eventuality, it is necessary to reduce the aerodynamic resistance by properly shaping the radome in which the antenna is housed. One of the ideas in the mind of the scientists at the DRDO Laboratory was a planar antenna made of linear arrays of thin cross section, so that the aerodynamic resistance is minimised. The work reported in this thesis was started with a view to achieve this requirement. How this antenna can actually be used in making a 2-D antenna for airborne applications, whether such an antenna can be used on an aircraft at all, whether the backlobe performance of such an antenna meets the specification required etc. are still to be studied and decided. Our main objective in this study is to come up with a Linear array configuration with thin cross sections and low sidelobe level. The specification were worked out mainly based on these requirements. The specifications of the linear array worked out were the following:

- Centre frequency = 3.2 GHz
- Band Width = 400 MHz
- Length of array $\approx$ 2 mtrs
- Side lobe level = $<$ -30 db
- Power handling $\approx$ 1 KW peak, 10 W average
- Input VSWR = $<$ 1.5
- Directivity $\approx$ 15 db
- Polarisation - linear, horizontal

First task was to select an appropriate radiating element with the desired characteristics. Apart from the electrical characteristics of horizontal polarisation and power handling capability, we also had to consider structural and fabrication aspects. Considering various radiating elements such as, horn, dipole, slot, notch etc., it was decided that notch element is the best choice. Notch antenna element is an extension of a slot line. The slot transmission line is widened to make it radiate in the end fire direction.

1.2 Notch antenna element

A notch antenna is a travelling wave antenna when the taper is slow and long (several wavelengths) and has an advantage over resonant antennas in its ability to work over a large band width. It is also referred to as a Tapered Slot Antenna (TSA) or Vivaldi antenna. These antennas have the fields confined to the slotline which decouple from the slot edge and radiate as the slot width is increased. The radiated electrical field of the antenna is linearly polarised and is parallel to the plane of the slot. Since the structure is open ended, there is virtually no reflection of the outgoing wave and current reflections along the edges are small. The TSA consists of a tapered slot cut in a thin film of metal with or without an electrically thin substrate on one side of the film, as shown in Fig. 1.1. [1]

The power handling capacity of this antenna could be increased by fabricating it on a thick metal plate instead of a thin one, without dielectric substrate, so as to reduce dielectric loss. Various types of feed lines can be used to couple energy to the slot, like a strip line, microstrip line, coaxial line, etc. These antennas have been found suitable for many integrated circuit applications, imaging and phased array.[2]. Although the

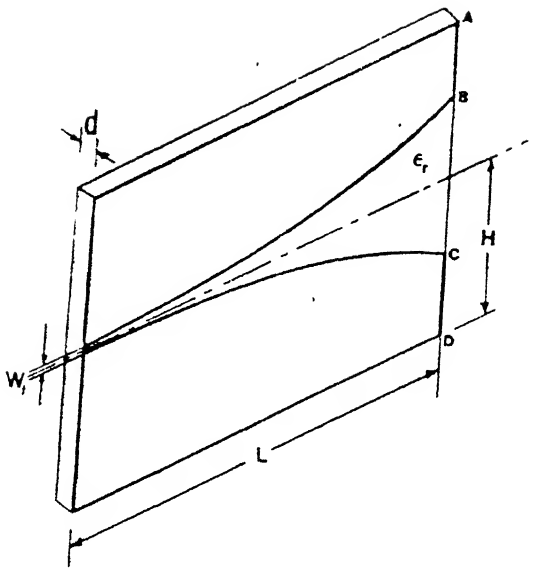

Figure 1.1: A notch antenna

electrical characteristics of this radiator is suitable for the present application, its size is rather large for array application. For array application, the optimum element size is of the order of half wavelength. It was also necessary to keep the length of the taper small to make the antenna thin in cross section. Since the bandwidth required is 10 percent, which even resonant type antennas can give, it was decided to make a short TSA, length and width approximately half wavelength, making it near resonant structure at the operating frequency, resulting in narrow bandwidth. This is the price we had to pay for smaller size.

1.3 Literature Survey

The earliest mention of TSA, in IEEE Transactions, has been found in [3]. S.N. Prasad and S Mahapatra had introduced a slot line antenna, on Alumina substrate ($\epsilon_r = 9.8$), coated with copper of thickness 5 micro mtr, operating at 9 GHz. The results showed

the antenna capable of high gain, low side lobes, wide band of operation and very small cross polarisation. Yngvesson et al. carried out further investigation on TSA on dielectric substrate in [2]. The effects of dielectric substrate and shape on various types of TSA's was studied. It also makes a mention of Vivaldi antenna, with exponentially tapered slot, having a low side lobe level and wide band operation. Janaswamy et al. have presented a theoretical analysis of the radiation characteristics of linear TSA with air dielectric in [4] and [1]. The analysis is limited to electrically large aperture antennas. Janaswamy developed a more accurate moment method analysis for LTSA in [5], capable of accounting for finite width of the antenna aperture. The method had a limitation in that it required a large CPU time for obtaining the solution, as acknowledged by the author in [5]. Characterisation of Tapered slot antenna feeds and feed arrays has been done by Young et al. in [6]. A model which enables prediction of element gain and aperture efficiency of a LTSA and LTSA array has been made. Lai et al. have proposed an ultra wide band antenna based on a slot line feed structure in [7]. A slot line antenna was used alongwith a bow tie antenna with rolled termination for ultra wide band application from 2 - 18 GHz. A ultra wide band microstrip to slot transition is also proposed. Eric Thile and Allen Taflowe have presented a FD-TD analysis of Vivaldi flared horn antenna and array in [8]. They have computed the E/H plane gain patterns and input impedance across 6 to 18 GHz. A strip line was used to feed the Vivaldi antenna fabricated on 2 pieces of duroid substrate, with the feed line between the 2 pieces, which were joined together. The FD-TD analysis, as stated by the authors, is numerically intensive and requires the use of Super Computers. Schaubert et al. have presented a full wave moment method analysis of Infinite stripline - fed, TSA arrays in [9].

Literature survey was also carried out for slot line transitions. Seymour B.Cohn has

studied a slot on dielectric substrate and mentions that a slot to microstrip transition, at right angles to each other, has very good coupling.[10]. The paper gives formulae for slot line wavelength, impedance etc. for substrates of ϵ_r between 10 and 40. Mariani et al. have also investigated the slot line characteristics, on dielectric substrate, for ϵ_r between 9.6 and 20 in [11]. A comparison between slot line and microstrip impedance has also been carried out. Robinson et al. describe the transition from slot on dielectric substrate to coaxial line and microstrip line in [12]. The VSWR of transition between microstrip and slot has been shown almost 1.03 for 8 - 10 GHz band. Dispersion characteristics of wide slot lines on low permitivity substrate have been analysed using Galarkins method by Janaswamy et al. in [13]. Substrates of ϵ_r 2.22 to 9.8 have been analysed over 2 - 6 GHz band. The same authors have presented empirical formulae for calculation of normalised slot wavelength and characteristic impedance in [14], on low permitivity substrates.

1.4 Organisation of the thesis

This thesis presents the detailed procedure followed and results obtained in development of a low sidelobe notch antenna array. Chapter 2 explains the experimental procedure followed for finalisation of the design of a notch antenna element and the feed line for it. It also gives the results of experiments carried out on all the models developed and inferences drawn from it. Chapter 3 explains the mutual impedance evaluation of the array and the results obtained. Chapter 4 describes the designing of the array, calculation of active impedances and array coefficients, and design of the complete feed network. Final fabrication of the array and its near field testing has been explained in Chapter 5. The results obtained have been compared to the theoretical

values. Chapter 6 concludes the thesis and suggests the scope for further work.

Chapter 2

Experimental study of Notch Antenna Element

2.1 Introduction

In order to design and fabricate an array of notch antenna elements with very low side lobe level ($< -30db$) with centre frequency of 3.2 GHz, band width of 3 to 3.4 GHz and capable of handling 1 KW peak power, it was necessary to design one notch antenna element which was well matched from 3 to 3.4 GHz and was capable of handling high power. The option to design the antenna on a dielectric substrate or metal were considered. Glass epoxy substrate is lossy, hence has a poor power handling capability. Duroid substrate has low loss and therefore can handle high power, but the cost of the substrate is very high. Among the metals, Aluminium was the cheapest and easiest to work with. Metals also provide structural rigidity and can handle high power. Hence it was decided to fabricate the antenna element in Aluminium. Initially, to have an idea regarding the bandwidth and VSWR of the notch antenna, it was decided to print the antenna on a glass epoxy substrate and study its characteristics before fabricating it in Aluminium. The feed network envisaged for the notch antenna comprised of a microstrip feed line with a microstrip to slot transition for coupling the energy to the antenna. This chapter describes the various configurations studied, their advantages

and disadvantages, the experimental results achieved and inferences drawn from them, and the final antenna design chosen alongwith its characteristics.

2.2 Experimental study of notch antenna configuration

In order to study the characteristics of a notch antenna, the first model was printed on glass epoxy substrate of $\epsilon_r = 3.8$ and thickness of 1.6mm. The taper of the element was chosen in such a manner so as to enable a smooth transition of the impedance away from the feed point. The optimal taper was not tried for since any taper which could fulfil the requirement of impedance transition in the pass band was adequate for the antenna element. With this in mind, a taper equation of

$$y = 0.1x^2 + 0.2x^3$$

was used in model No.1. A 50 Ω microstrip feed line was designed to feed the slot whose width for 50 Ω was found to be 0.3mm using the design equations given in [14]. The width of the microstrip line was found to be 3.4mm using the commercial software package PUFF. The feed line was short circuited at the feed point of the slot. A circular open circuit was used to terminate the slot so as to provide a wide band operation for the antenna. The size of the opening of the antenna to free space was kept $\approx \lambda_o/2$ and the length less than $\lambda_o/2$ so that the antenna is not a pure travelling wave type but a resonant structure suitable for operation in 3 to 3.4 GHz band. Refer Fig.2.1 for the design of the first model.

The second model was also printed on glass epoxy substrate. The taper of the antenna element was changed to

$$x = 23.075 + 46.808\sqrt{y} \qquad for\ 0 \leq y \leq 1$$

MODEL No. 1

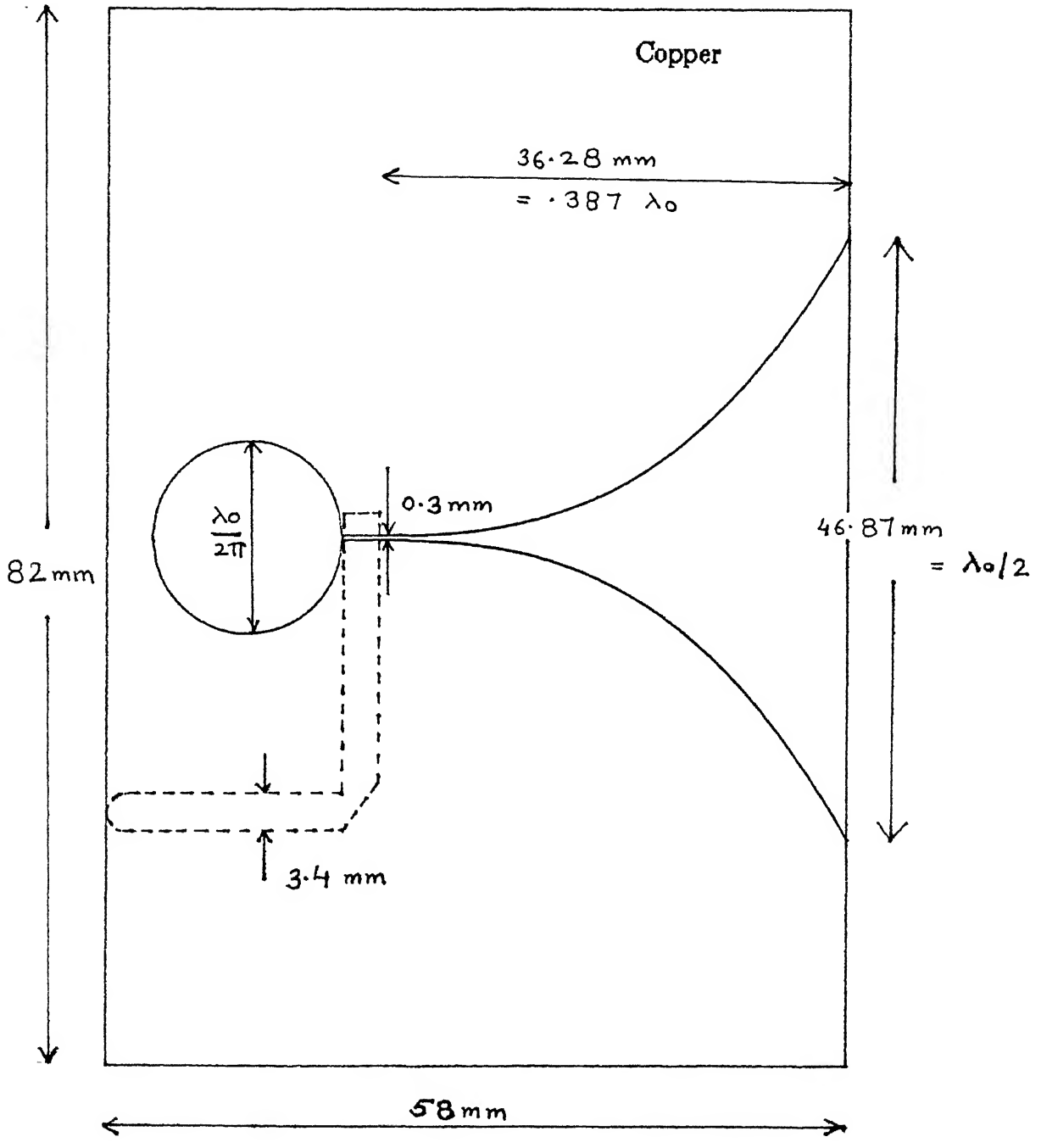

Fig. 2.1 Model No. 1 on glass epoxy substrate

so as to increase the length of the taper to $\lambda_o/2$. The circular open circuit was replaced by a rectangular open circuit to save space and make the antenna element smaller in size. Both configurations, circular as well as rectangular open circuit are designed for broad band operation of the antenna. The microstrip feed line was terminated in a $\lambda_g/4$ open circuit stub instead of a short circuit for ease in fabrication of the open circuit. Refer Fig.2.2 for the design of the second model.

Since the final antenna was to be fabricated in Aluminium and the first two models showed satisfactory characteristics, further antennas were developed and fabricated in Aluminium. Aluminium plate has a finite thickness unlike the very thin conducting layer of copper on the dielectric substrate. No design equations were available for calculation of impedance of a slot in a conducting plate of finite thickness. Therefore it was decided to experimentally match the 50 Ω input microstrip line, printed on glass epoxy substrate, to a slot in a Aluminium plate of finite thickness, by varying the slot width and comparing the match for each slot width. A 1.6mm Aluminium plate was used for fabrication of this experiment. The slot width was gradually increased from 0.54mm to 2.3mm in eight unequal steps and the best match was ascertained with a 50 Ω microstrip feed line. Refer Fig.2.3 for the dimensions of the experimental antenna fabricated. Thereafter since the final antenna was to be radiating in one direction only, one side of the experimental antenna was shorted with a movable short. The short circuit distance was varied for different slot width and the best match between slotwidth shorted at a distance and the feed line ascertained. It was experimentally found that a slot width of 1.0mm, in a 1.6mm Aluminium plate, with the slot shorted at a distance of 11.5mm from the feed point gave the best match for a 50 Ω microstrip feed line on a glass epoxy substrate.

These results, obtained experimentally, were used for fabrication of the next model

MODEL No. 2

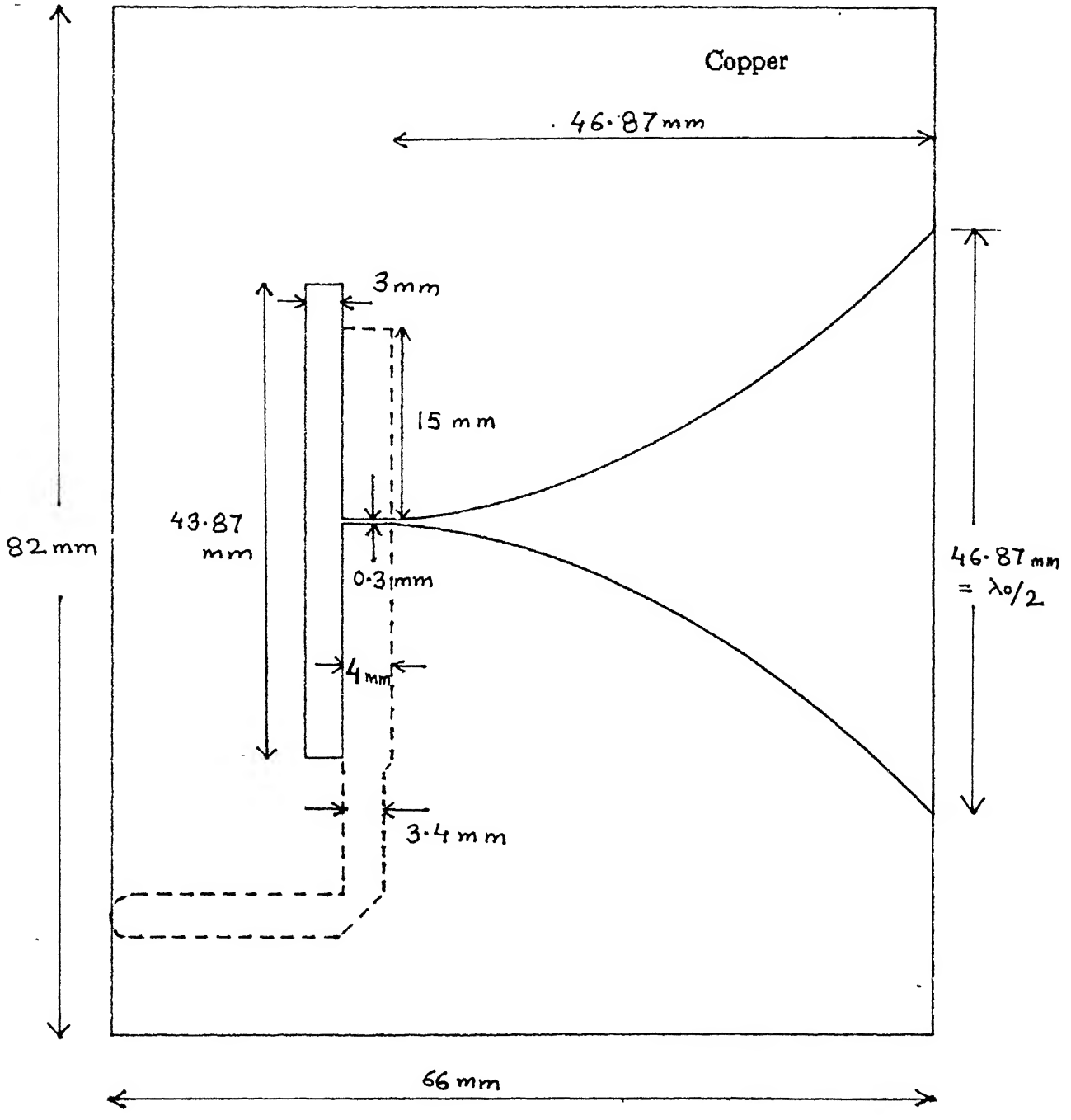

Fig. 2.2 Model No. 2 on glass epoxy substrate

MODEL No. 3

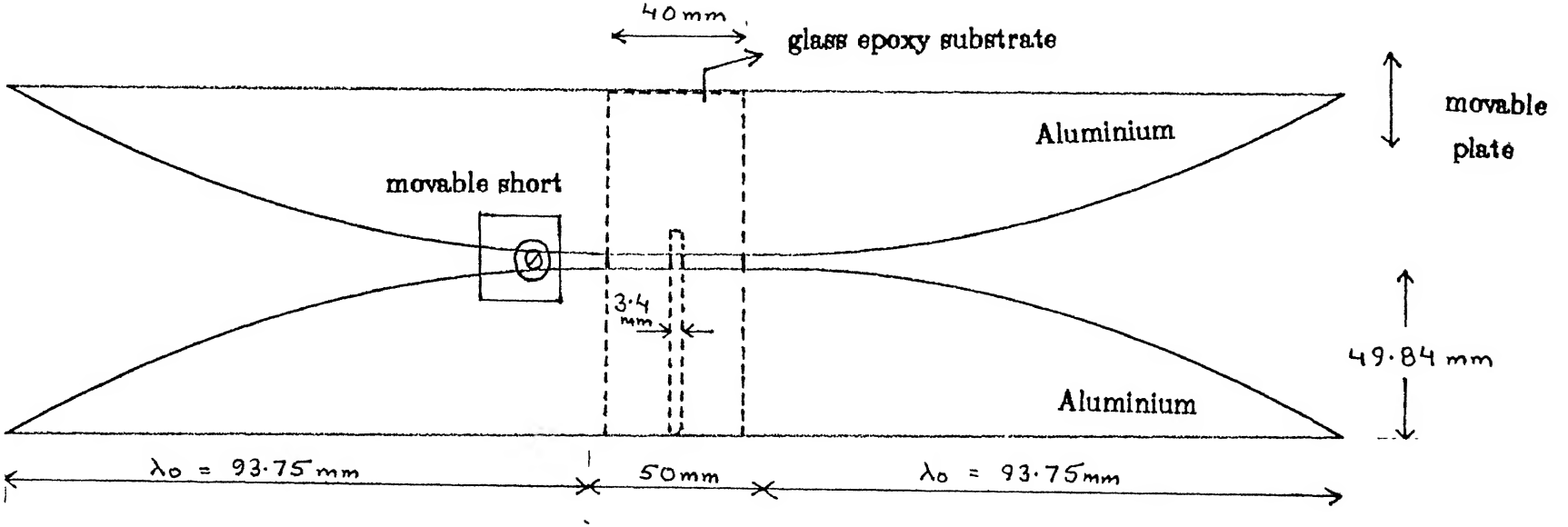

Fig.2.3 Model No. 3 Experimental Antenna

of antenna. The taper of the antenna was kept

$$x = 60\sqrt{y} \qquad for 0 \leq y \leq 1$$

so as to reduce the size of the notch antenna element taper to 6.0 cms (more than $\lambda_o/2$) at 3.0 GHz, the lower frequency of the required band. The microstrip feed line, printed on glass epoxy substrate, was terminated in an open circuit stub. The length of the stub was adjusted to obtain the best match, which was found for a stub length of 12mm. Refer Fig.2.4 for the design of the fourth model.

The glass epoxy substrate is very lossy in nature and fabrication of the feed network on it for the full array of 2 meter would greatly enhance the loss. Hence it was decided to try other means for feeding the slot of the notch antenna. The first method tried was by using a coaxial cable to feed the antenna used in model No.4. A 50 Ω coaxial cable RG 58 was used. The other method tried was by making a Suspended Strip line feed. Suspended Strip line is a low loss transmission line. This was fabricated in a notch antenna consisting of 4 plates of antenna joined together. A channel was left between the 4 plates for the suspended strip line. Refer Fig.2.5 for the configuration of suspended strip line used.

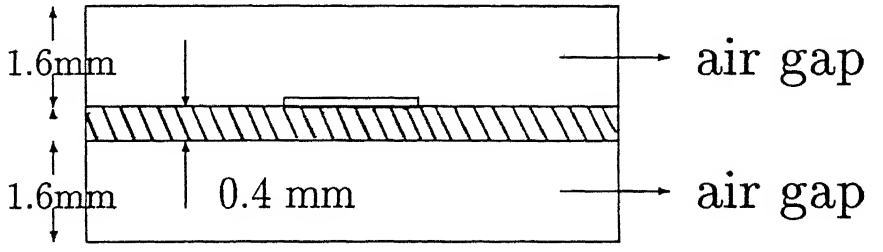

Fig 2.5 Suspended strip line

This configuration was used to couple energy to the slot of the antenna. The slot width of the 4 plate antenna was kept adjustable so as to achieve a good match with

MODEL No. 4

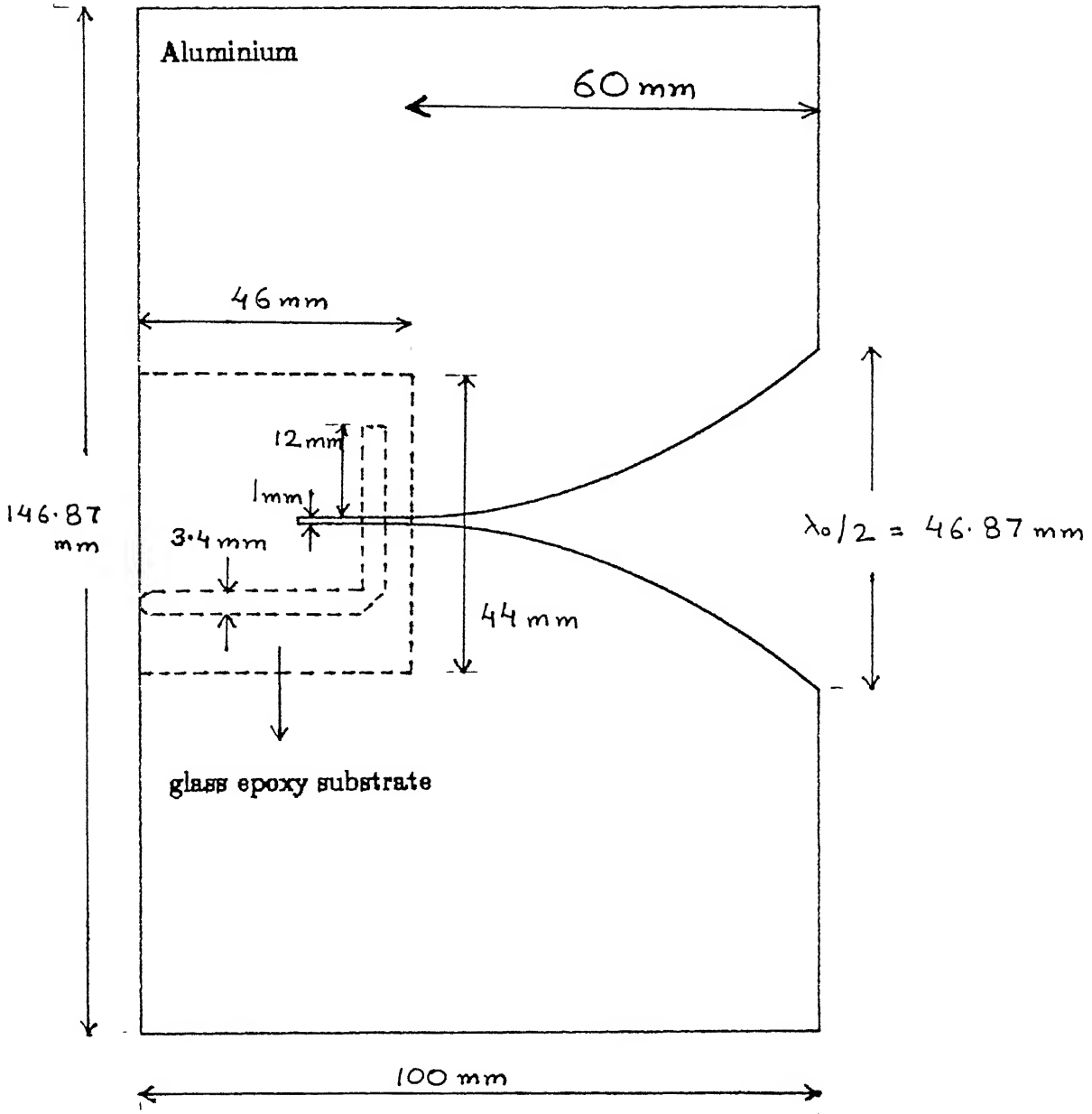

Fig. 2.4 Model No. 4 Aluminium Antenna

the feed line. The dimensions for the 50 Ω suspended strip line on a 0.4mm glass epoxy substrate were found using the design equations given in [15]. Initially the feed line was shorted at the feed point and the antenna characteristics studied. Thereafter the suspended strip line was terminated in a $\lambda_g/4$ open circuit stub. The characteristics of this antenna model, with suspended strip line feed, gave poor results. One of the specifications of the antenna to have a thin cross section was not fulfilled. Refer Fig.2.6 for the antenna model.

The next model used suspended strip line feed again for a single plate notch antenna element. The slot width was again varied to achieve the best possible match with the 50 Ω feed line. This also gave a very poor result due to weak coupling between the feed line and antenna slot.

It was decided, after all these experiments, to continue the microstrip feed line for the notch antenna element. The power loss in case of this feed line on a glass epoxy substrate was reduced to some extent by using a Aluminium plate to shield the microstrip line at a height of 6mm. The dimensions for a shielded microstrip line were found using the design equations given in [15].

2.3 Experimental Results and Inferences

The experiments conducted on each of the models of notch antenna element consisted of measurement and recording of S_{11} characteristics of the antenna both in magnitude and phase, over a frequency band of 2 to 4 GHz so as to get the antenna performance over a wide band of frequency. The S_{11} magnitude was plotted Vs frequency on a graph. The slot impedance was calculated at the feed point of the slot looking from the microstrip input, by measuring the S_{11} magnitude and phase at the connector plane

MODEL No. 6

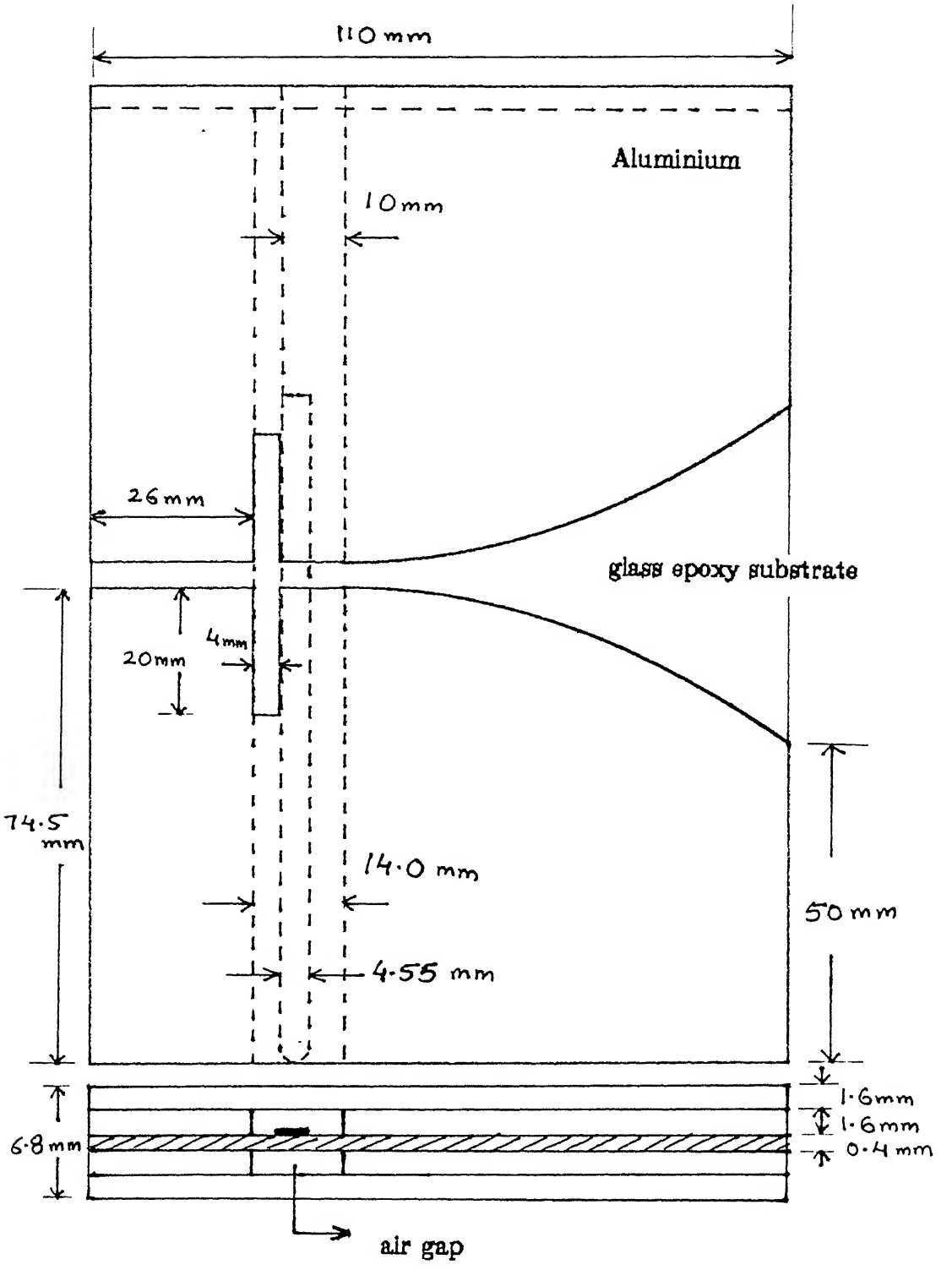

Fig. 2.6 Model No. 6.4 Plate Aluminium Antenna

and then transforming the S_{11} on to the feed point of the slot depending on the length of the transmission line. The slot impedance was calculated from this transformed S_{11}. The following formulae were used for transforming S_{11} on to the slot and for calculation of slot impedance :

$$\Gamma(l) = \Gamma_l \, e^{2l\gamma}$$

$\Gamma(l)$ – *S_{11} phase and magnitude at the slot*

Γ_l – *Measured S_{11} phase and magnitude*

l – *length of the microstrip line*

$$\gamma = \alpha + \iota\beta$$

γ – *propagation constant*

α – *attenuation constant*

β – *phase constant*

$$\alpha = \frac{\beta}{2Q} = \frac{2l\pi}{2Q\lambda}$$

λ – *wavelength*

Q – *Q factor = 50*

$$Z_{slot} = Z_o \frac{1+\Gamma(l)}{1-\Gamma(l)}$$

Z_o – *characteristic impedance of the line = 50Ω*

Z_{slot} – *impedance at the slot as seen by the microstrip feed line.*

The slot impedance was also plotted Vs frequency on a graph so as to obtain the resonant frequency of the fabricated structure.

The measurement set up involved the following equipment,

1. 1-4 GHz Microwave Source (Wavetek Model 952)

2. Network Analyser Set (Hewlett Packard Model 8410 A)

3. S Parameter test set (Hewlett Packard Model 8746 B 001)

Refer Fig.2.7 for the measurement set up.

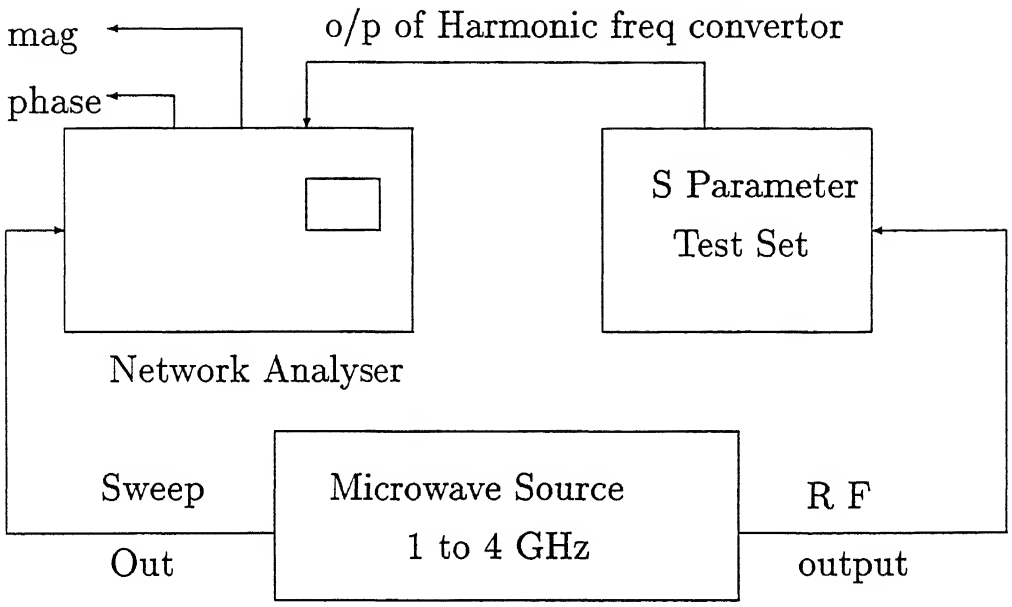

Fig 2.7 Experimental set up for measurement of S_{11} characteristics

Experiments were performed on each of the models discussed in section 2.2. The results measured and computed were plotted on graphs so as to gauge the behaviour of each model of antenna and arrive at the best model for extending into an array. The first model showed a good match of less than -15 db in the required frequency band of 3 to 3.4 GHz. This validated the contention that a notch antenna of this shape could

be used in designing an array with the required specifications. Fig 2.8 shows the plots obtained for model No.1.

In the second model on glass epoxy substrate, where the circular open circuit was replaced by a rectangular open circuit, the performance seen on performing experiments as done on model 1, showed a lower match as compared to the first model. The match achieved was about -10 db over the band of 3 to 3.4 GHz. The slot impedance plot showed a wide variation of 25-30 Ω in the frequency band. The reason attributed to the drop in performance was the removal of ground plane on one side of the microstrip feed line due to the rectangular open circuit. Refer Fig.2.9 for the plots of the second model.

The third model was made in Aluminium for finding the slot width, in a finitely thick conducting plate, best matched to a 50 Ω microstrip feed line. Only the magnitude of S_{11} was plotted Vs the frequency to obtain the best match for various slot widths. Initially the measurement was carried out without the movable short on one side. The measured values obtained were plotted and the plots showed that slot widths varying from 1mm to 2mm approx, showed a less than -10 db match with the 50 Ω microstrip feed line. This was better than the match got for the other slot widths in the frequency band of 3 to 3.4 GHz. Refer Figs.2.10, 2.11, 2.12, 2.13 for the plots obtained.

A movable short was introduced on one side of the antenna to direct the radiation in one direction since the array to be fabricated was required to radiate in one direction. The slot width was varied in 4 unequal steps between 1mm and 2mm. The short circuit distance was also varied for each slot width to obtain the best match. The measured values were plotted and the plots showed that the best match was obtained for a slot width of 1.08mm and a short circuit distance of 11.5mm from the feed point. Refer Figs.2.14 and 2.15 for the plots of the experiment.

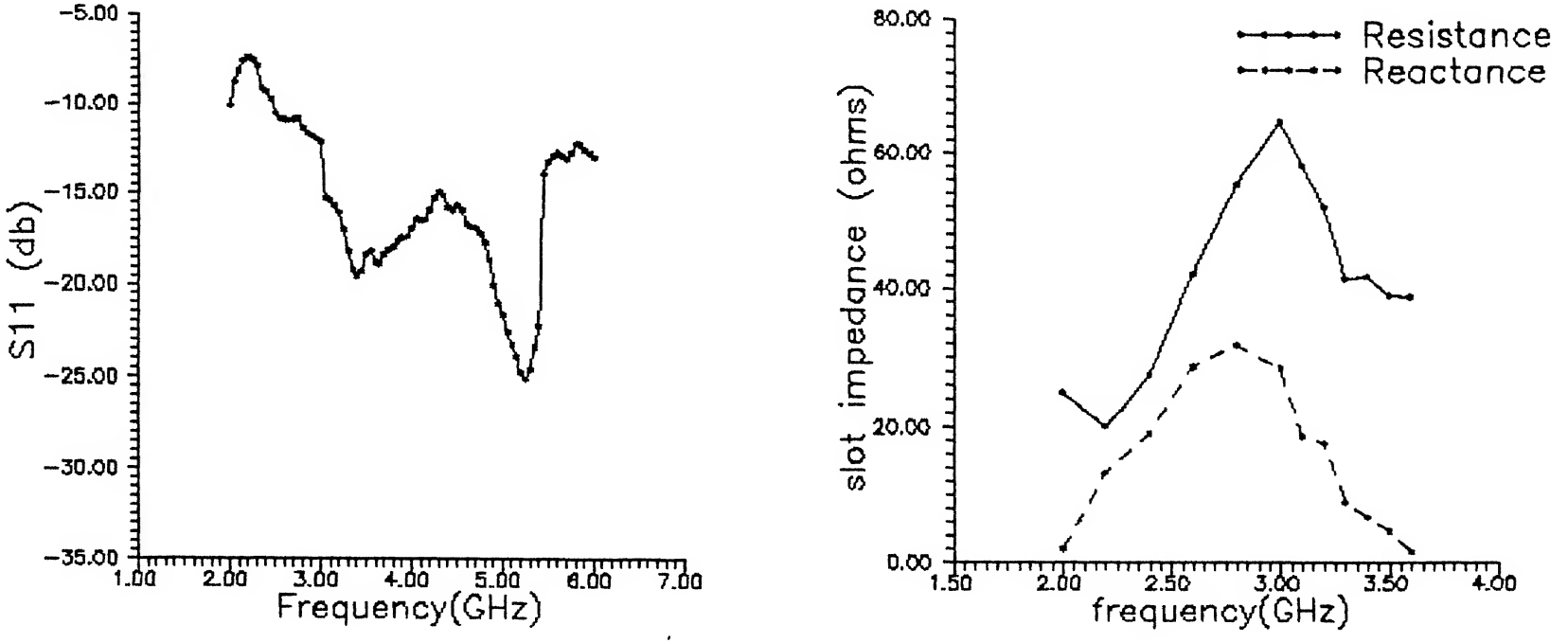

Fig. 2.8 Plots of Model No.1

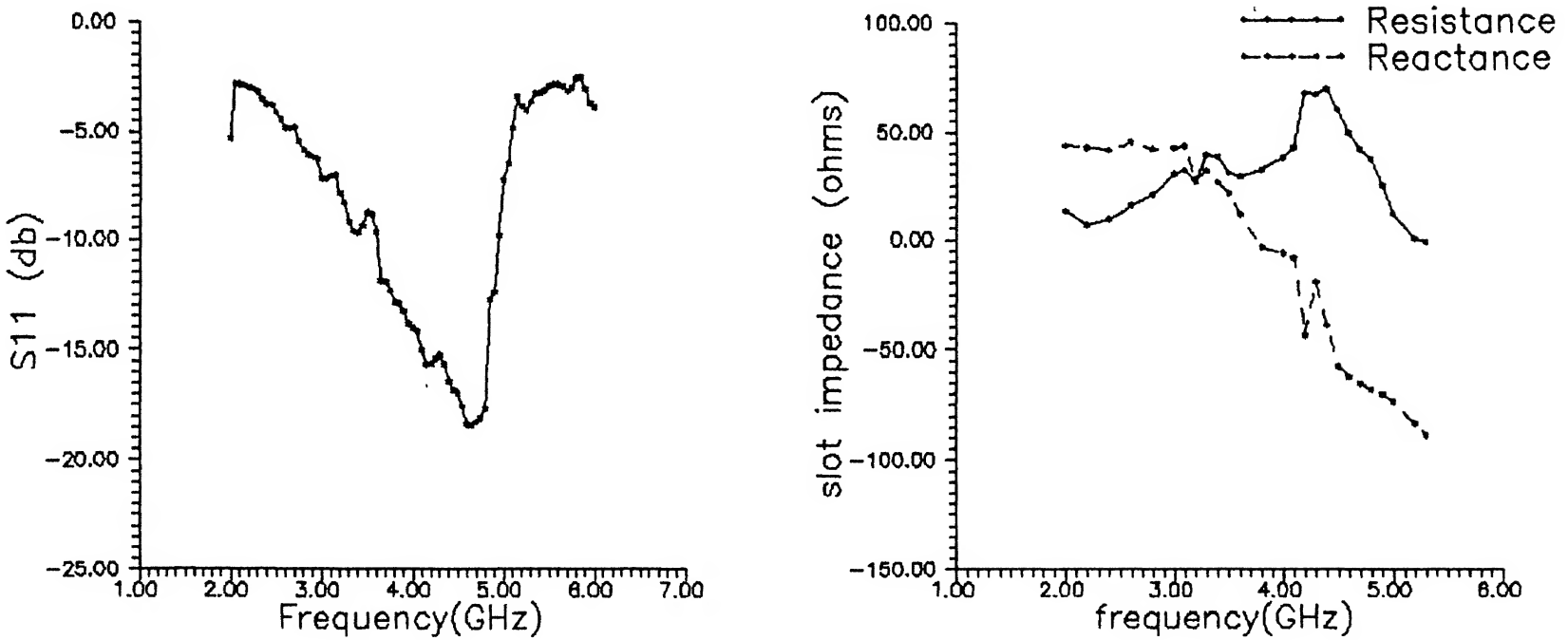

Fig. 2.9 Plots of Model No.2

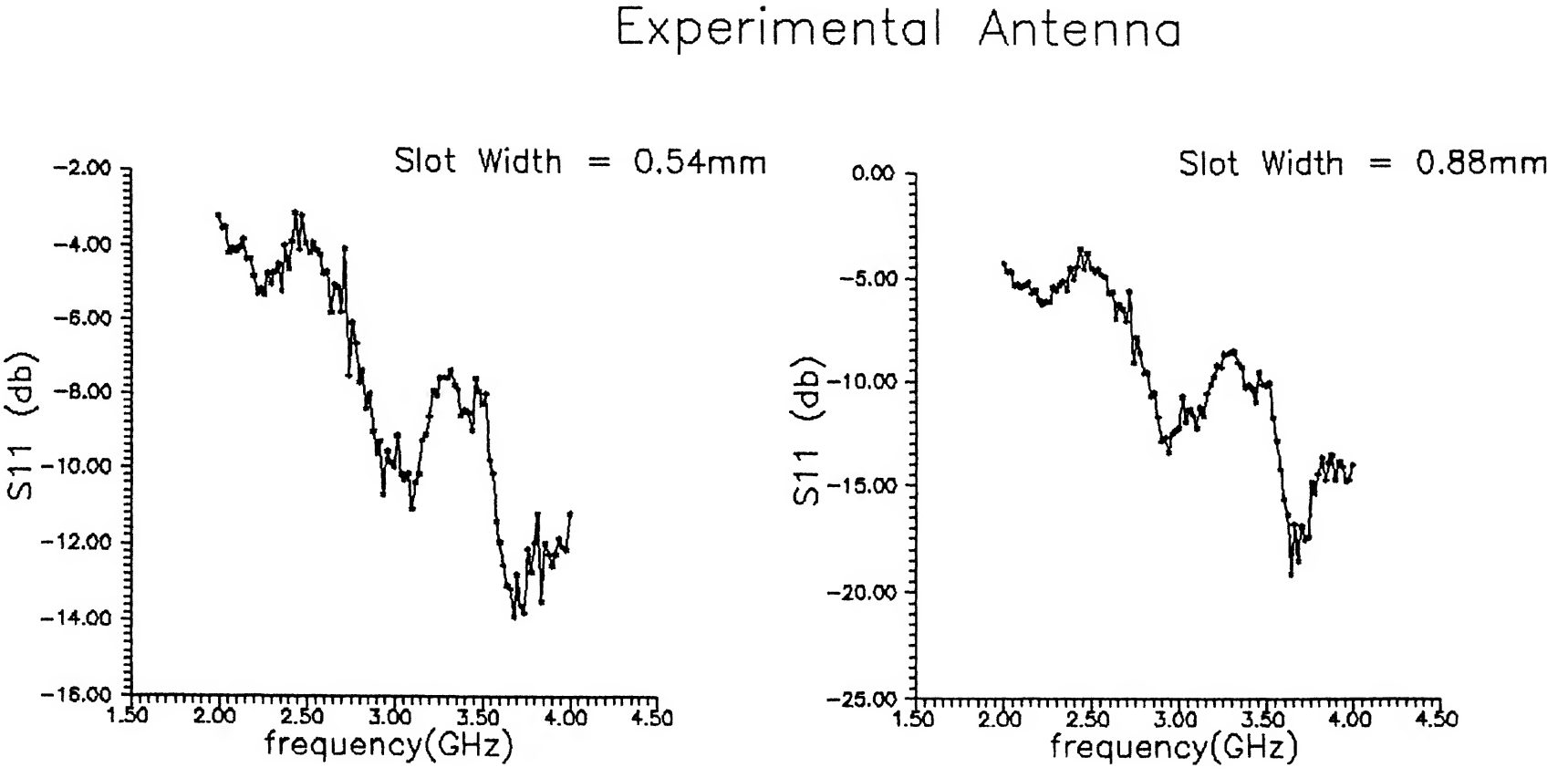

Fig. 2.10 Plots of Model No.3

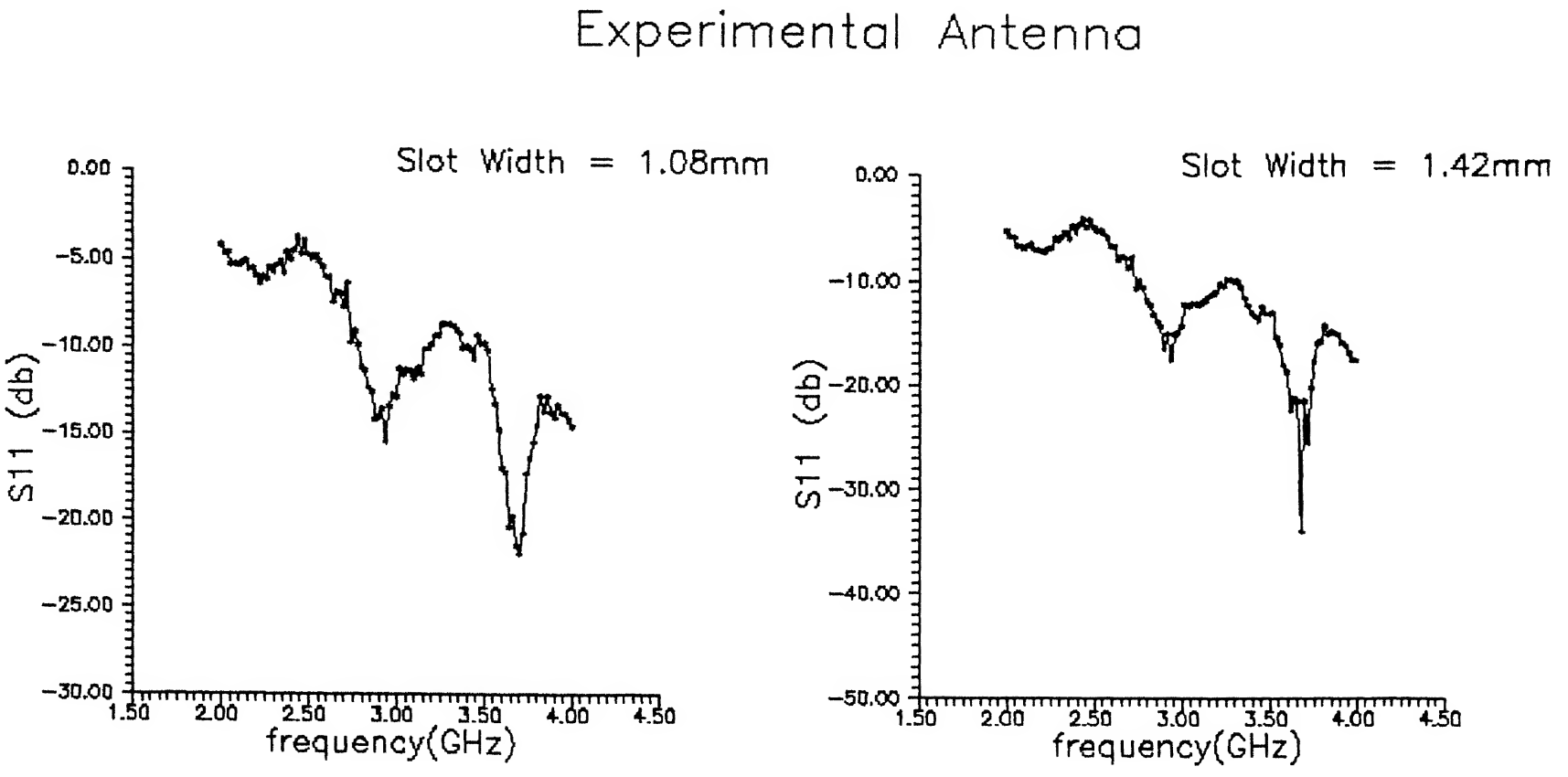

Fig. 2.11 Plots of Model No.3

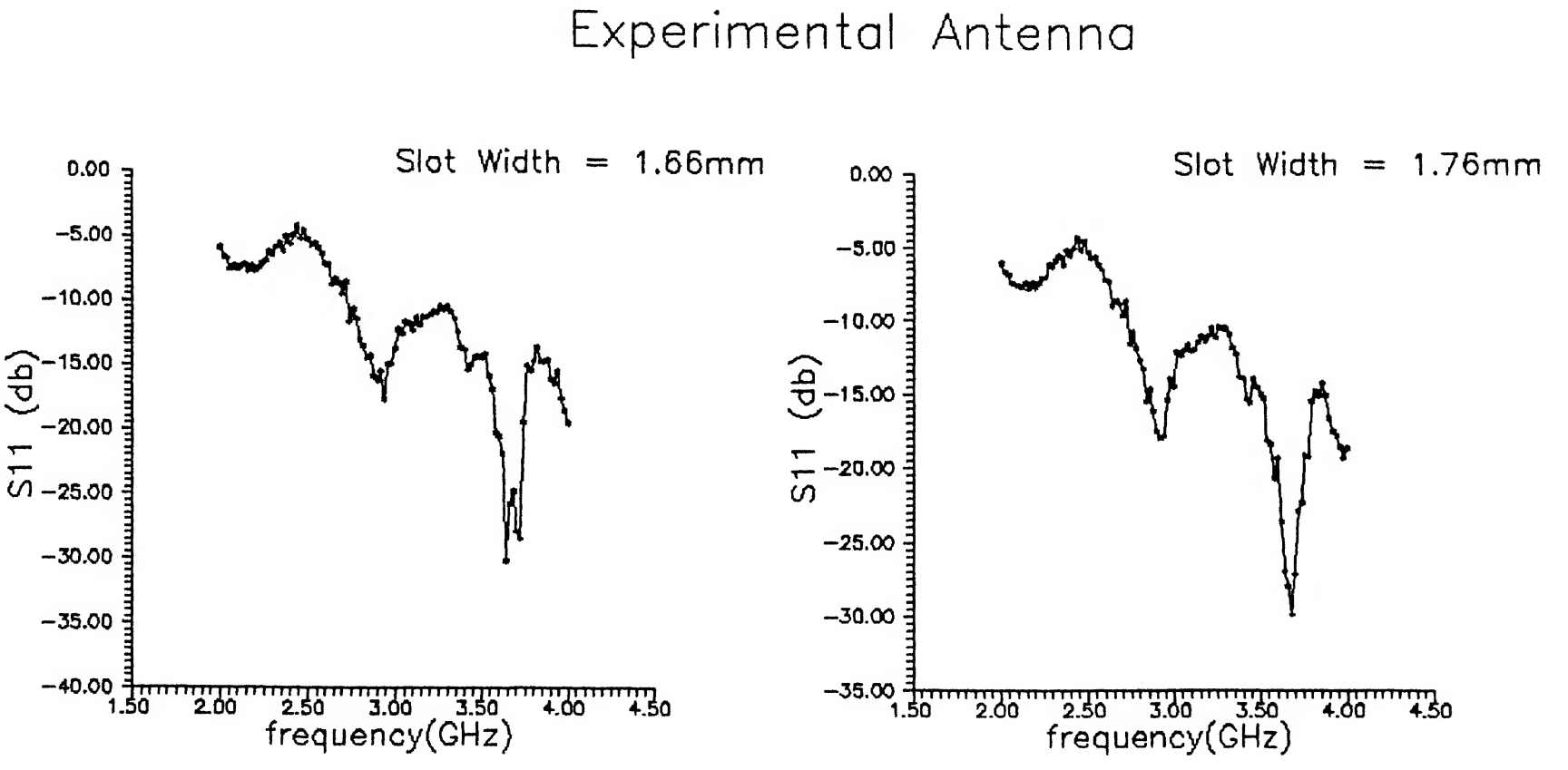

Fig. 2.12 Plots of Model No.3

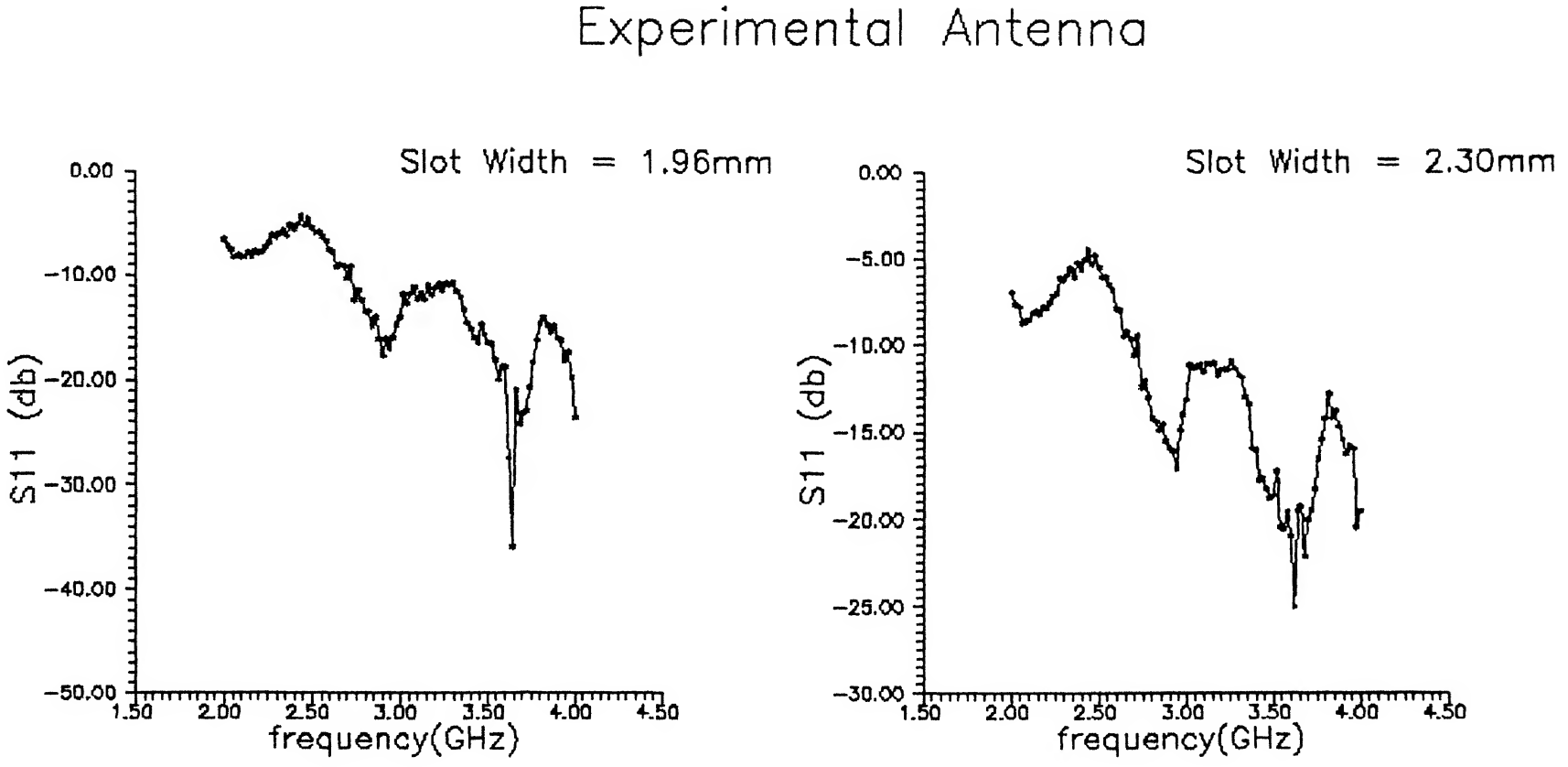

Fig. 2.13 Plots of Model No.3

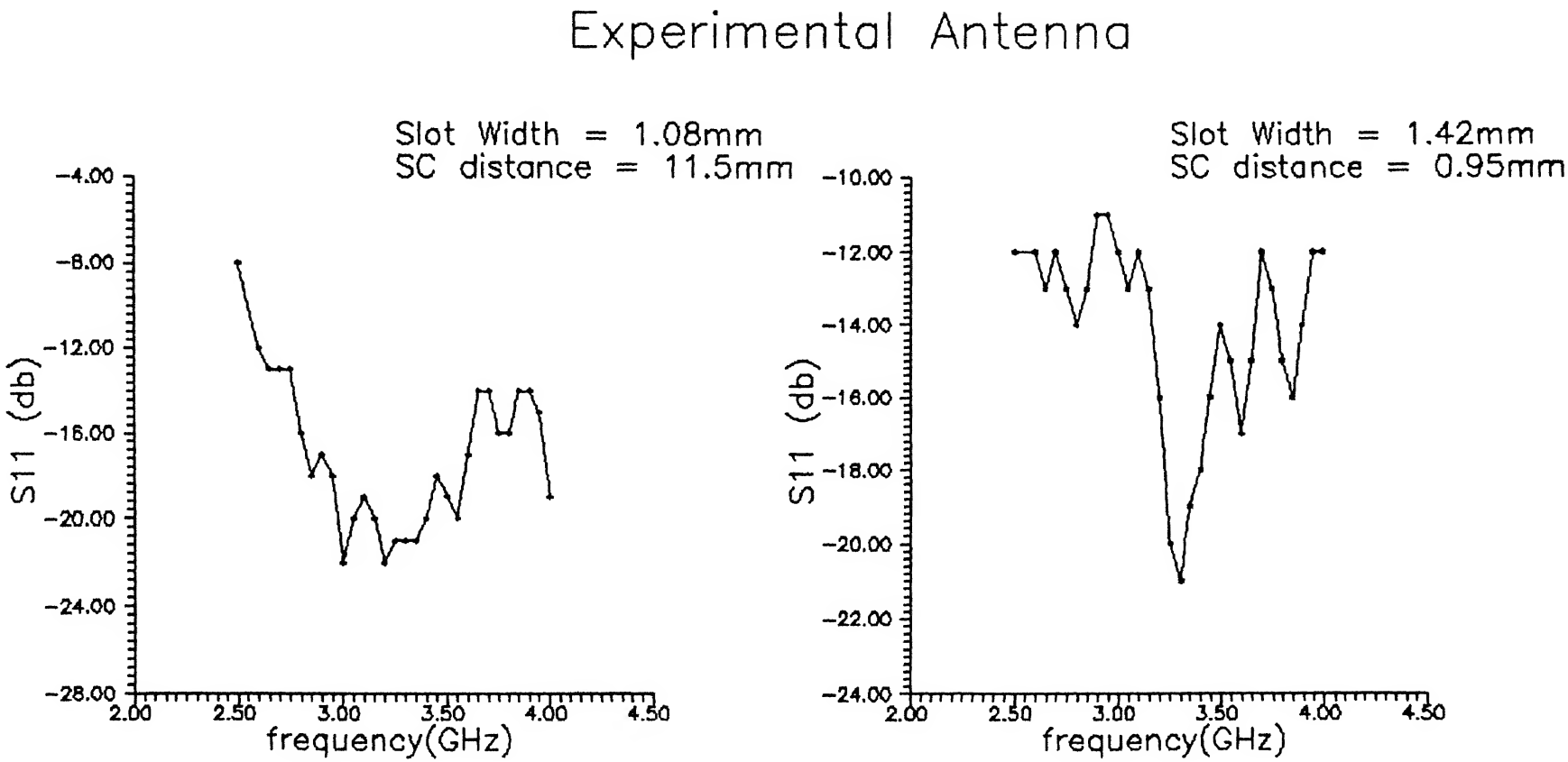

Fig. 2.14 Plots of Model No.3 with short circuit

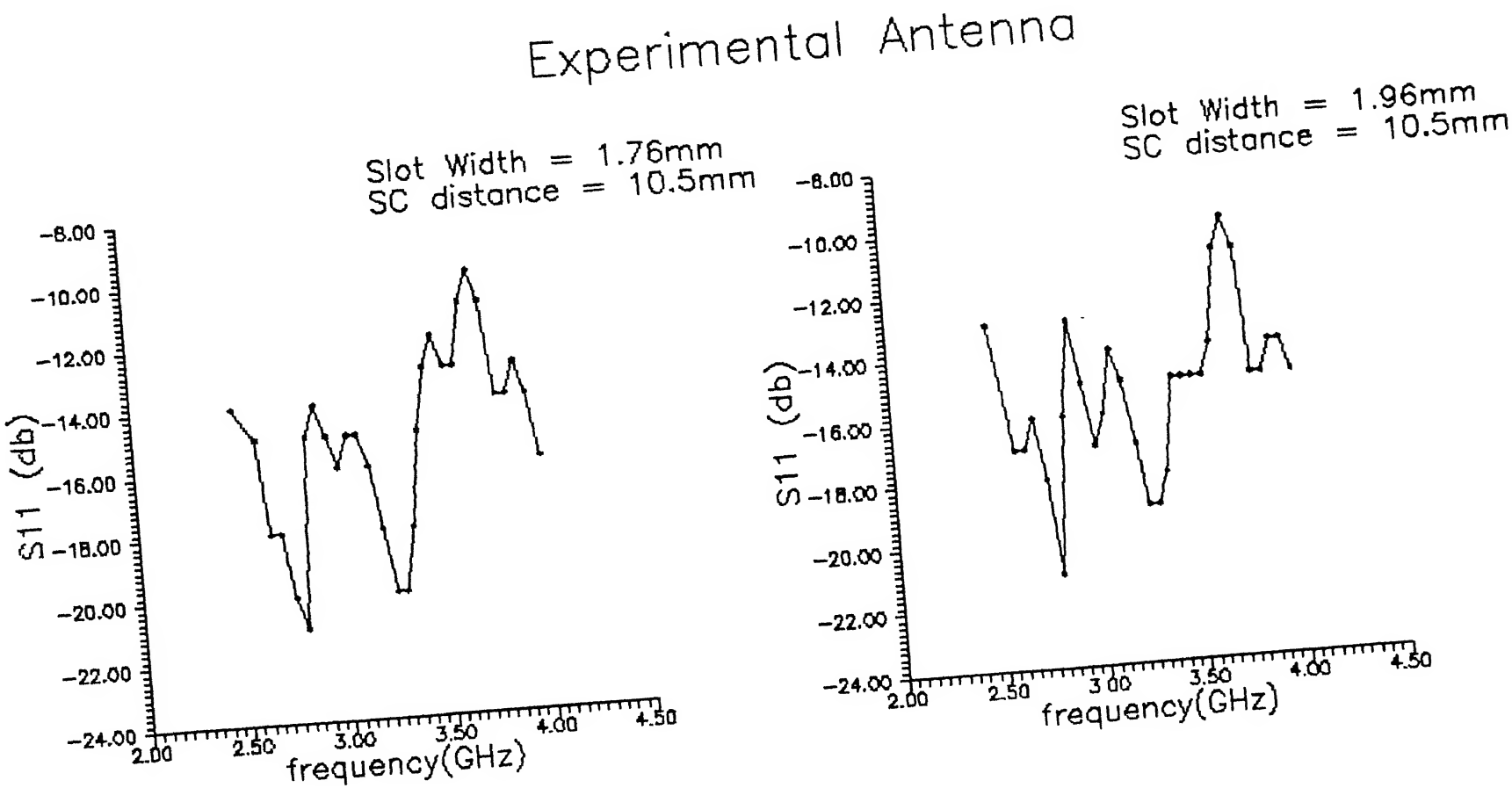

Fig. 2.15 Plots of Model No.3 with short circuit

The fourth model was based on the dimensions obtained from the previous experiments. This model was also attached with the Network Analyser to measure the S_{11}. The data recorded and plotted showed that this antenna gave a very good match (less than -18 db) over the required frequency band of 3 to 3.4 GHz with -26 db match at 3.15 GHz. The slot impedance curves showed almost a 50 Ω impedance at 3.15 GHz, thereby providing a good match for the input line. The variation of slot impedance was only around 10 Ω in the required frequency band. This antenna model gave the best results achieved so far among all the model of antennas fabricated. Refer Fig.2.16 for the plots of model No.4.

The next model involved change in the feed line to coaxial feed line. The model of the antenna was the same as in model no.4, only the microstrip feed was replaced with coaxial feed. The results obtained did not show a good match most probably due to poor coupling between coaxial feed line and slot. The match obtained was less than -10 db over the band of 3 to 3.4 GHz. The slot impedance also showed a wide variation of 20 to 30 Ω over the frequency band. Refer Fig.2.17 for the plots of model No.5.

The suspended strip line feed with the 4 plate antenna was the next model. The 4 plate antenna with the feed line shorted at the feed point gave the best match for a slot width of 1.34mm. The match obtained was -11 to -13 db over 3 to 3.4 GHz. The slot impedance showed a very wide variation ($\approx$ 30 Ω) in the frequency band. Refer Fig.2.18 for the plots obtained. The suspended strip line was terminated in a $\lambda_g/4$ open circuit instead of a short circuit in the next model, so as to see if it improves the performance. The match obtained on experimentation was only -10 to -11 db in the required frequency band. The slot impedance showed $\approx$ 30 Ω variation in the 3 to 3.4 GHz frequency band. Refer Fig.2.19 for the plots obtained. The next model used suspended strip line feed to a single plate notch antenna. Experiments carried

Model No. 4

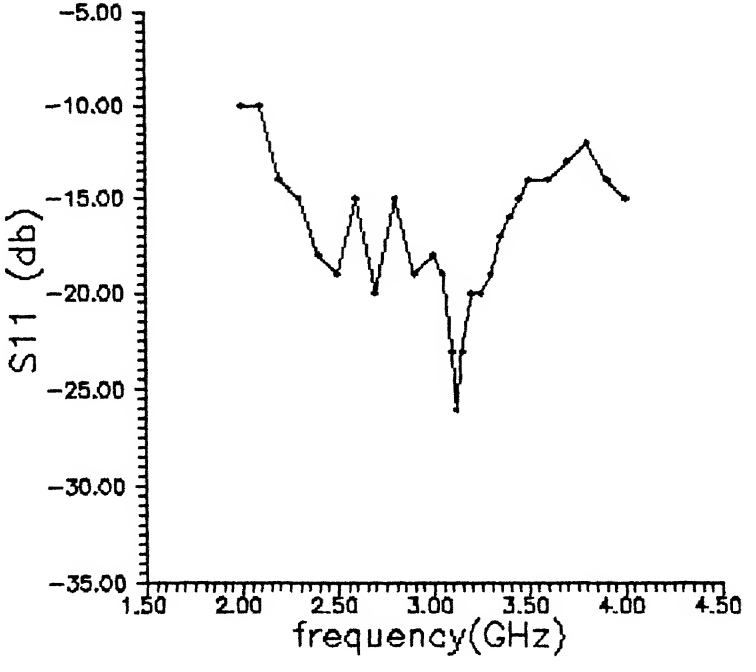

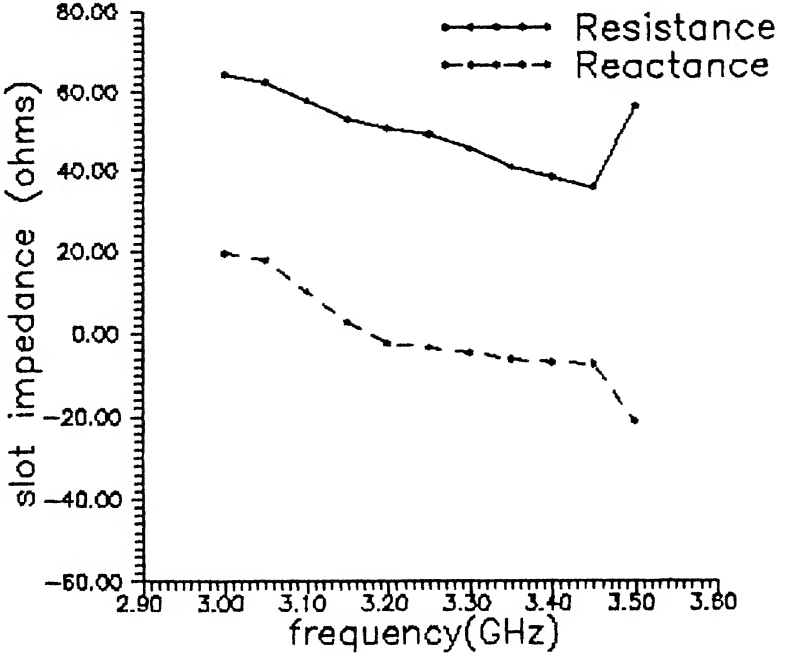

Fig. 2.16 Plots of Model No.4

Model No. 5
Coaxial feed

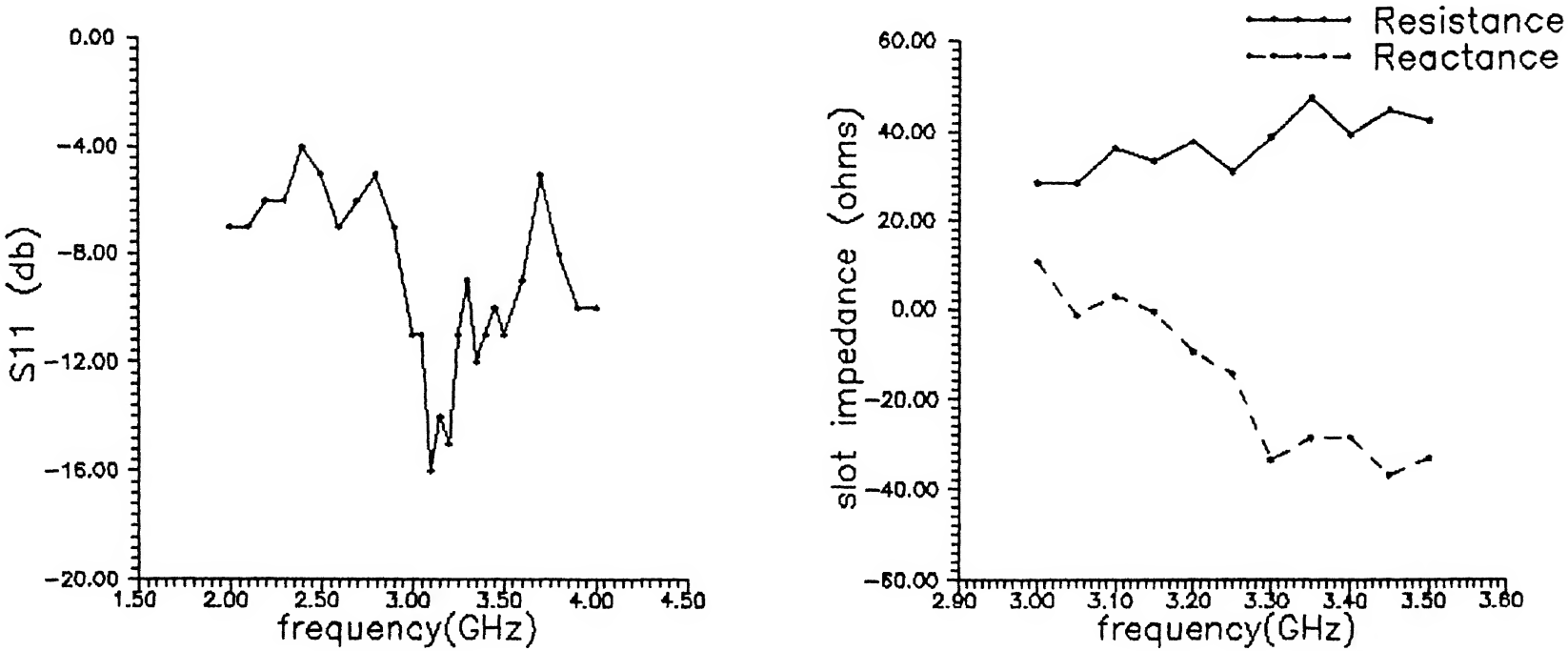

Fig. 2.17 Plots of Model No.5

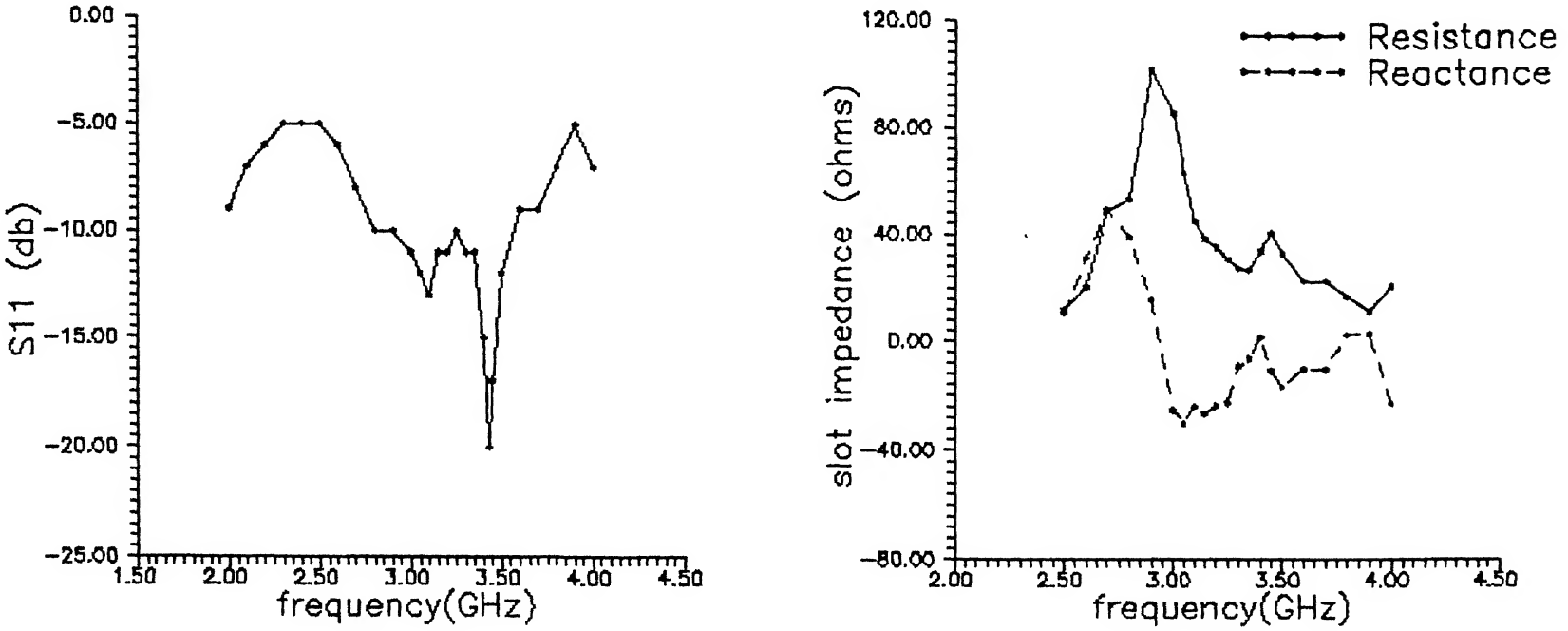

Fig. 2.18 Plots of Model No.6

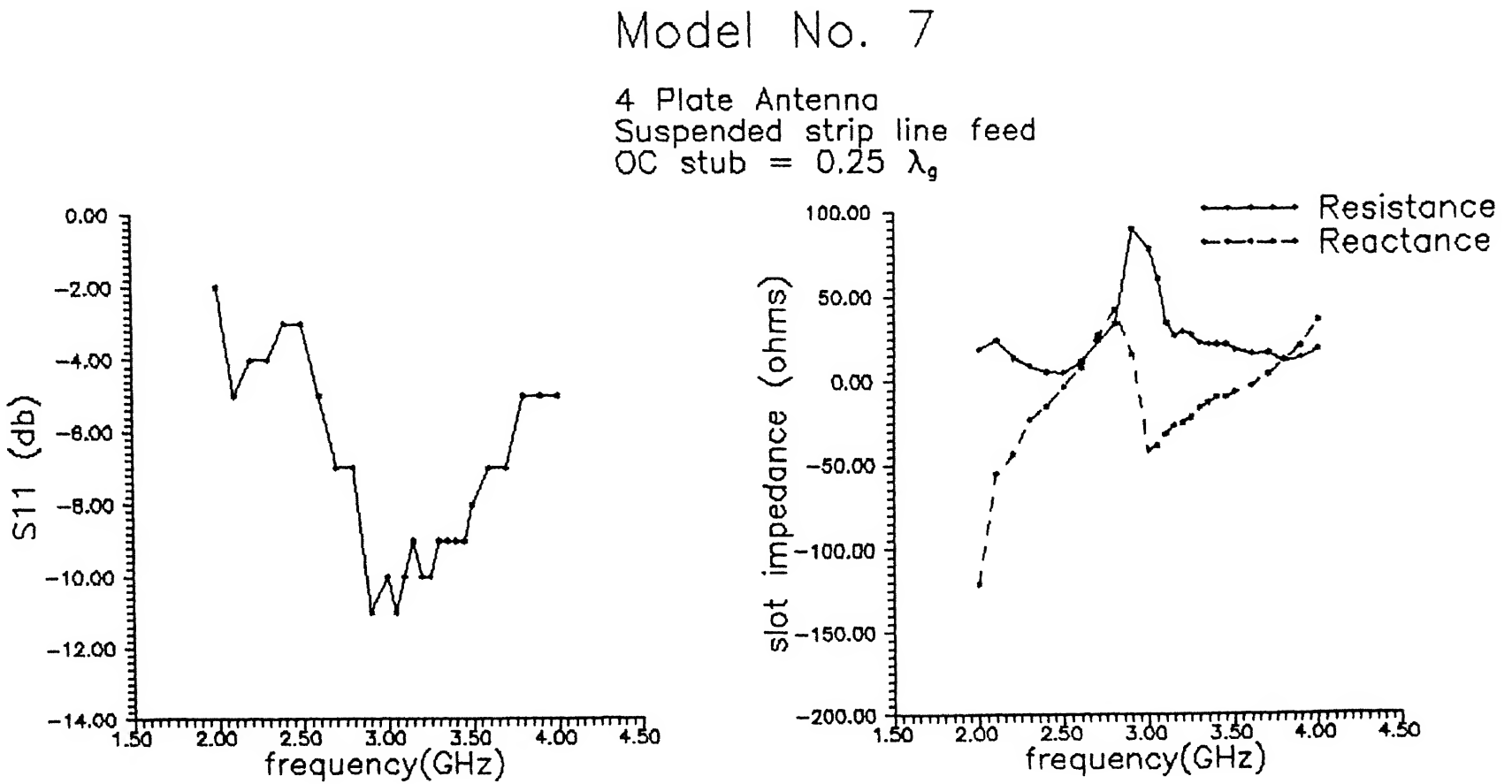

Fig. 2.19 Plots of Model No.7

out on this with the Network Analyser showed a match of only -10 to -11 db. The slot impedance showed an even wider variation of $\approx$ 70 Ω in the frequency band of 3 to 3.4 GHz. Refer Fig.2.20 for the plots obtained.

The poor match obtained using the suspended strip line feed was attributed to a poor coupling between the feed line and the slot. Therefore it was decided to continue with microstrip feed on glass epoxy substrate for feeding the notch antenna element.

2.4 Final Antenna Element

The various models of notch antenna element fabricated along with the different types of feed lines, and the experiments carried out on each showed that model No.4, refer Fig.2.4, gave the best results. Refer Fig.2.16 for the results. It was decided to use this design of the notch antenna element for making the array. The power loss occurring in the microstrip feed line on glass epoxy substrate was reduced to some extent by placing an Aluminium plate, as a shield, on the feed line PCB. The dimensions of the microstrip feed line with shield at a height of 6mm were found using the design equations given in [15]. Experiments, similar to the ones performed on other models, were performed on the shielded microstrip fed notch antenna element. The results obtained showed a good match of less than -18 db in the frequency band of 3 to 3.4 GHz. At 3.1 GHz the match was about -37 db. The slot impedance matched the input feed line impedance of 50 Ω over the entire frequency band with only about 10 Ω variation. Refer Fig.2.21 for the plots obtained.

The results obtained from this model of notch antenna element were adequate for using this element to fabricate an array. Therefore this model was finalised and further developed into an array as explained in the subsequent chapters.

Model No. 8
Suspended strip line feed

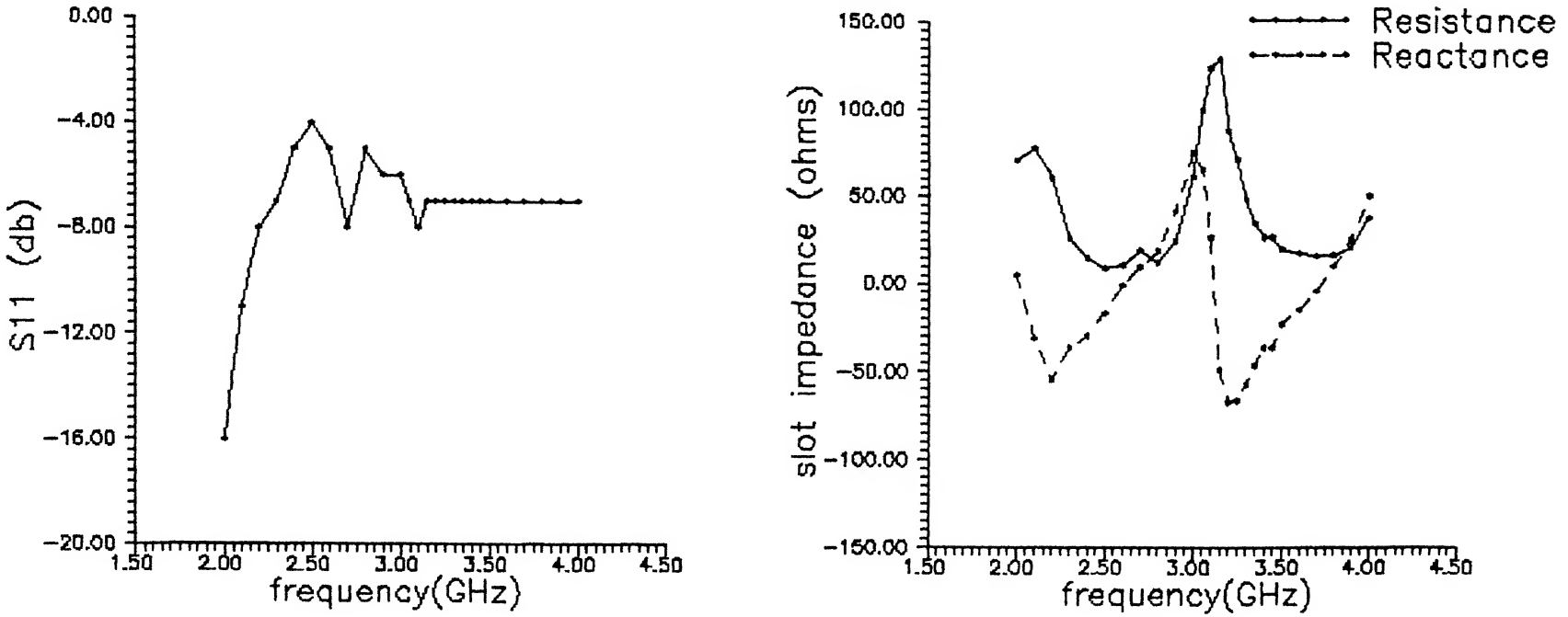

Fig. 2.20 Plots of Model No.8

Model No. 9

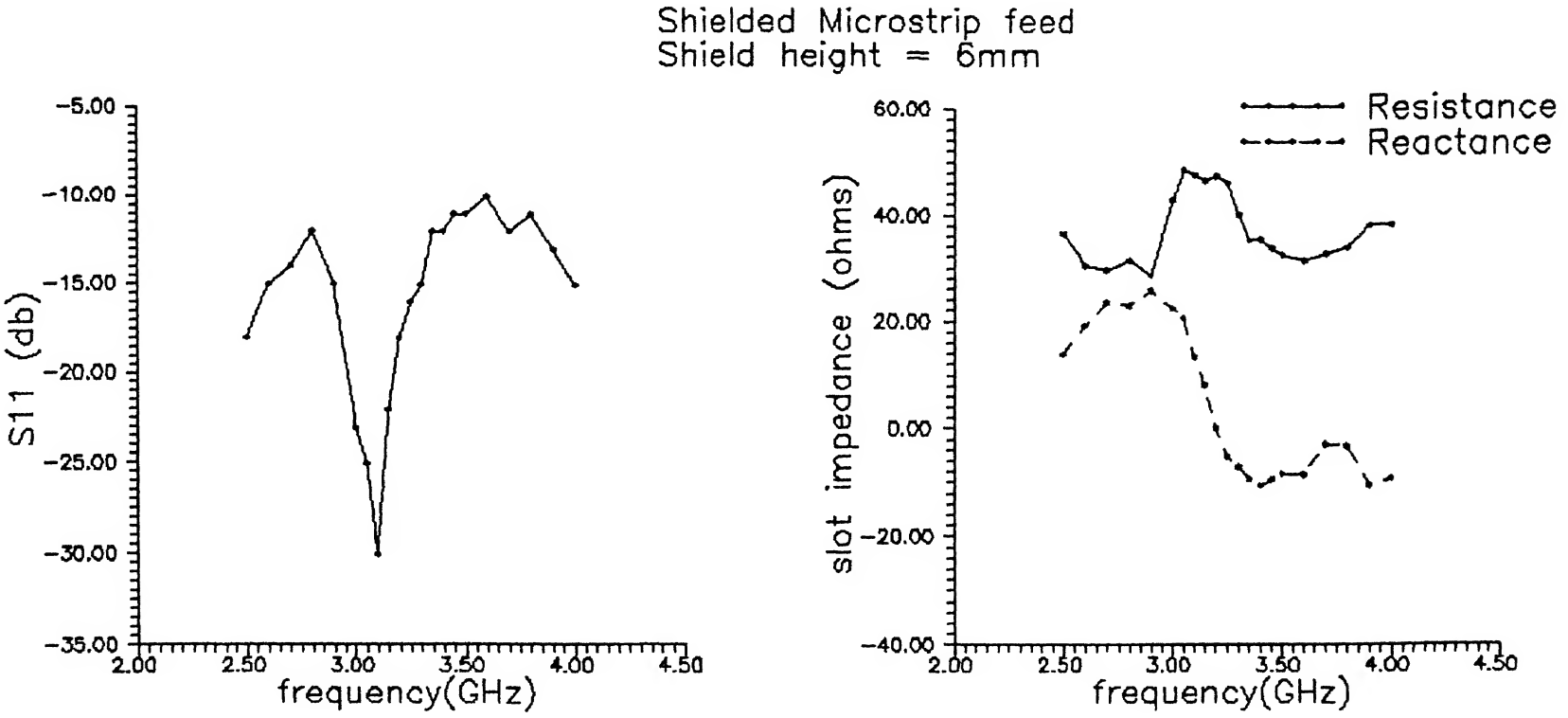

Fig. 2.21 Plots of Model No.9

Chapter 3

Evaluation of mutual coupling

3.1 Introduction

In the design of an array, it is important to estimate the mutual coupling between the antenna elements. Mutual coupling is caused by the simultaneous effect of interaction through free space and interaction through surface waves, between the various elements of the array. No theoretical formulation was available for evaluation of mutual coupling, therefore it was decided to experimentally evaluate the mutual coupling between the notch antenna elements of the array.

The dimensions of the array and the interelement spacing at 3.2 GHz central frequency were designed using LAARAN software. The designed side lobe level was -30 db. It was decided to fabricate a 32 element array with 0.64 λ (6 cms) spacing between the elements. The length of the array for these dimensions came to 6.097 feet ($\approx$ 2 mtrs). These dimensions were used in fabrication of elements for evaluation of mutual coupling.

The methods thought of for experimental evaluation of mutual coupling were the following,

- S matrix approach.

- Z matrix approach.

- Y matrix approach.

The S matrix approach required fabrication of the complete array of 32 elements in Aluminium and measurement of S_{12}, S_{13}, S_{14} etc. one by one, while keeping all the other elements match terminated. Fabrication of the complete array and match terminating 30 elements at one time was a difficult task. The Z matrix approach involved open circuiting all the elements, except the two under measurement, instead of match termination. The 2 X 2 matrix obtained from each measurement, converted to 2 X 2 Z matrix would have given values of Z_{12}, Z_{13}, Z_{14} etc. for the complete array. This Z matrix converted to S matrix would have given the complete S matrix for the array.

The Y matrix approach involved shorting of all 30 elements of the array except the 2 under test. Each 2 X 2 S matrix got from measurement, converted to Y matrix would have given values of Y_{12}, Y_{13}, Y_{14} etc. for the array. The Y matrix so formed could be converted to S matrix for the array, thereby getting the mutual coupling of the elements. This approach was the easiest for evaluation of mutual coupling since it did not involve fabrication of the complete array elements and match/open terminating them. Although, ideally one must short the input points of the elements with the entire array present, a nearest approximation is to close all elements with a Aluminium plate. It is not necessary to fabricate the entire array for approximate mutual coupling evaluation using Y matrix approach. Before adopting this approach it was decided to fabricate a 2 element array and evaluate the mutual coupling between the 2 elements so as to get an idea regarding the level of mutual coupling involved. Thereafter an attempt was made to further reduce the mutual coupling by providing an isolating slot, to act as an open circuit for the coupling energy, between the 2 elements. This

chapter describes the experimental procedure adopted to evaluate the mutual coupling of the array and the results obtained from the same.

3.2 Two Element Array

Based on the notch element finalised in the second chapter, a 2 element array was fabricated, with interelement spacing of 0.64 λ, as designated for the array. Each element was provided with separate microstrip feed lines shielded at a height of 6mm. Refer Fig.3.1 for the model of the 2 Element Array. The S_{11} and S_{22} of the model were measured using the Network Analyser. Both elements showed a good match of less than -15 db in the frequency band of 3 to 3.4 GHz. The slot impedance calculated for each of the elements also showed a good match with the input feed line. Refer Figs.3.2 and 3.3 for the graphs got on performing experiments on the 2 elements. The mutual coupling S_{12}/S_{21} was measured between the 2 elements, using the Network Analyser. It was seen that a very low mutual coupling of less than -20 db existed between the 2 elements over a very wide frequency band.

The mutual impedance calculated from S_{12}/S_{21} magnitude and phase also showed a very low value of $-2+j7\,\Omega$, as seen at the microstrip input to the slot, at the design frequency of 3.2 GHz. The self impedance seen at the same point was around 40 Ω. Also the variation in mutual impedance in the required frequency band of 3 to 3.4 GHz was very low. Refer Fig. 3.4 for the plots of the mutual coupling and impedance.

3.3 Isolation between adjacent elements

The notch antenna element was not a proper travelling wave antenna since the length of the antenna was shortened to $\approx \lambda/2$, but was resonant in nature. Therefore coupling

2 Element Array

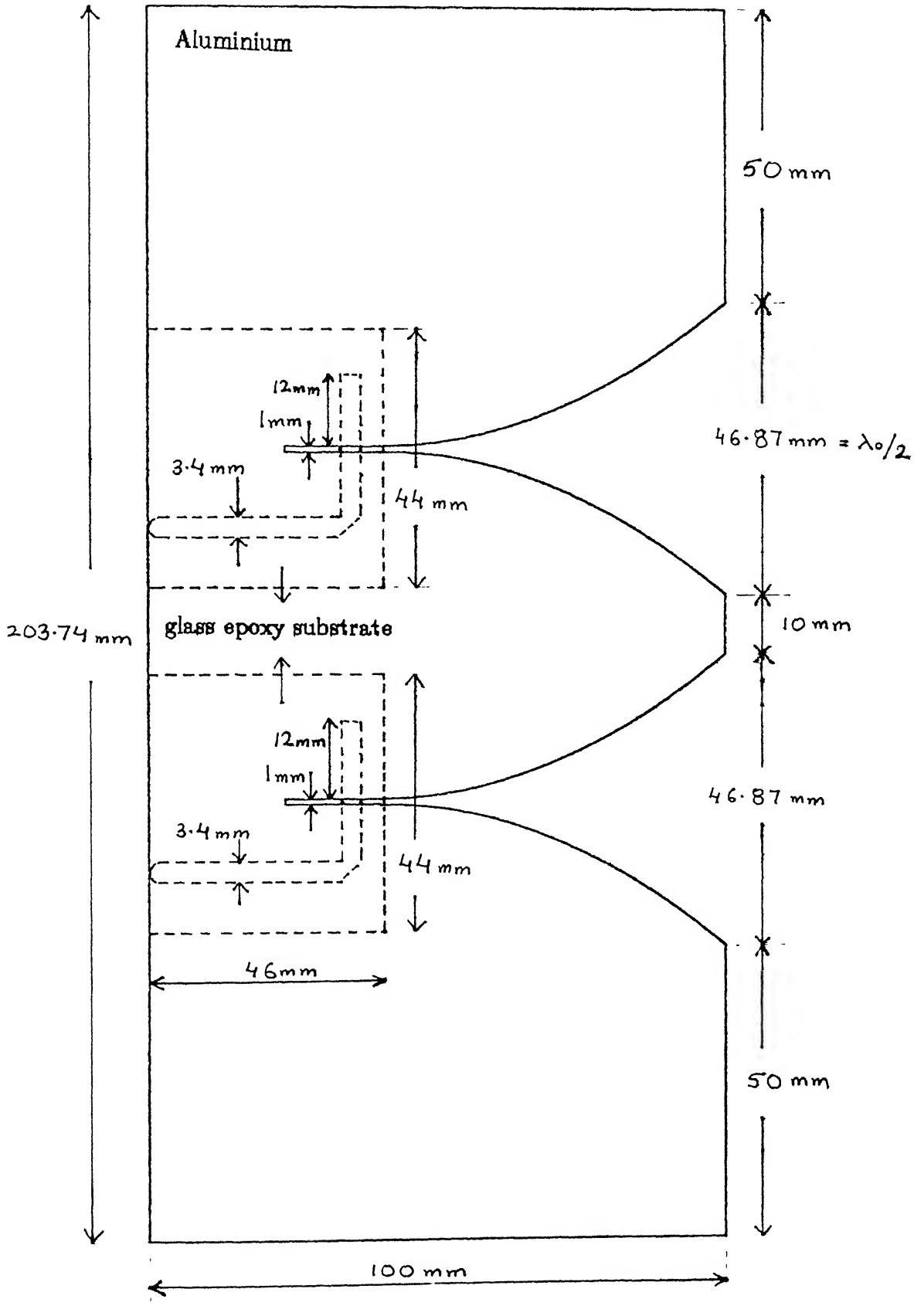

Fig. 3.1 Model of 2 Element Array

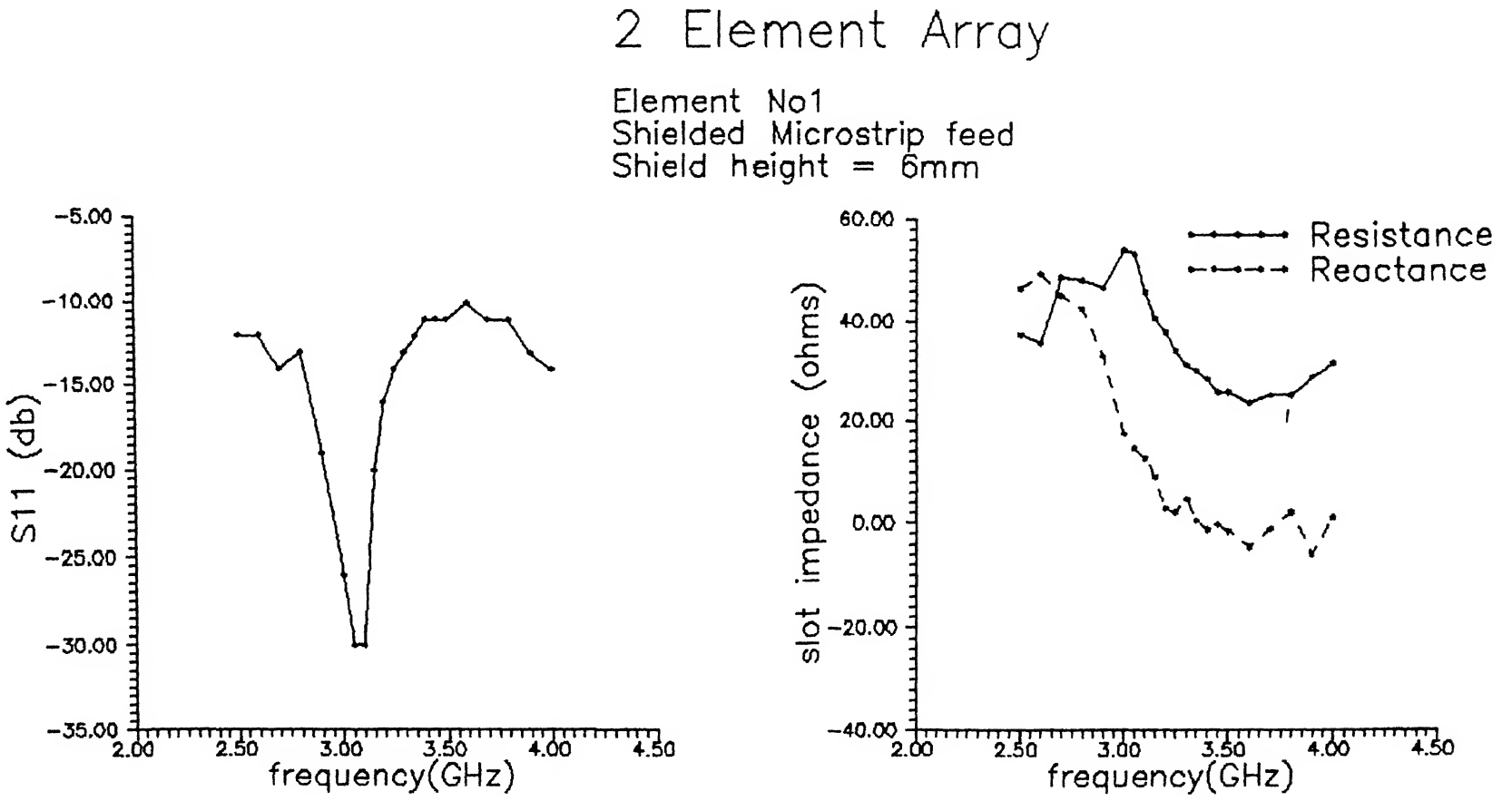

Fig. 3.2 Plots of 2 Element Array (Element 1)

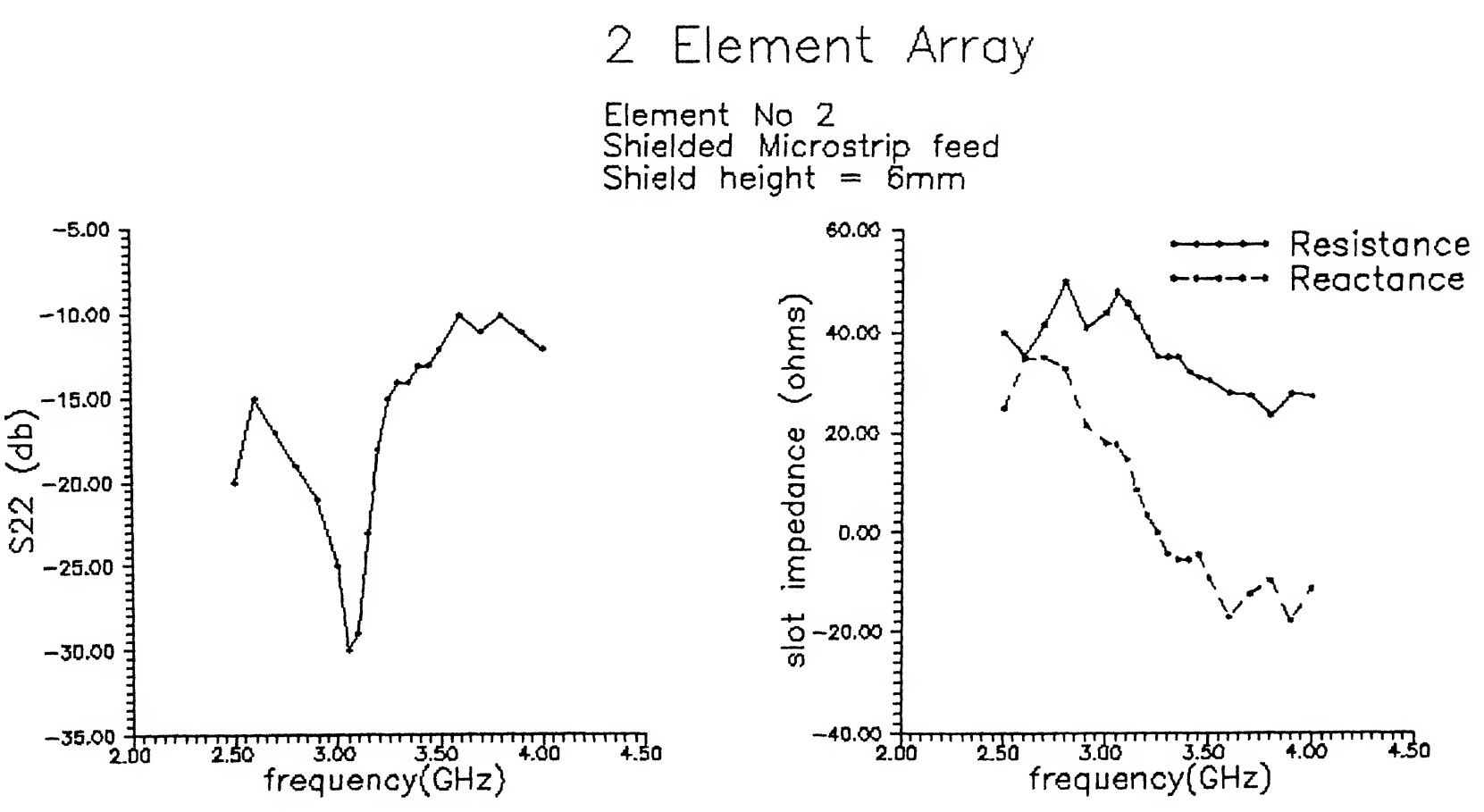

Fig. 3.3 Plots of 2 Element Array (Element 2)

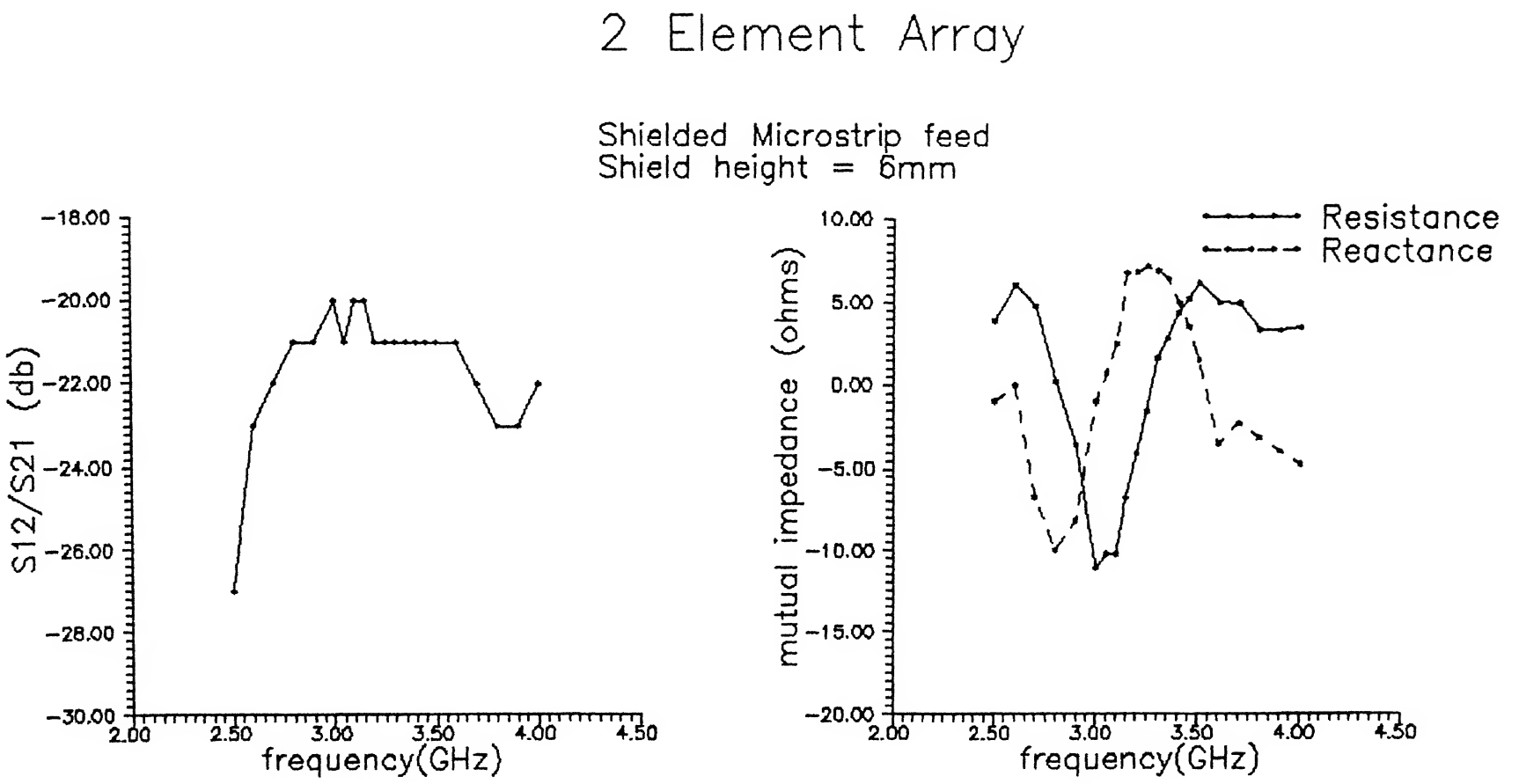

Fig. 3.4 Plots of 2 Element Array (Mutual coupling)

existed between the elements of the array. This coupling could be free space coupling, surface coupling caused due to the dielectric substrate of the feed structure, and direct coupling caused by flow of current on the edge of the antenna from one element to the other. The surface coupling was neglected. Since there was no way of reducing the free space coupling, the direct coupling was reduced by providing a $\lambda/4$ slot in the Aluminium plate between the 2 elements. A short circuit at one end of the slot caused an open circuit to the flow of current on the other end. This prevented the flow of current from one element to the other along the edge of the element thereby reducing the direct mutual coupling. The length of the slot was further adjusted since the slot length caused the phase of the coupled portions to change which in turn could improve the mutual coupling by cancelling the phase of free space coupling. Therefore the slot length was experimentally adjusted to a length of 32mm to get the lowest mutual coupling, of around 24 db, between the 2 elements. The mutual impedance further reduced to almost ι 5 at the design frequency of 3.2 GHz. Refer Fig.3.5 for the 2 element array model with the isolation slot. Figs 3.6, 3.7 and 3.8 give the plots obtained from the measurements.

3.4 Experimental evaluation of Mutual coupling

The low value of mutual coupling obtained for the 2 element array with isolation slots, prompted the use of a different technique for evaluation of mutual coupling of the array. Instead of following the Y matrix approach of shorting all 30 elements of the array and then measuring the mutual impedance between the balance 2 elements, the 2 element array itself was used with distance between the elements gradually increased by inserting shorting plates of Aluminium of increasing widths. Therefore in effect the

2 Element Array

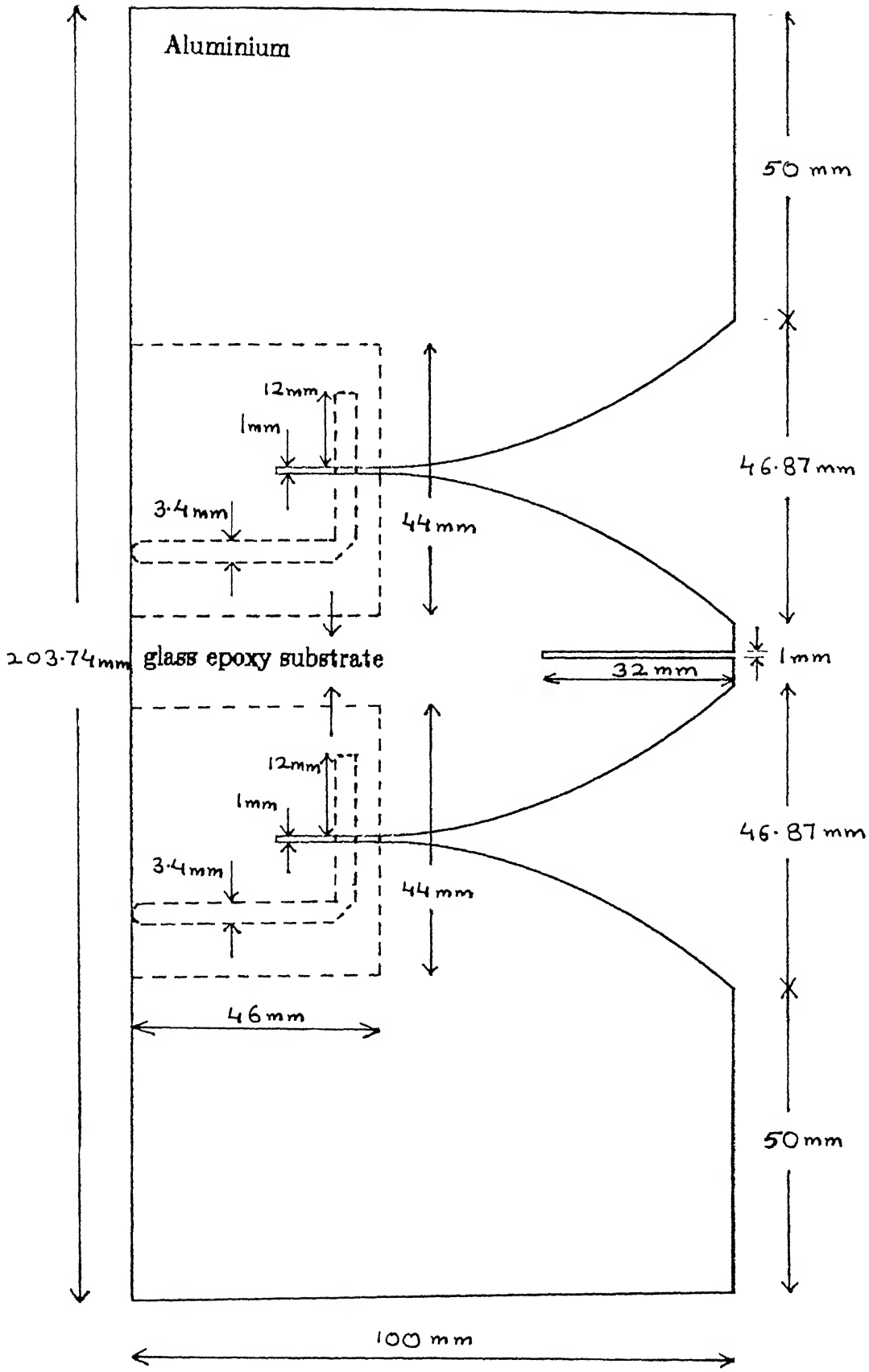

Fig. 3.5 Model of 2 Element Array with isolating slot

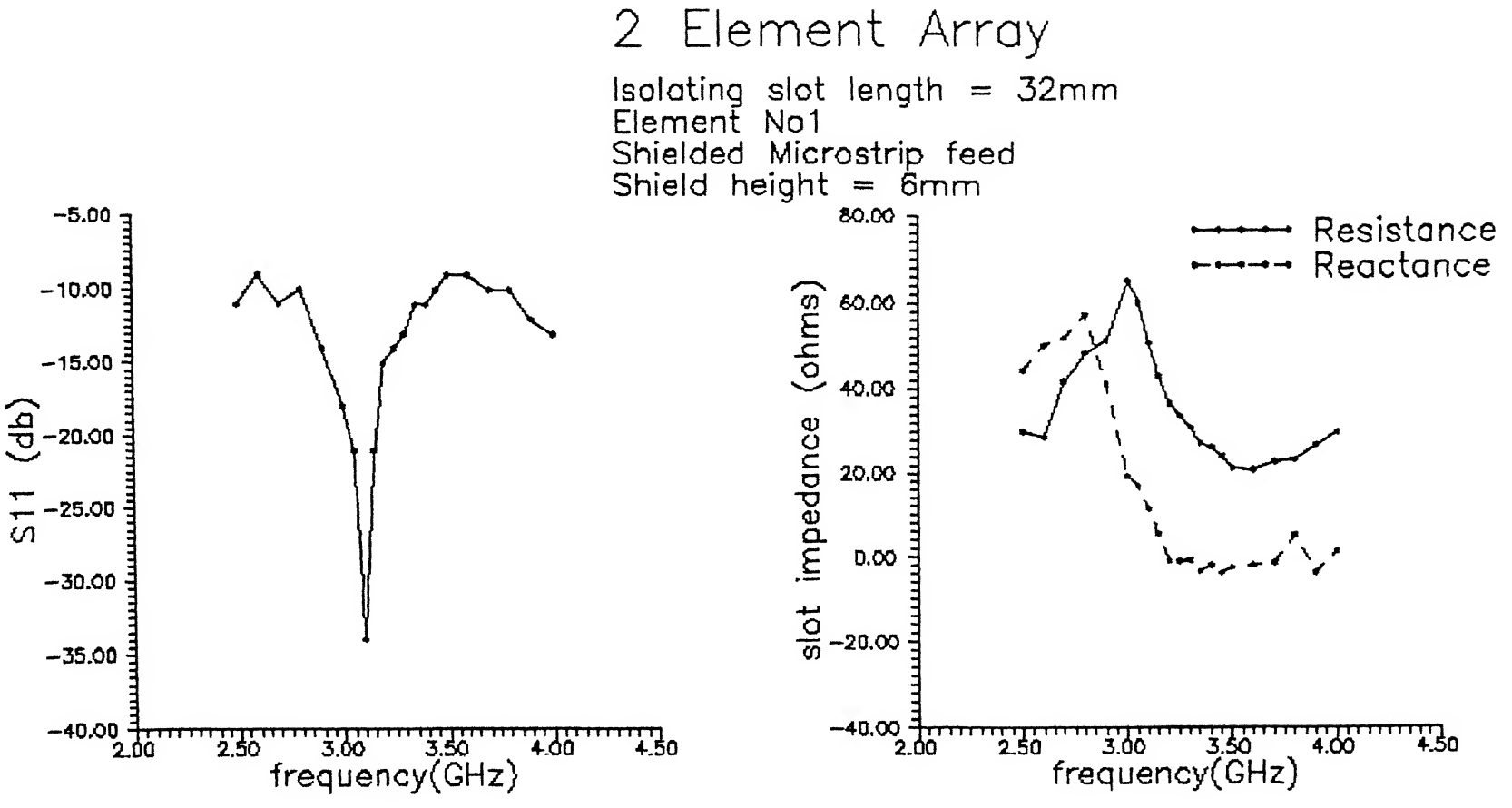

Fig. 3.6 Plots of 2 Element Array with isolating slot (Element 1)

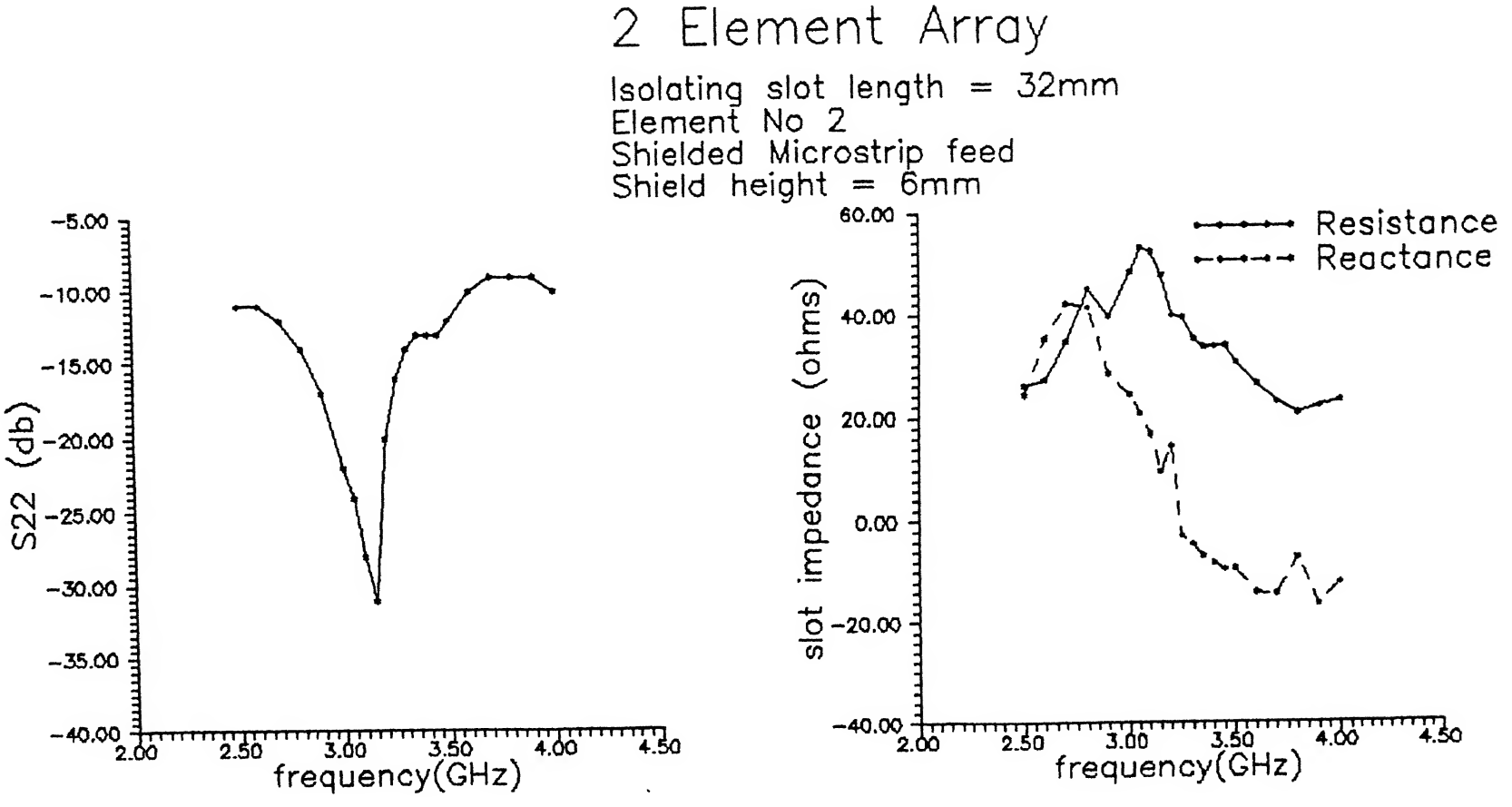

Fig. 3.7 Plots of 2 Element Array with isolating slot (Element 2)

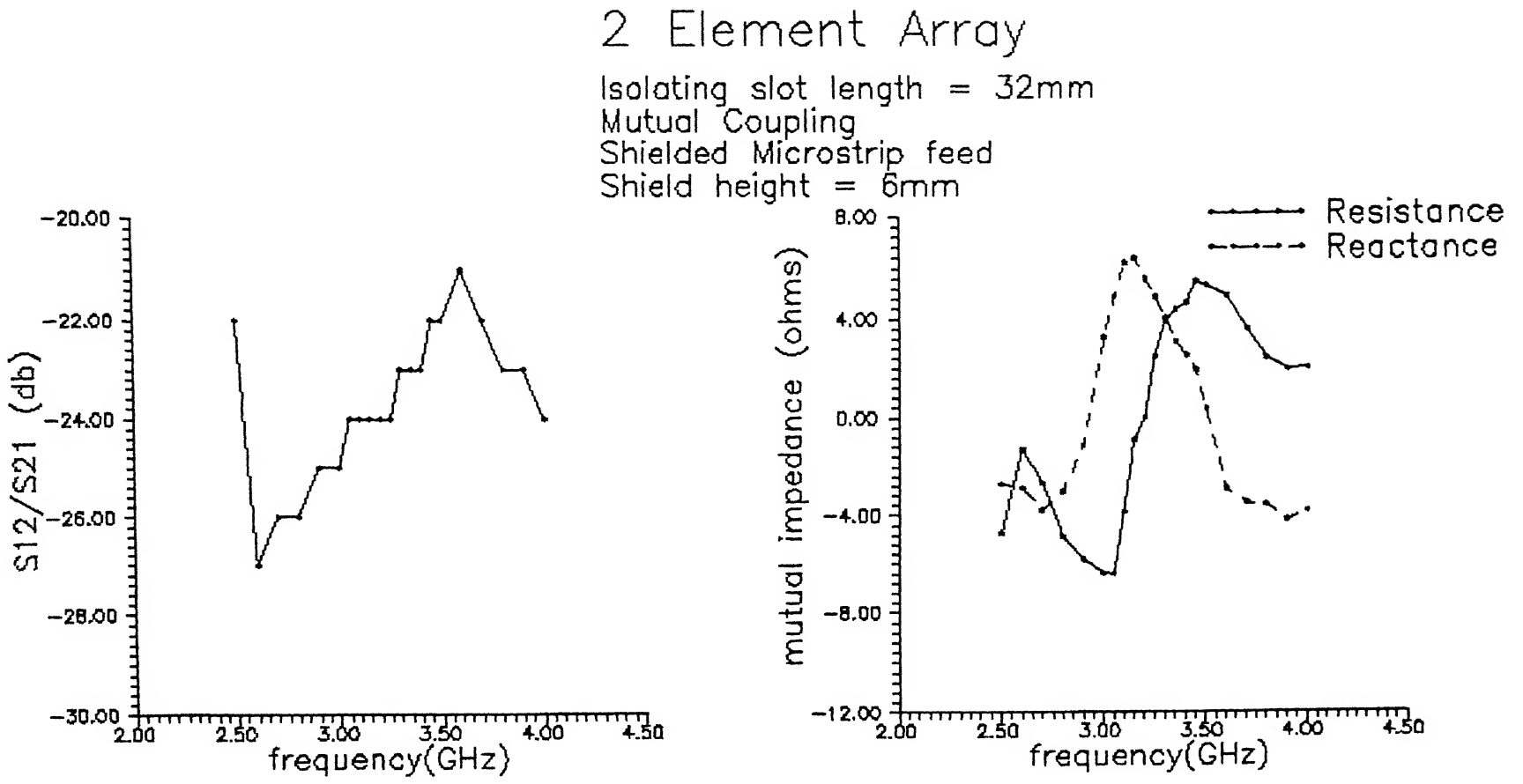

Fig. 3.8 Plots of 2 Element Array with isolating slot (Mutual coupling)

elements in between the 2 elements were shorted while a shorting plate of 5cms was kept on the outside of each of the elements. A 5cm shorting plate is in effect almost equal to one shorted element on the outside of the elements. The S_{12}/S_{21} magnitude and phase for each increase in the distance between the elements was measured and plotted Vs the distance. The measurement was done at 3 frequencies of 3.1, 3.2 and 3.3 GHz so as to know the behaviour of the mutual coupling over the entire frequency band of 3 to 3.4 GHz. The plate size in between the 2 elements was increased to a maximum size of 12cms, equivalent to 2 shorted antenna elements. The readings recorded were plotted Vs the distance and curve fitting was done to extend the mutual coupling values to whatever distance required. Refer Fig.3.9, 3.10 and 3.11 for the curves obtained alongwith curve fitting equations.

These curve fitting equations were used to calculate the mutual coupling between the elements of the array directly instead of conversion to Y matrix and then forming the S matrix of the array. The procedure for evaluation of the mutual coupling was thereby shortened since the 2 element array showed a fairly low value of mutual coupling. The curve fitting equations used for calculation of mutual impedance were as follows,

$$y = -0.892857\,x - 19.6786 \qquad -\,for\ magnitude$$

$$y = -31.1786\,x + 151.114 \qquad -\,for\ phase$$

The S matrix of all 32 elements of the array was formulated using the above mentioned equations. The value of S_{11} used in the matrix was the one got during measurement of 2 element array. Refer Fig.3.12 for the values of S matrix obtained. This 32 X 32 S matrix, of mutual coupling between the elements of the array, was used for the computation of active impedance of each element, at the input of the microstrip line

to the slot. The active impedance computed was used for designing the feed network. The procedure for this and the values obtained are explained in Chapter 4.

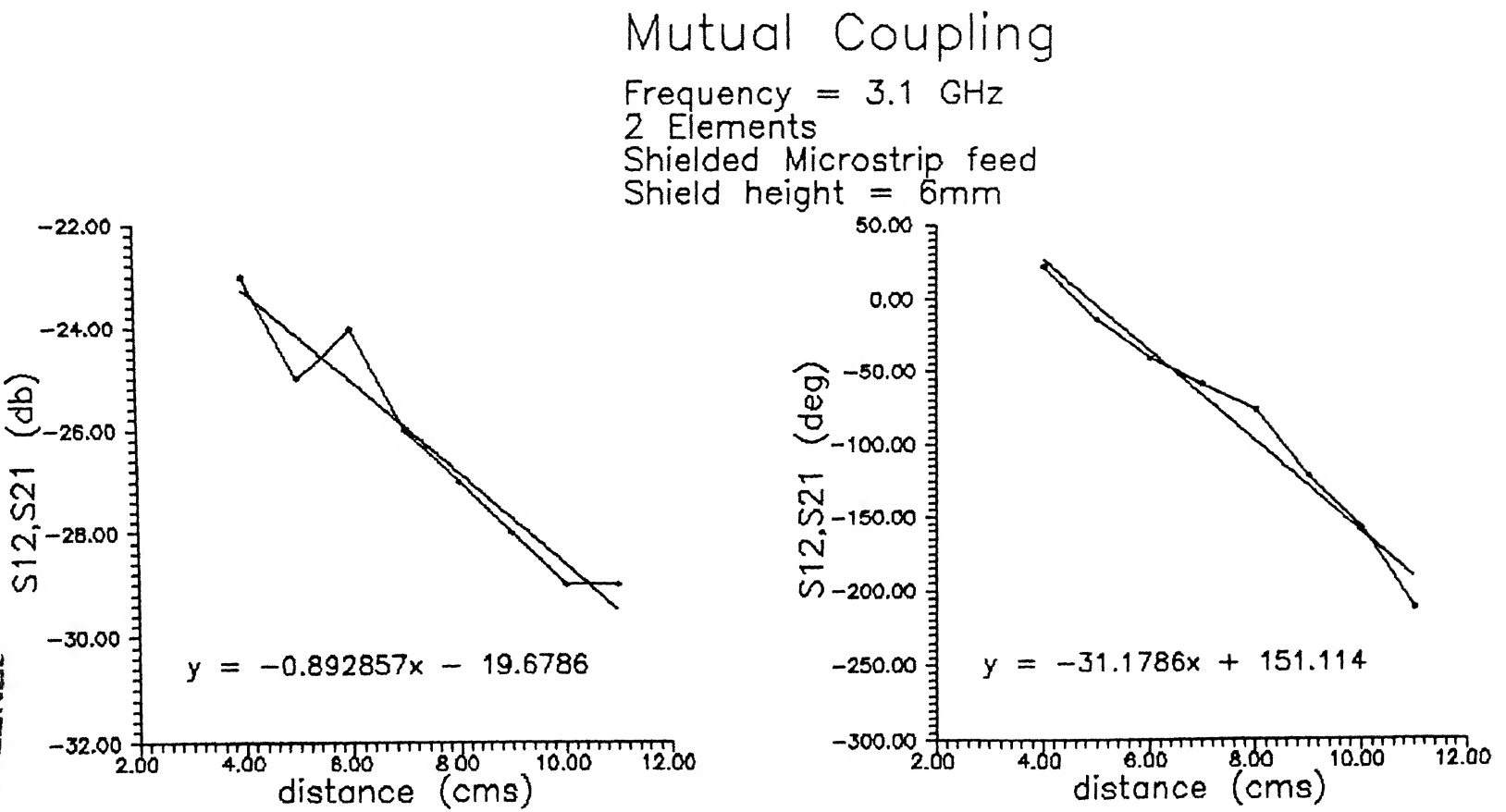

Fig. 3.9 Plots of Mutual Coupling Vs distance (2 Elements)

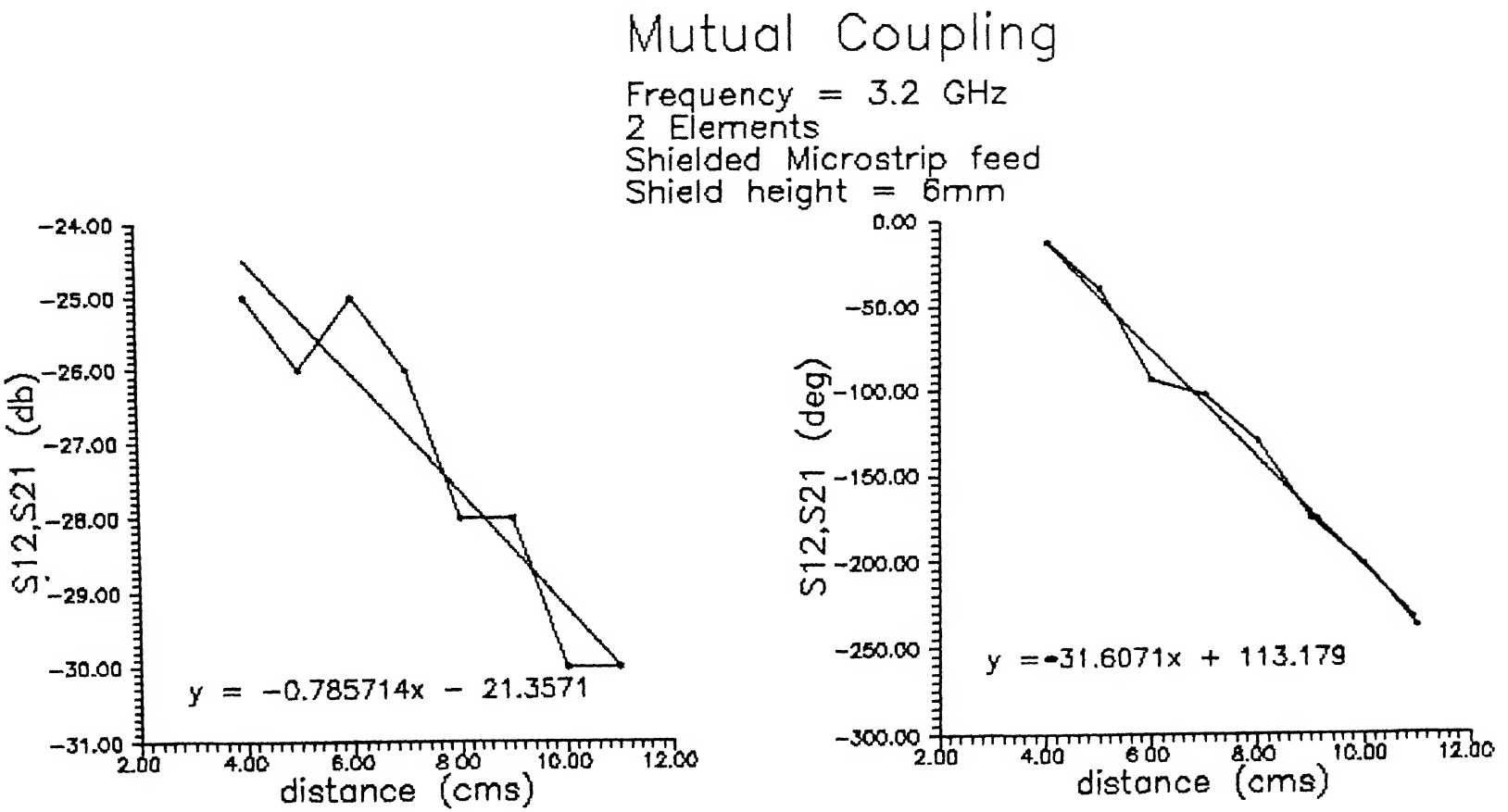

Fig. 3.10 Plots of Mutual Coupling Vs distance (2 Elements)

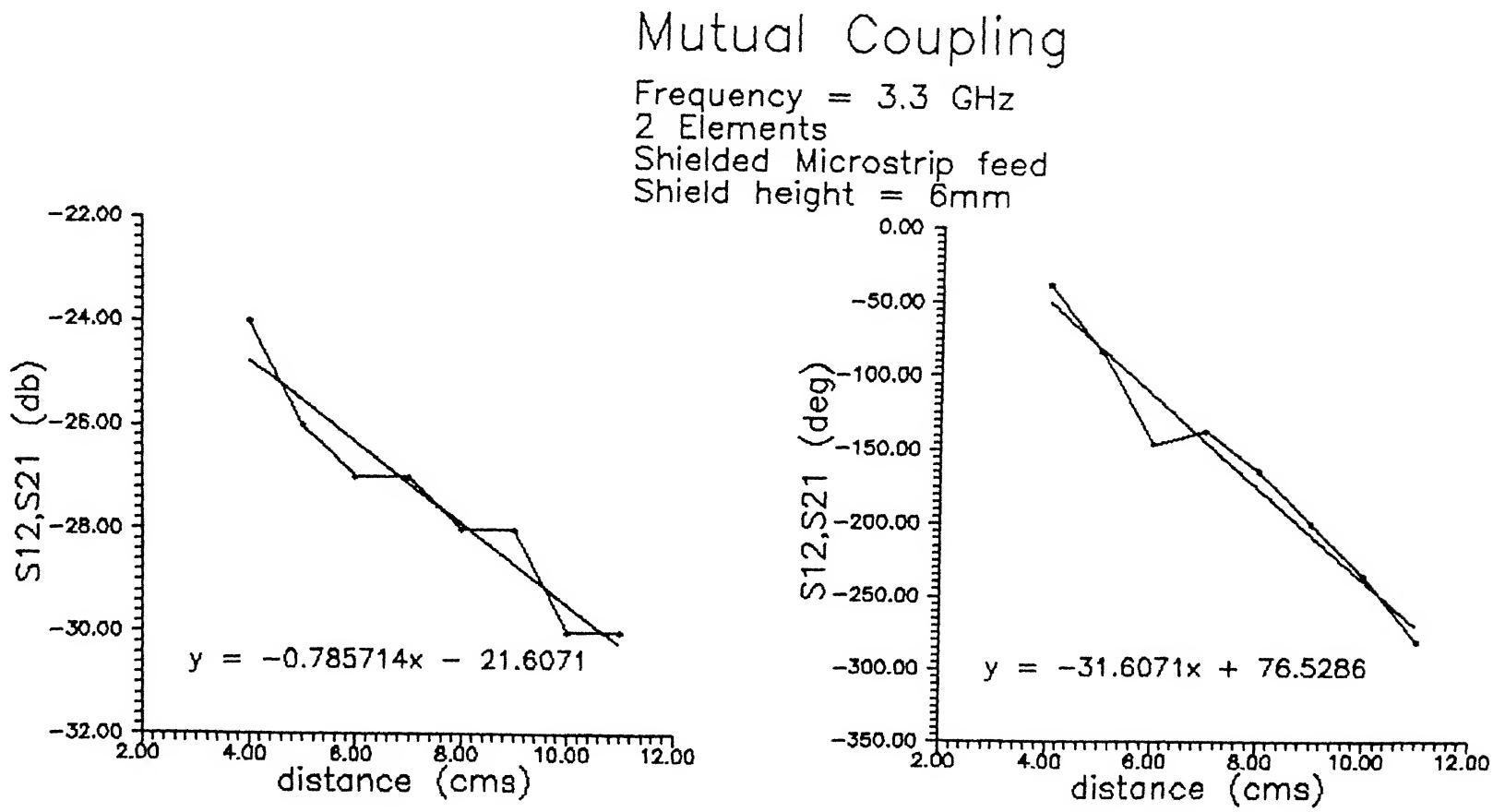

Fig. 3.11 Plots of Mutual Coupling Vs distance (2 Elements)

n	S_1n (db's)	S_1n (deg)
1	-20.0	-50.5
2	-26.0713800	-76.4635800
3	-30.7856700	86.1061900
4	-35.4999500	-84.2512400
5	-40.2142300	74.6086400
6	-44.9285200	-64.9659800
7	-49.6428000	55.3233300
8	-54.3570900	-45.6807700
9	-59.0713700	36.0382200
10	-63.7856500	-26.3956700
11	-68.4999400	16.7531200
12	-73.2142200	-7.1104580
13	-77.9285000	-2.5323110
14	-82.6427900	12.1748600
15	-87.3570700	-21.8174100
16	-92.0713600	31.4599600
17	-96.7856400	-41.1025200
18	-101.4999000	50.7450600
19	-106.2142000	-60.3876200
20	-110.9285000	70.0301700
21	-115.6428000	-79.6727200
22	-120.3571000	89.3155700
23	-125.0713000	-81.0417300
24	-129.7856000	71.3993900
25	-134.4999000	-61.7570600
26	-139.2142000	52.1142900
27	-143.9285000	-42.4715200
28	-148.6428000	32.8291900
29	-153.3570000	-23.1864200
30	-158.0713000	13.5436500
31	-162.7856000	-3.9008800
32	-167.4999000	-5.7414530

Fig. 3.12 S Matrix of the Array

Chapter 4

Array Design

4.1 Introduction

The basic groundwork for the design of the array had been completed by finalising the design of one element of the array and evaluation of mutual coupling between the elements of the array. The number of elements in the array had also been decided to be 32 with 0.64 λ (6cms) interelement spacing. It was decided to design the array on Taylor Pattern having decaying side lobes instead of Tchebychev Pattern which has equal side lobes. Tchebychev Pattern gives optimum beam width but the side lobe level extending to the edge of the array gives rise to back lobes. Contrary to this, in Taylor Pattern, the excitation gradually decreases towards the edges of the array and so no back lobe is formed.

The general configuration of the array was decided based on ease in fabrication and assembling of the 32 elements. Design of the feed network was also based on ease in printing and assembling. Corporate feed network was designed for the array. The division of power in the elements of the array was done as per the incident power coefficients got from computations. The LAARAN coefficients were suitably modified for calculation of the active impedance of each element at the input of microstrip feed

line. S matrix of the array was used for computation of active impedance. The feed line design was based on microstrip line on glass epoxy substrate with simple power dividers designed in the feed line for dividing the power into the 32 elements. This chapter describes the general configuration of the array, array factor design and results obtained using LAARAN, procedure followed for computation of active impedance of the elements, design of feed line and power dividers and the final feed network designed for the array.

4.2 General configuration of the Array

The array of notch antenna elements was to be 2mts long as per specifications. Thirty two elements had to be fabricated on a 2 meter long Aluminium plate, 1.6mm thick, with precise 6cm distance between each element. Each element of the array had a slot of precise 1mm thickness with a specific taper which had to be same for all the elements. It was not practical to do precision work on a single sheet of Aluminium. So it was decided to divide the array into 8 pieces with 4 notch antenna elements fabricated on each piece. These 8 pieces could later be joined together to form the complete array. The 2 meter feed network PCB could also not be printed at one go. Therefore it was decided to make individual feed network for each Aluminium piece, feeding the 4 elements on that piece. The 8 inputs to these 8 feed networks had to be combined on a single feed network. For this it was envisaged that another microstrip feed network on glass epoxy substrate would be printed with 8 way power division, one for each feed network. In this manner the amount of glass epoxy substrate used was reduced, thereby reducing the dielectric loss. The combining of the 8 way power divider PCB to the 8 feed networks was done using coaxial cables. This was the

general configuration planned and later implemented, for the array. Refer Fig.4.1 for the general configuration.

4.3 Array Factor Design

The specification given for the array were as follows,

- Centre Frequency - 3.2 GHz
- Band Width - 10 percent or higher
- Length - 2 meters
- Peak Side lobe level - < -30 db
- VSWR - < 1.5
- Gain - 16 db
- Power - 1 KW peak, 10 W average
- Array should be radiating along an edge and have a thin cross section.

LAARAN software was used for calculating the array coefficients for a 32 element array, with 0.64 λ interelement spacing, at 3.2 GHz. The side lobe level specified was -30 db and $\overline{n} = 4$. For a Taylor pattern design, the excitation coefficients of the array were found using LAARAN which also gave the plot of distribution Vs element position and the pattern of the array. Refer Fig.4.2 for these coefficients, Fig.4.3 for the plot of the distribution Vs element position and Fig.4.4 for the pattern of the array as given by LAARAN.

General configuration of the array

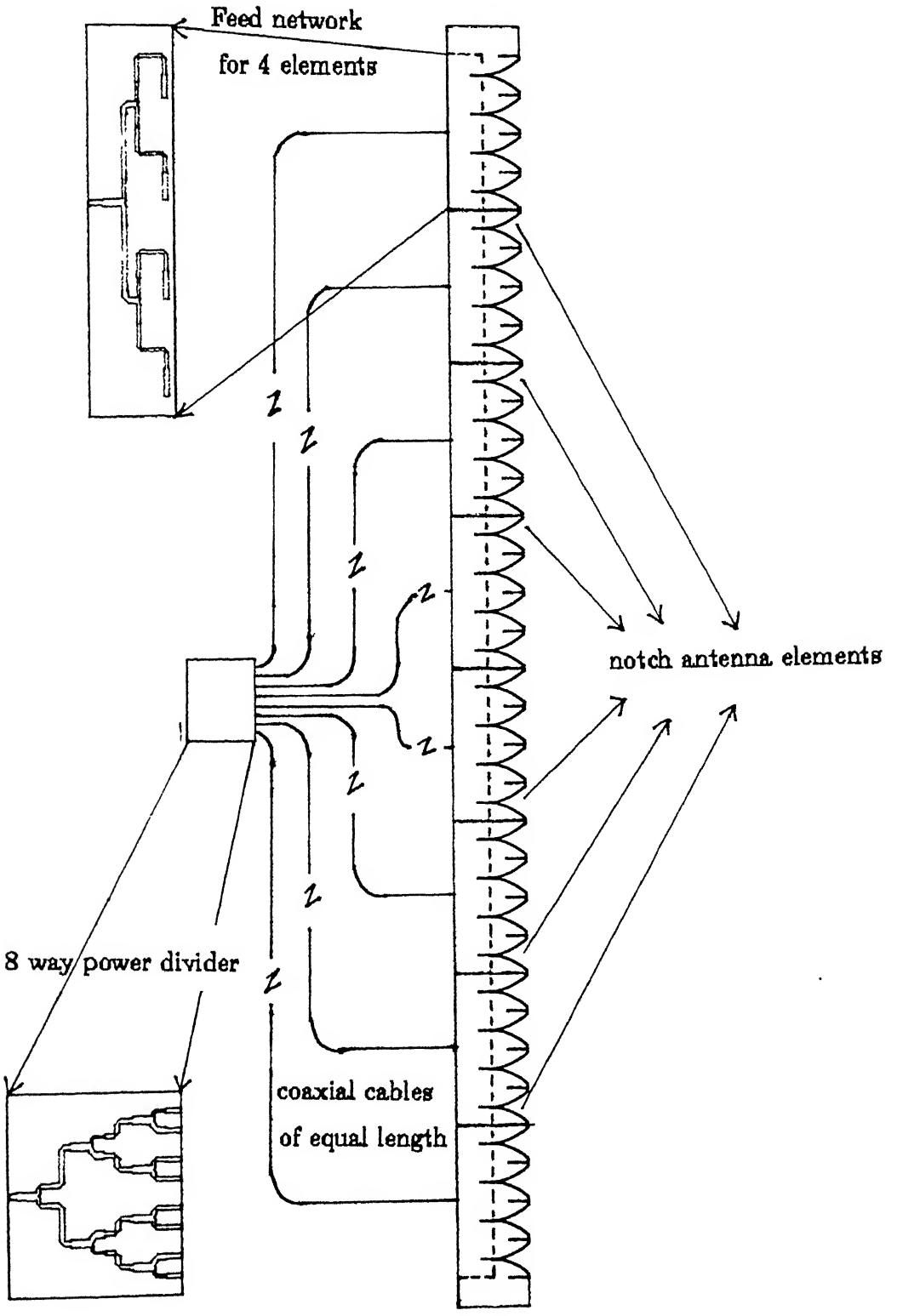

Fig. 4.1 General configuration of the array

Element No.	magnitude	phase(deg)
1	0.24486499	0.00000000
2	0.26323655	0.00000000
3	0.29865253	0.00000000
4	0.34865478	0.00000000
5	0.41000009	0.00000000
6	0.47907534	0.00000000
7	0.55229223	0.00000000
8	0.62638485	0.00000000
9	0.69856948	0.00000000
10	0.76656574	0.00000000
11	0.82851779	0.00000000
12	0.88287497	0.00000000
13	0.92828953	0.00000000
14	0.96357369	0.00000000
15	0.98772496	0.00000000
16	1.00000000	0.00000000
17	1.00000000	0.00000000
18	0.98772496	0.00000000
19	0.96357369	0.00000000
20	0.92828953	0.00000000
21	0.88287497	0.00000000
22	0.82851779	0.00000000
23	0.76656574	0.00000000
24	0.69856948	0.00000000
25	0.62638485	0.00000000
26	0.55229223	0.00000000
27	0.47907534	0.00000000
28	0.41000009	0.00000000
29	0.34865478	0.00000000
30	0.29865253	0.00000000
31	0.26323655	0.00000000
32	0.24486499	0.00000000

Fig. 4.2 Excitation coefficients of the array as got from LAARAN

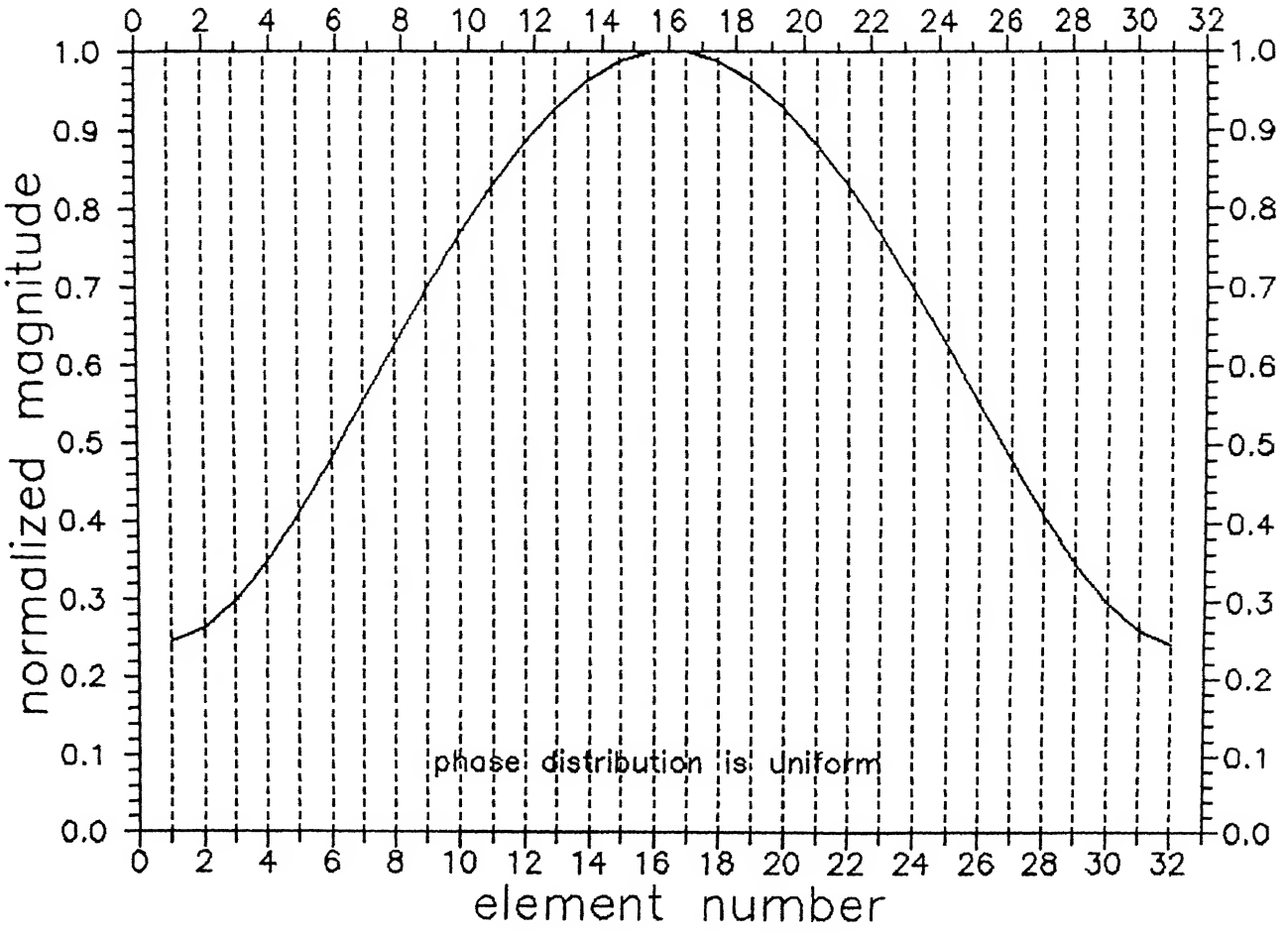

Fig. 4.3 Theoretical distribution of the array

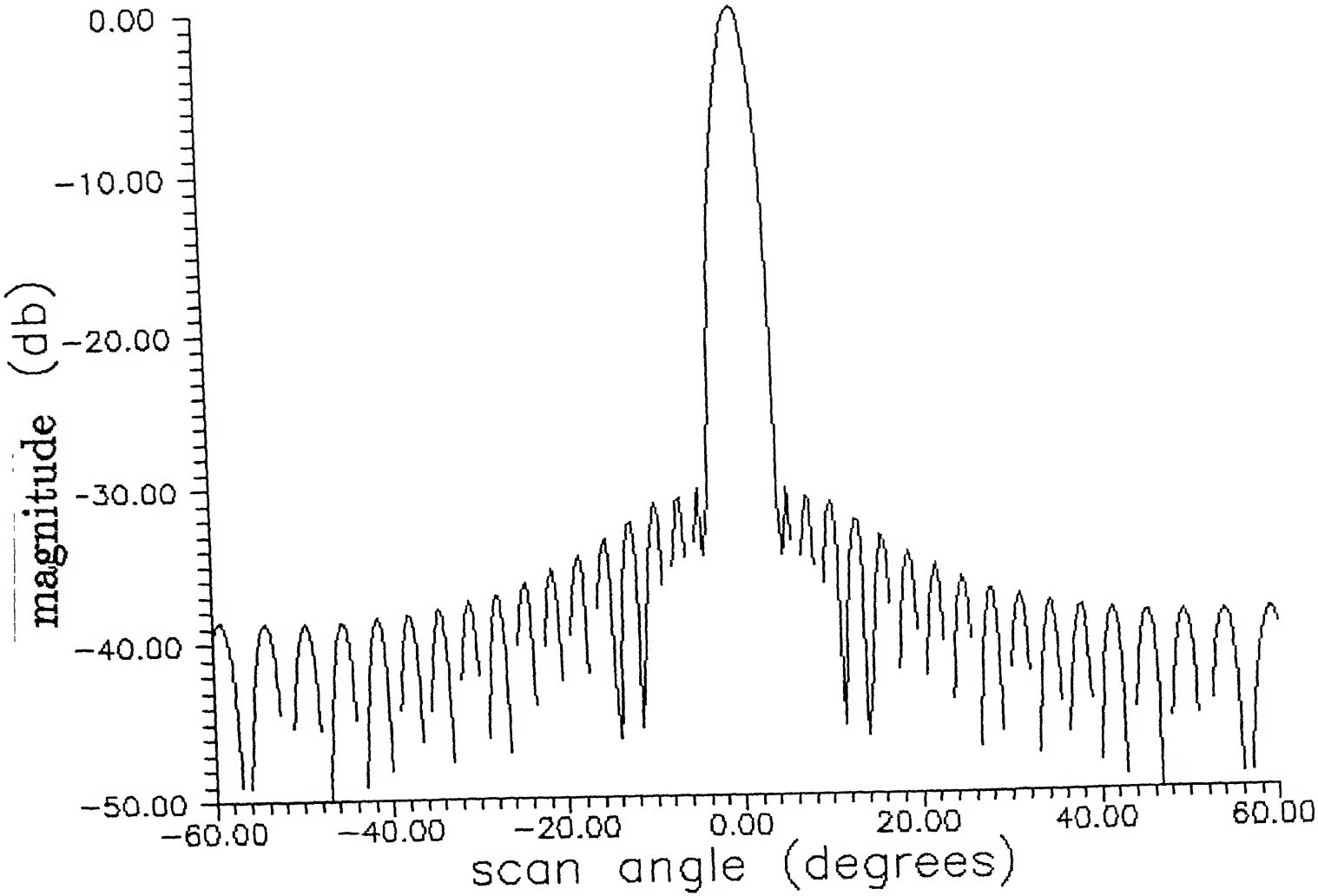

Fig. 4.4 Theoretical pattern of the array (from LAARAN)

4.4 Active Impedance Calculation

The feed network design of the array was to be based on the active impedance evaluated at the element slot as seen by the microstrip input. The microstrip line printed at that point had to be of that impedance. Active impedance is the impedance found at the feed point of an element as a combined effect of both self and mutual impedance due to the mutual coupling effect of all elements of the array. For calculation of the active impedance of each element of the array, the excitation coefficients of the array and the S matrix of the array were used. The coefficients of the array as given by LAARAN could not be used directly since they could not be directly equated to voltage across the slot. This was so since the stub termination of the feed line was not $\lambda_g/4$ resulting in a value of stub impedance at the slot. Refer Fig.4.5 for the equivalent circuit of the slot.

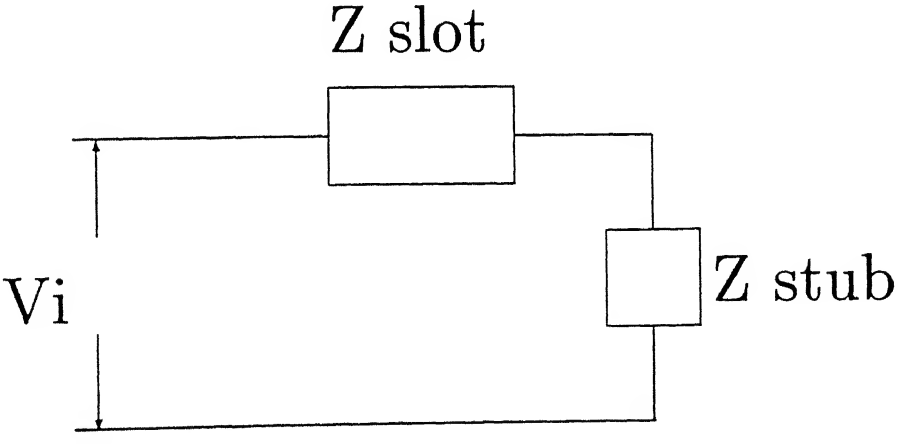

Fig 4.5 Equivalent circuit of slot

Therefore the method adopted for finding the voltage across the slot was by using a scaling factor and iteratively finding the coefficients. The algorithm adopted for this is explained below,

$$C_i = V_i \times d_i \quad where\ C_i - known\ coefficient\ from\ LAARAN$$

$$V_i - actual\ coefficient\ to\ be\ found$$

$$d_i - scaling\ factor = \frac{Z_{slot}}{Z_{slot} + Z_{stub}}$$

The value of d_i was used as a scaling factor for computation of V_i. The value of Z_{stub} was constant since the stub length was constant. The value of Z_{slot} was equated to Z_{self} for the first value of d_i, and subsequently equated to Z_{active} due to interaction caused by mutual coupling. Therefore

$$d_i = \frac{Z_{active}}{Z_{active} + Z_{stub}}$$

The first value of d_i was used for calculation of first V_i, which was used for active impedance calculation in the following manner,

$$V_i = a + b \quad where\ a - incident\ voltage$$

$$b - reflected\ voltage$$

$$\Rightarrow [V_i] = [a] + [b] = [a] + [S][a] = [1 + S][a]$$

$$\Rightarrow [a] = [1 + S]^{-1}\,[V_i]$$

The [a] matrix was found from this and $|a|^2$ gave the incident power in each element of the array. From [a], [b] matrix was found using

$$[S][a] = [b]$$

Once [a] and [b] were known, $\frac{b_1}{a_1}$ gave Γ_{in} (input reflection coefficient) from which Z_{active} was computed by

$$Z_{active} = \frac{1+\Gamma_{in}}{1-\Gamma_{in}}$$

This value of Z_{active} was substituted in $d_i = \frac{Z_{active}}{Z_{active}+Z_{stub}}$ for computing the new value of d_i. This process was iteratively carried out until the value of d_i converged. A convergence factor of 0.001 was used for d_i. The active impedance of the elements and the incident power in each element was computed using this procedure.

4.5 Design of feed line and power divider

The value of active impedances for each element had been evaluated and also the ratio of power division in each element had been found from the incident power coefficient for each element. The feed line structure could be now planned based on these values. There was an option between designing a corporate feed network or a serial feed network. The corporate feed network has a broader bandwidth because the phase of excitation is independent of frequency, since the path length for each line is the same. On the other hand the serial feed has a narrower band width but has lower loss. It was decided to formulate a corporate feed network for the array to cater for a wide band of operation. Therefore a corporate feed network of microstrip feed lines on glass epoxy substrate was decided on. The general configuration of the feed network had already been decided as explained in section 4.2. The feed lines were to be made as small as possible in length so as to reduce the dielectric loss. Power division was incorporated in the microstrip lines by making simple power dividers in microstrip line. One example of the power divider design as incorporated in the feed network is given below. Refer Fig.4.6.

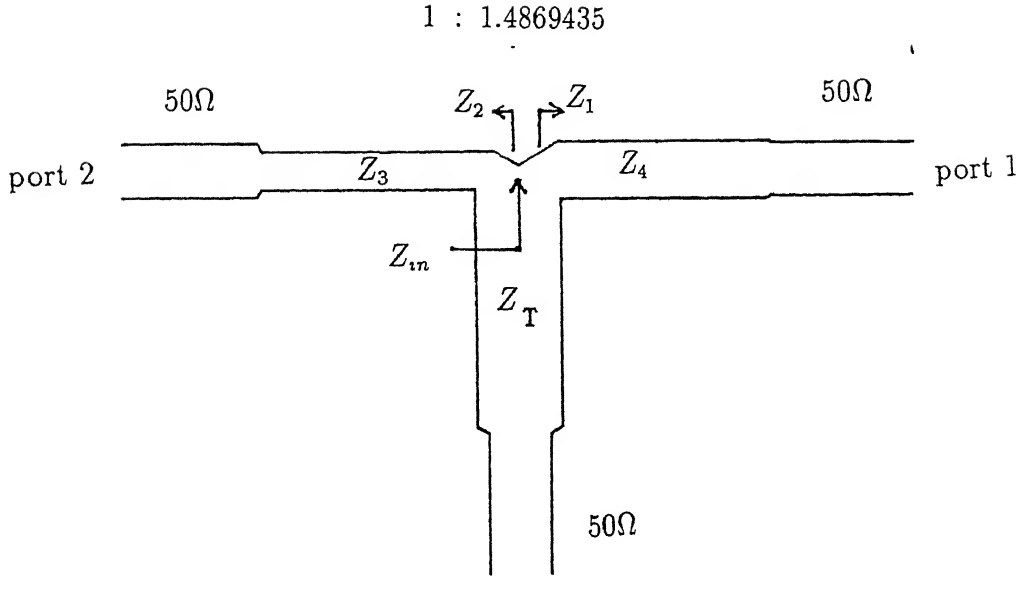

Fig. 4.6 Power divider example

The ratio of power division required :

$\frac{P_1}{P_2} = \frac{Z_2}{Z_1} = \frac{2.9724}{1.999} = 1.4869435$

For a total input of 2.9724 + 1.999 = 4.9714, the higher ratio of power division is in port 2. Therefore compensation is required between the input port and port 2.

$$
\begin{aligned}
Compensation &= \sqrt{\frac{4.9714}{1.999}} = 1.577 \\
Z_{in} &= \frac{50}{1.577} \approx 31.7\Omega \\
Z_{in} &= \frac{Z_1 Z_2}{Z_1 + Z_2} \Rightarrow Z_{in}(1 + \frac{Z_2}{Z_1}) = Z_2 \\
\Rightarrow \quad & 31.7(1 + 1.4869435) = Z_2 = 78.85\Omega \\
& Z_1 = 53.03\Omega \\
\Rightarrow \quad & Z_3 = \sqrt{Z_2 \times Z_0} = \sqrt{78.85 \times 50} = 62.79\Omega \\
& Z_4 = \sqrt{Z_1 \times Z_0} = \sqrt{53.03 \times 50} = 51.49\Omega \\
& Z_T = \sqrt{Z_{in} \times Z_0} = \sqrt{31.7 \times 50} = 39.8\Omega
\end{aligned}
$$

4.6 Feed Network Design

The dimensions of the microstrip feed line, shielded at a height of 6mm, and the power divider dimensions for different values of impedances were calculated using design equations given in [15]. The active impedance computed, as explained in section 4.3, was including the open circuit stub impedance in which the feed line was terminated. Therefore for calculating the actual active impedance, the stub impedance was subtracted from the active impedance. The final values of active impedance are as shown in Fig.4.7. These values have a real and imaginary portion. The imaginary portion had to be tuned out by adjusting the length of the open circuit stub. Therefore the impedance of different lengths of the stub lines was computed and a length

Element No.	Resistance (ohms)	Reactance (ohms)
1	61.633	-2.473
2	64.424	-17.045
3	61.346	-21.702
4	65.182	-19.397
5	63.061	-19.756
6	63.670	-18.802
7	63.101	-18.888
8	63.090	-18.454
9	62.873	-18.418
10	62.770	-18.231
11	62.666	-18.184
12	62.588	-18.098
13	62.534	-18.058
14	62.489	-18.015
15	62.465	-17.992
16	62.451	-17.977
17	62.451	-17.977
18	62.465	-17.992
19	62.489	-18.015
20	62.534	-18.058
21	62.588	-18.098
22	62.666	-18.184
23	62.770	-18.231
24	62.873	-18.418
25	63.090	-18.454
26	63.101	-18.888
27	63.670	-18.802
28	63.061	-19.756
29	65.182	-19.397
30	61.346	-21.702
31	64.424	-17.045
32	61.633	-2.473

Fig. 4.7 Final Active impedance of the elements

of stub which tuned out the reactive part at each element was decided upon. In other words, each element had a different open circuit stub length, depending on the reactive portion of the active impedance.

The feed network of microstrip feed lines was designed taking into account the stub lengths for each element and the compensation required for bends, T junctions, and steps in the microstrip line. The design equations given in [16] were used for the compensations. Eight separate feed networks were designed each to feed 4 antenna elements. Refer Fig.4.8 for the etching pattern of one of the feed networks. The 8 way power divider feed net work was also designed in a similar manner. Size of this PCB was kept small so as to reduce the dielectric loss. Refer Fig.4.9 for the 8 way power divider feed network etching pattern. The power division to each element was done based on the incident power values calculated in section 4.3. Refer Fig. 4.10 for the incident power coefficients on which the feed network is made. The design of the feed network was to be symmetrical around the centre since the pattern of the array was symmetrical around the centre. Therefore 4 feed networks were designed for 16 antenna elements in half of the array and each feed network was flipped around the inner edge to give the feed network of the other 16 elements. The direction of feeding of the slots of the elements was however kept the same because difference in direction of feed would have not given any pattern since the feed was required to be in phase for getting a sum pattern.

The combining of the 8 way power divider network with the 8 feed networks was done using RG 58, a 50 Ω coaxial cable. Equal lengths of cable, 8 in number, were used for extending the feed line from one feed network to another. RG 58 offers a loss factor of 0.5 db / foot. This, however, had to be accepted since this was the simplest method to extend the feed line,compared to the costly way of using waveguides and

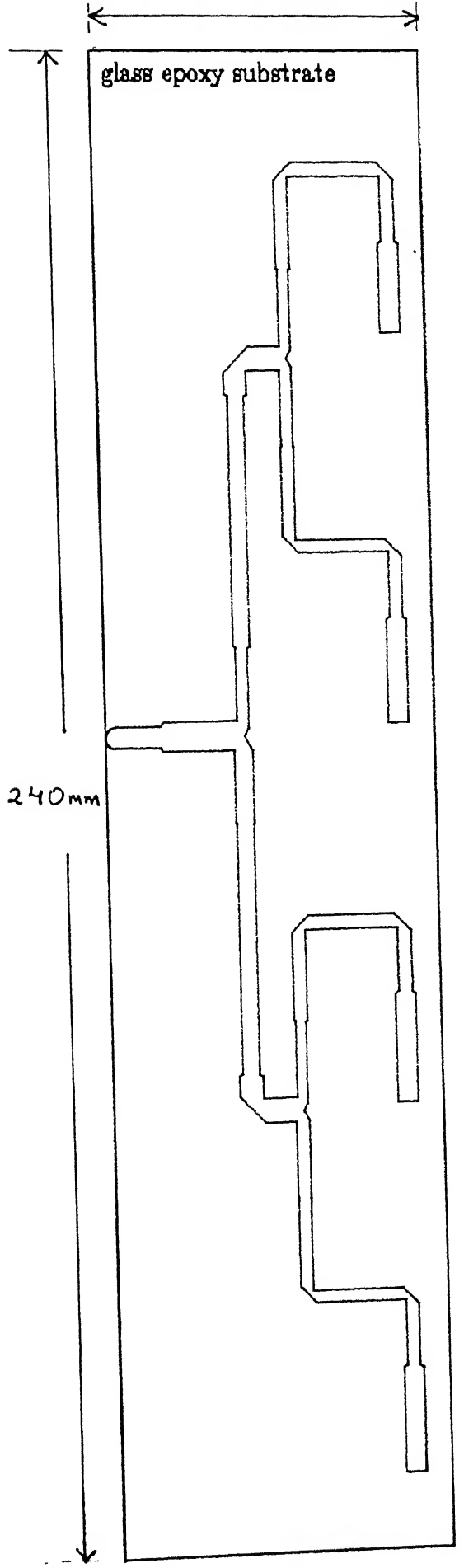
glass epoxy substrate
240mm

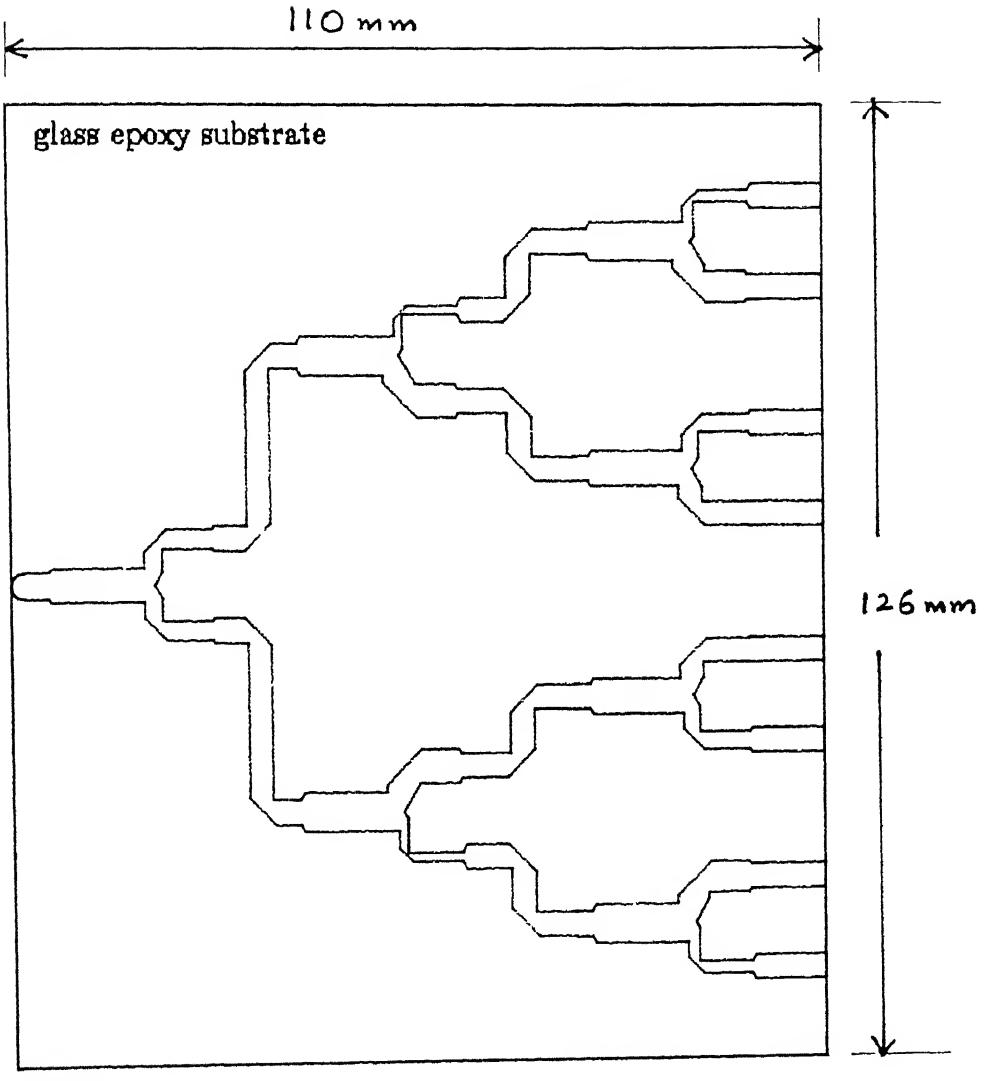

Fig. 4.9 Etching pattern of 8 way power divider

Element No.	magnitude	phase (deg)
1	.0490	0.0
2	.0536	0.0
3	.0702	0.0
4	.0925	0.0
5	.1308	0.0
6	.1780	0.0
7	.2381	0.0
8	.3069	0.0
9	.3828	0.0
10	.4618	0.0
11	.5402	0.0
12	.6142	0.0
13	.6796	0.0
14	.7328	0.0
15	.7703	0.0
16	.7897	0.0
17	.7897	0.0
18	.7703	0.0
19	.7328	0.0
20	.6796	0.0
21	.6142	0.0
22	.5402	0.0
23	.4618	0.0
24	.3828	0.0
25	.3069	0.0
26	.2381	0.0
27	.1780	0.0
28	.1308	0.0
29	.0925	0.0
30	.0702	0.0
31	.0536	0.0
32	.0490	0.0

Fig 4.10 Input Power Coefficients

the lossy way of using dielectric substrate. Refer Fig. 4.11 for feed network parameters and Fig 4.12 for 8 way power divider parameters.

With the feed network design having been completed and the general configuration of the array finalised, the last step was fabrication of the array and testing of the same to see the results achieved. The procedure adopted for this and the results achieved is explained in chapter 5.

Ele. #	R_act (ohms)	S L (mm)	i/p line Zo (ohms)	1st level PD (ohms) Zo1	Zo2	Zot	o/p line Zo (ohms)	2nd level PD (ohms) Zo1	Zo2	Zot	o/p line Zo (ohms)
1	61.63	14.4	63								
2	64.42	16.8	65	70.8	68.7	45.7	55				
3	61.34	17.6	63								
4	65.18	17.2	66	72.5	64.6	44.5	55	66.4	52.7	39.4	50
5	63.66	17.3	64								
6	63.67	17.1	64	73.2	62.7	44.2	55				
7	63.10	17.1	64								
8	63.09	17.1	64	74.6	65.7	45.7	55	67.5	50.8	38.7	50
9	62.87	17.1	63								
10	62.77	17.0	63	72.8	66.1	45.7	55				
11	62.66	17.0	63								
12	62.58	17.0	63	71.5	67.1	45.7	55	67.5	57.7	41.8	50
13	62.53	17.0	63								
14	62.49	17.0	63	63.6	60.5	41.8	55				
15	62.46	16.9	63								
16	62.45	16.9	63	69.6	68.8	45.7	55	63.6	60.5	41.8	50

Notes:-
* Feed network for elements 17 to 32 is symmetrical about the centre.
* R_act - Active Resistance
* S_L - Stub Length, Zo = 50 ohms
* The reactive part of active impedance is compensated by adjusting the stub length.
* PD - Power Divider
* The 50 ohms o/p lines are connected to coaxial cables.
* Zo1,Zo2,Zot are the transformer impedance values. The length and width of the transformers has been calculated using [15].

Fig. 4.11 Feed Network Parameters

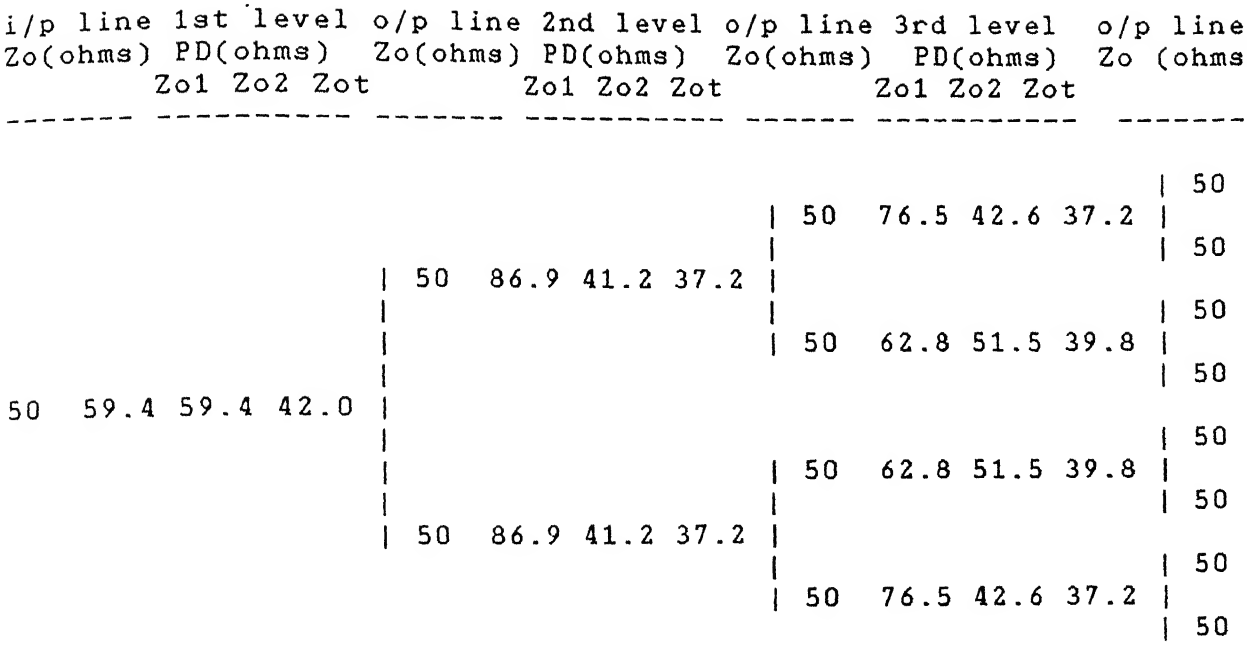

Notes:-

* The eight 50 ohms o/p lines are connected to coaxial cables.
* PD - Power divider
* Zo1,Zo2,Zot are the transformer impedance values.The length and width of the transformers has been calculated using [15].

Fig. 4.12 Eight Way Power divider Parameters

Chapter 5

Fabrication of Final Array and Testing

5.1 introduction

With the design of the feed network completed and the general configuration of the array envisaged, the fabrication of the complete array was started. The fabrication of the 32 notch antenna elements on a sheet of Aluminium, 1.6mm thick, was done in 8 pieces, with 4 elements on each piece. The feed network was cut on rubylith and printed on glass epoxy substrate 1.6mm thick and of ϵ_r of 3.8. the shielding of the feed network was also made of 1.6mm thick Aluminium plate. Spacers of 6mm height were used for providing spacing between the feed network and the shields. The 8 pieces of the array were individually assembled first and then mounted on a 3mm thick Aluminium rail of L shape, 1.5 inches wide on each side. A 2.25m length of rail was used so as to provide handling support on both sides of the array.

Once the array had been fabricated, it had to be tested for ascertaining its radiation pattern and VSWR. An array, 2m in length, required an antenna measuring range of 80m minimum for far field conditions. This was calculated using the formula $\frac{2D^2}{\lambda}$ where D is the physical aperture equal to 2m. Also a microwave source of 3.2 GHz of sufficient power was required to overcome the loss resulting from the use of glass epoxy

PCB's, coaxial cables and range attenuation. This chapter explains the actual procedure adopted for fabrication of the array notch antenna elements and feed network, the method used for carrying out the measurements on the array and the results obtained and comparison with the theoretical values.

5.2 Mechanical Fabrication of the Array

The mechanical fabrication of the array involved precise cutting of the antenna elements and the slots on a Aluminium plate 1.6mm thick. The coordinates of 4 notch antenna elements on one piece were generated with the isolating slots between them. The edge pieces on both sides of the array were made 5cms longer on the outer sides of the array. These coordinates were plotted and the drawings were pasted on pieces of Aluminium plate 1.6mm thick, and given to the Central Workshop for cutting of the slots and the taper. Refer Fig. 5.1 for the drawing of the 4 notch antenna element piece. The feed network coordinates were generated and cut on a rubylith sheet, for printing on glass epoxy substrate 1.6mm thick ($\epsilon_r = 3.8$), by the conventional photo etching technique. The Aluminium pieces for shielding of the feed network were cut in the Electrical Department Workshop.

After the array pieces and the feed network pieces were made by the respective agencies, final filing and finishing was done on them to make them exactly to size. The feed network pieces were placed on the notch antenna elements along with the shielding pieces and holes drilled in them for fixing them together with proper alignment. Thus each of the 8 array pieces were completely assembled individually for ease in mounting on the Aluminium rail. The notch antenna plates were mounted first on the rail ensuring that there was no gap left between the pieces.

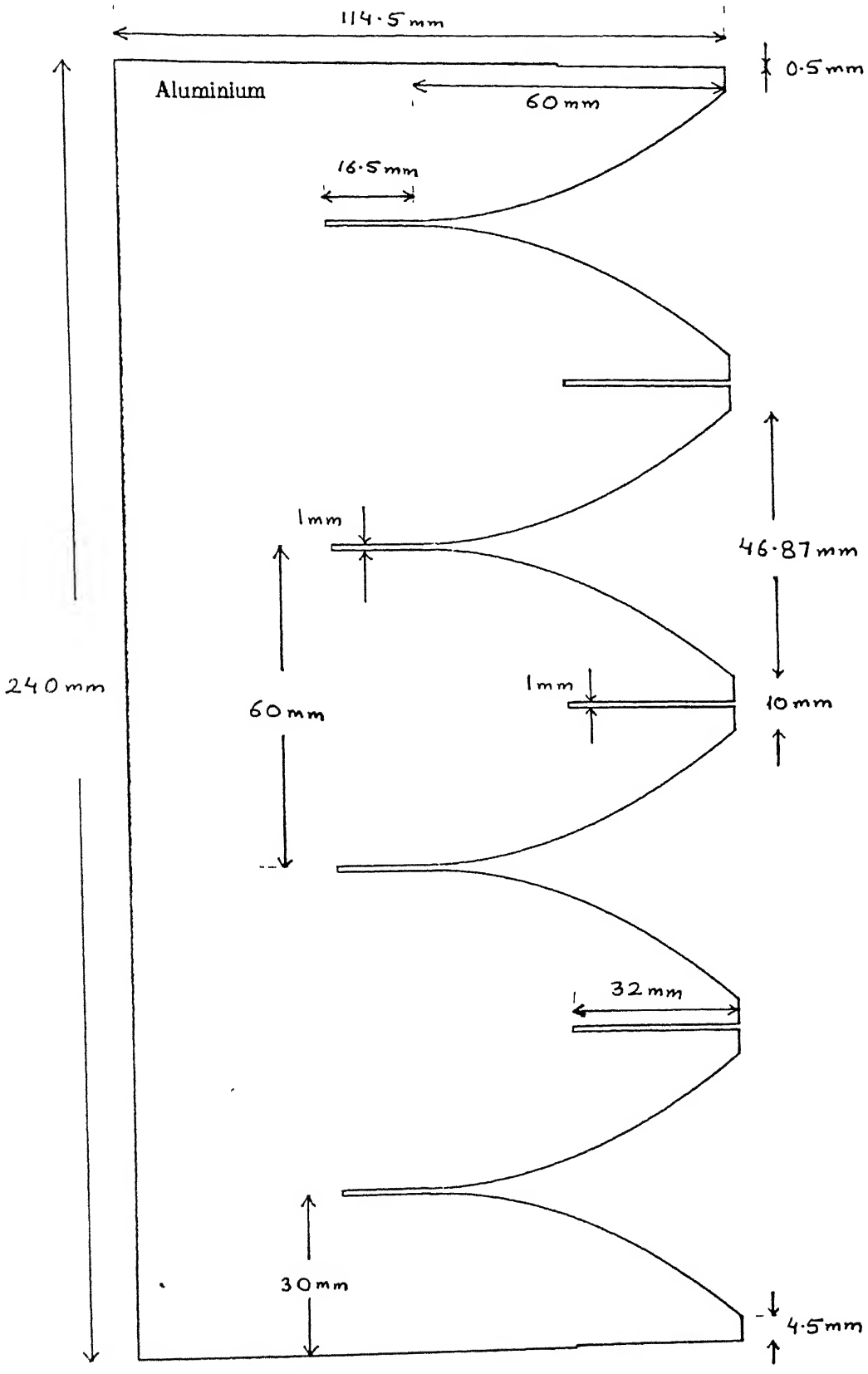

Fig. 5.1 Drawing of 4 notch antenna elements

Thereafter coaxial cable, RG 58, was cut into 8 equal pieces and exposed at both ends equally. One end of each was soldered to each of the 8 feed network pieces which was then attached to the notch antenna element plates fixed to the Aluminium railing. Clamps had to be made to hold the coaxial cables steady on the rail so that the soldered cable does not come out. After this the shield plates were attached on the feed network PCB's with 6mm spacers in between. The 8 way power divider, which was also printed by conventional photo etching technique, was fixed to the rail in the centre of the array, behind the notch elements. Another Aluminium plate was fixed to the rail for supporting the 8 way power divider. The other ends of the coaxial cable were then soldered to the respective outputs of the 8 way power divider. Clamps were used again to hold the cable steady close to the 8 way power divider. A shield was placed on the 8 way power divider also at a height of 6mm. A N type connector was connected to the input of the 8 way power divider for connecting the source to the array. The coaxial cable was looped and attached to the railing so as to avoid it hanging loose. This completed the mechanical fabrication of the array.

5.3 Testing of the Array

Testing of the array required a antenna testing range of at least 80m so as to enable measurement of the array pattern in the far field. The value of 80m was got from the formula $\frac{2D^2}{\lambda}$ where D is the physical aperture of the antenna. This formula gives the far field distance for an antenna where the spherical wave front radiating from the antenna becomes a plane wave front. This facility was not available in this institute. Even if this facility was created, a microwave source of the required band of 3 to 3.4 GHz was required with enough power to overcome the lossy nature of the glass epoxy substrate

and coaxial cables, and cause the antenna to radiate properly. This again was not available in this institute. The lack of such a source did not permit gain measurements to be conducted on the array.

With these limitations measuring the pattern in the far field was not possible. It was decided to carry out near field measurement of the E field of each of the antenna elements, convert the same to slot voltages and compare it with the excitation coefficients obtained from LAARAN. This would have enabled us to get a distribution Vs element position plot and the pattern of the array using LAARAN. For doing this, a probe in the form of a monopole was constructed using a piece of coaxial cable, RG 58. The procedure envisaged for the measurement was to connect the array to port 2 of the Network Analyser, the probe to port 1 of the Network Analyser, and measure the S_{12} of the array by placing the probe in the plane between the notch antenna element and free space. The measurement of phase of S_{12} was very critical since any variation in the probe position in the radiation direction resulted in a very drastic change in the phase value. For this a rigid structure was made using a thick Aluminium wire for holding the probe firmly at one end and the other end was attached to a movable clamp which was moved on the railing on which the array was mounted. This ensured that the probe remained in almost the same position, with respect to the notch, when measurement was taken by moving the probe from one notch to the other.

The phase value would have remained constant in all the elements if the lengths of all feed lines to the elements were exactly same and the accuracy in the measurement position was of the order of a few microns. This was not possible with the set up made for the measurement. The phase difference could also occur due to the coaxial cables used in the array not being exactly of the same size. The looping of the cables done in the elements closer to the centre also could introduce a phase change. Even the nature

of the discontinuities, in the form of solders, not being exactly identical could cause a difference in phase. Also it was not possible to maintain the cable, on which the probe was made, with exactly the same bends for measurements of all elements.

Despite all these limitations, the probe arrangement was set up and measurement of S_{12} at each antenna element carried out at 3.2 GHz with as much accuracy in positioning of the probe as possible with the help of a scale and the rigid clamping arrangement with the railing. The reference of the measurement of S_{12} was set by the values of S_{12} measured at the central 2 elements of the array. The values measured at both the elements were found to be the same. With respect to this reference, S_{12} in all the 32 elements of the array, was measured in magnitude and phase. The measured values of magnitude in dbs was converted to amplitude and the phase from degrees to radians. These were fed to LAARAN software and the excitation coefficients and pattern computed.

5.4 Results of the Array Measurements

The measurements of the phase of S_{12} from element to element in one Aluminium piece showed a difference of 4.5 to 9 degrees. The difference in phase from one piece of 4 elements to the other showed a maximum difference of around 22.5 degrees. This was since the feeding of each piece of 4 elements was done with a different coaxial cable. The phase difference was attributed to inaccuracies in measurements, difference in cable lengths, looping of the cables not being similar, and the nature of the soldered discontinuities not being same.

The measured S_{12} values, converted to amplitude and phase, were fed to LAARAN software. The coefficients of the array and the pattern showed a fair amount of simi-

larity with the theoretical values. The side lobe level of -30 db could not be achieved, however the pattern achieved showed a average side lobe level of around -25 dbs. Refer Fig. 5.2 for the excitation coefficients measured, Fig 5.3 for the plot of distribution Vs element position measured compared to the theoretical one, and Fig 5.4 for the measured pattern as compared to the theoretical one.

Neglecting the inaccuracies in phase measurement, that is by making the phase values 0, the amplitude values gave a even better pattern closer to the theoretical pattern. The peak side lobe level achieved was around -25 db. Refer fig 5.5 for the pattern of the array neglecting the variation in phase compared to the theoretical pattern. Gain measurements could not be performed on the array for want of a measurement range.

VSWR measurement of the array was performed using the Network Analyser. The S_{11} match at the input of the array showed a fairly good match of almost -20 db at the design frequency of 3.2 GHz. The VSWR computed from this value of S_{11} was 1.222 as compared to the required value of < 1.5. The VSWR value in the complete band of 3 to 3.4 GHz was found to be < 1.78. Refer Fig 5.6 for the plot of S_{11} of the array.

The results obtained from the measurements carried out showed a satisfactory outcome of the fabricated array design considering the constraints involved in construction and fabrication of the array. A -30 db side lobe level would require a accuracy of 1 in 1000,in fabrication, which was not possible to achieve. Therefore the results obtained were satisfactory.

Element No.	normalised magnitude	phase (radians)
1	0.334965	-0.314159
2	0.29854	-0.314159
3	0.354813	-0.157079
4	0.459727	-0.314159
5	0.515822	-0.157079
6	0.595662	-0.0
7	0.649381	-0.314159
8	0.707946	-0.157079
9	0.749894	-0.942477
10	0.794328	-0.628318
11	0.817523	-0.628318
12	0.891251	-0.942477
13	0.917275	-0.314159
14	0.971628	-0.157079
15	1.0	-0.314159
16	1.0	-0.0
17	1.0	-0.0
18	1.0	-0.157079
19	0.944061	-0.314159
20	0.971628	-0.628318
21	0.917275	-0.628318
22	0.841395	-0.471238
23	0.817523	-0.628318
24	0.794328	-0.942477
25	0.707945	-1.099557
26	0.595662	-0.785398
27	0.546386	-0.942477
28	0.501187	-0.942477
29	0.459727	-0.628318
30	0.334965	-0.942477
31	0.281838	-0.471238
32	0.316227	-0.628318

Fig. 5.2 Measured values of Excitation Coefficients

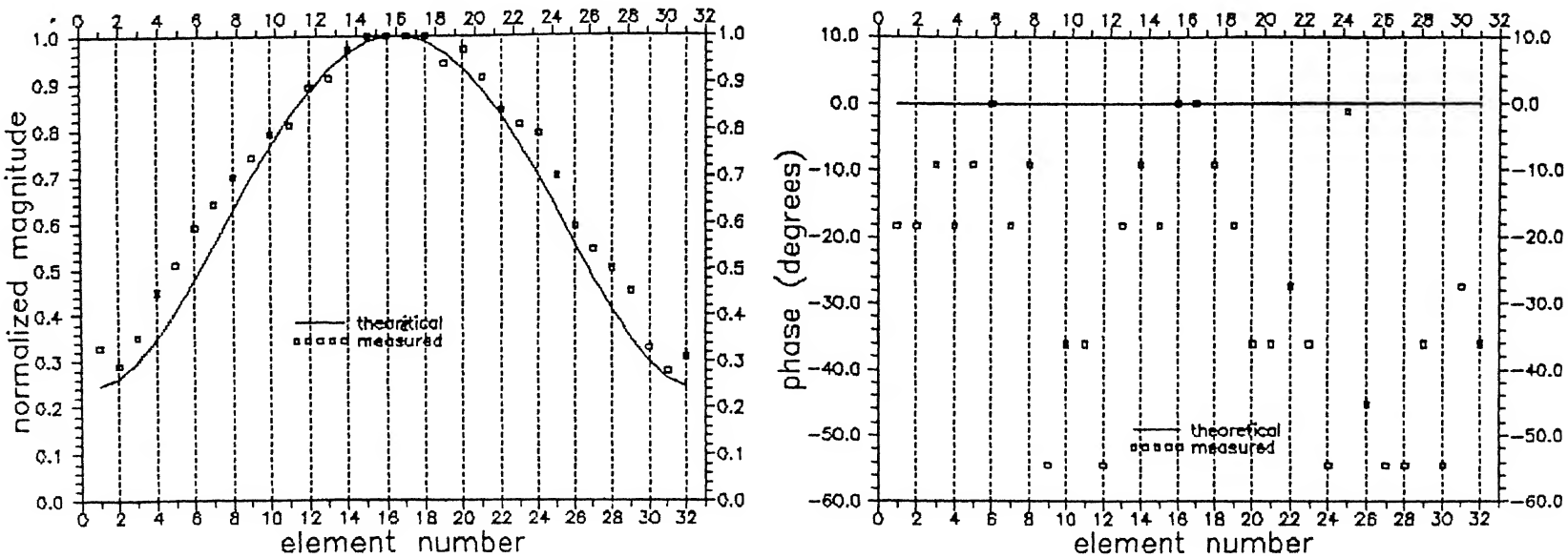

Fig. 5.3 Comparison between theoretical and measured distribution

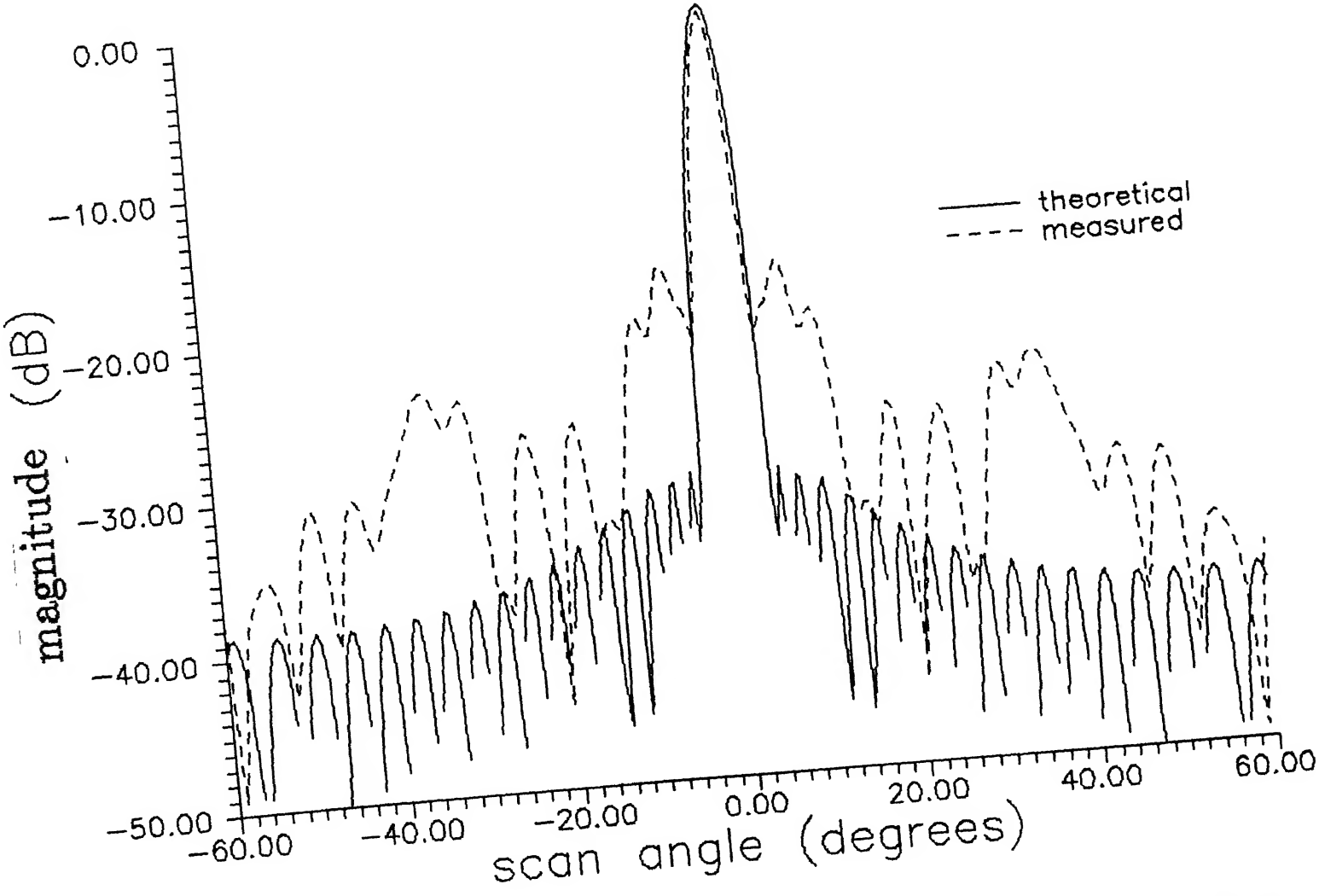

Fig. 5.4 Measured Vs Theoretical pattern of the array

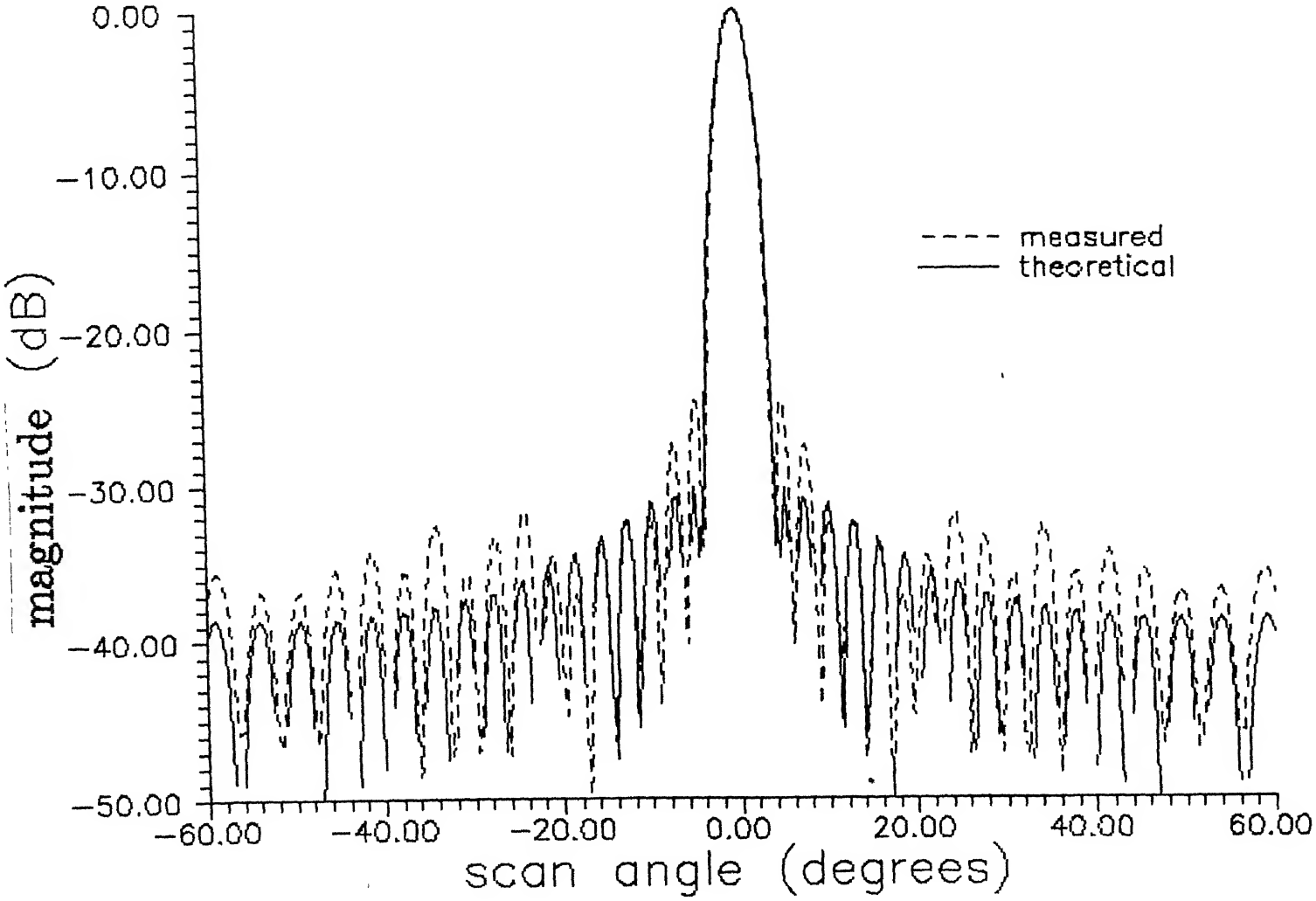

Fig. 5.5 Measured Vs Theoretical pattern (uniform phase distribution)

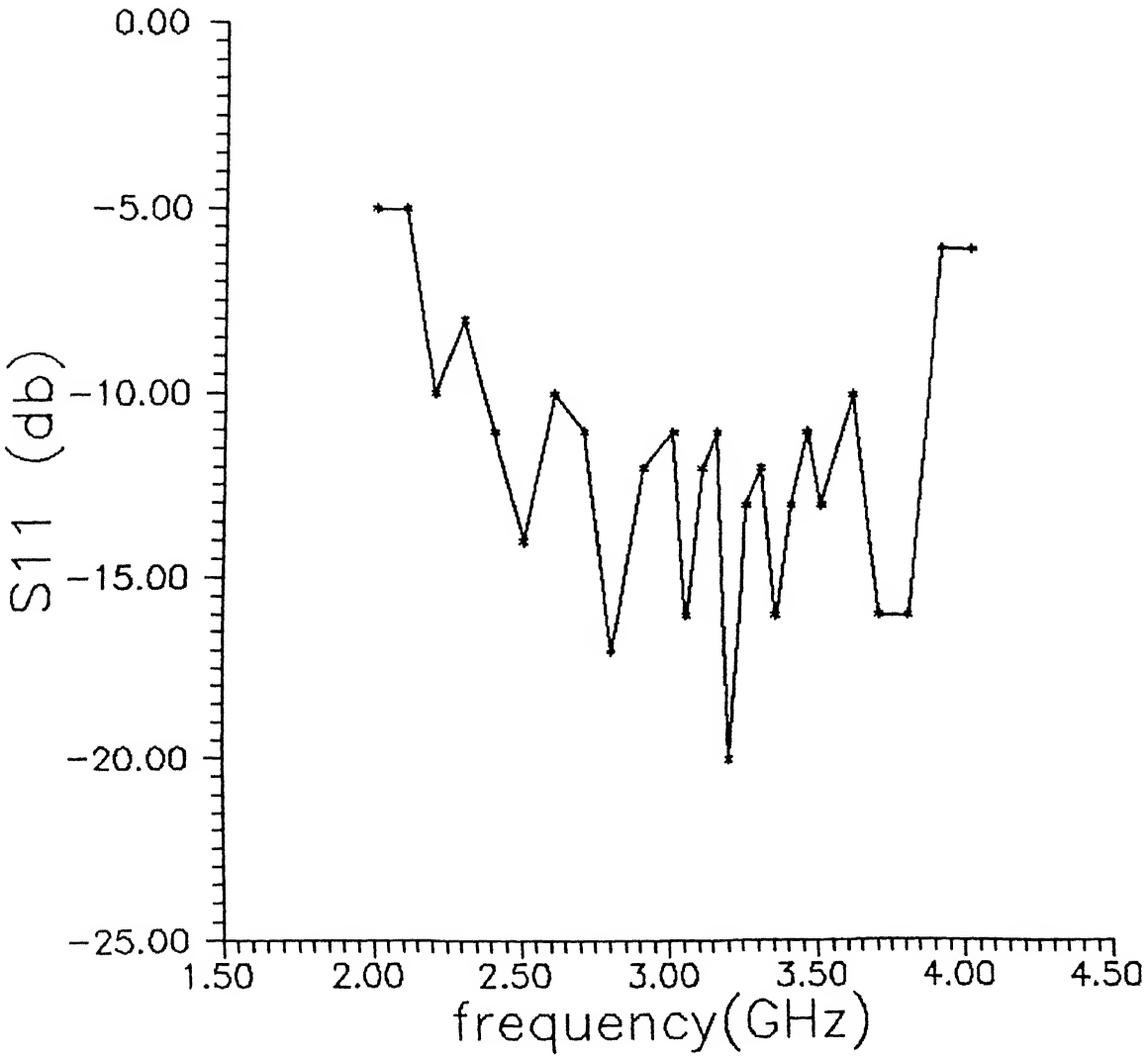

Fig. 5.6 Plot of S_{11} of the array Versus frequency

Chapter 6

Conclusion

In this study, the main objective was to experimentally fabricate a 2m long array with very low side lobe level (< -30 db), thin cross section and capable of handling high power (1 Kw peak). The VSWR specified was < 1.5 in the frequency band of 3 to 3.4 GHz. After studying the types of antenna elements which could be used for the array, a notch antenna element was finalised. The design of the notch antenna element was finalised after making models of the element on glass epoxy substrate and Aluminium metal sheet, and studying their characteristics. Different feed lines, like microstrip on glass epoxy substrate, coaxial cable, suspended strip line and shielded microstrip line were tried for feeding the element, with low loss factor. Finally a notch antenna element on Aluminium sheet, fed by a shielded microstrip feed line was selected for further extending into an array.

The mutual coupling between the antenna elements was evaluated experimentally by increasing the distance between 2 elements using shorting plates of varying widths. A low value of mutual coupling obtained between 2 elements prompted the use of this simplified method of mutual coupling evaluation instead of the proper procedure for the same. It was decided to make a 32 element array, with 0.64 λ spacing between them,

at 3.2 GHz central frequency, based on Taylor pattern for avoiding back lobes. Linear array design software, LAARAN, was used for computing the excitation coefficients of the array. These were suitably modified for calculation of active impedance and incident power to each element. The feed network was designed based on this, in microstrip form.

The array was mechanically fabricated in 8 pieces to facilitate ease in fabrication. The 8 pieces were assembled together to form the array and connected to a 8 way power divider feed network by coaxial cables of equal length. The testing of the antenna array was performed for near field since far field measurement was not possible for lack of a long antenna measurement range and a powerful microwave source. A test set up for measurement of the E field, as accurately as possible, on the edge of each antenna element, was made. The measured values obtained were fed to LAARAN and the pattern computed.

The results of the measurements showed a pattern fairly similar to the theoretical pattern with average side lobe level of -25 dbs. Considering the limitations in precise fabrication and precise measurement, the results achieved were satisfactory and showed a good scope for further improvement in the array for getting very low side lobe level. The VSWR achieved in the complete band of 3 to 3.4 GHz was < 1.78 with 1.22 VSWR at 3.2 GHz. The magnitude match between the array pattern and the theoretical pattern was reasonably good. The major problem was maintaining the phase balance and being able to carry out precise measurement of it. However by adjustment of the phase of each element it would be possible to achieve -30 db side lobe level. Gain measurement on the array could not be performed since the feed network used was very lossy.

6.1 Scope for further work

The results obtained from the array offers a lot of scope for further work. If a more sophisticated set up was used for precise fabrication of the array in one piece, and measurements also performed accurately, a side lobe level as low as -35 to -40 db could be achieved. Due to mutual coupling between the elements being very low, -20 db side lobe level design can be very simple. The mutual coupling need not be taken into account. The actual evaluation of mutual coupling should be carried out by match terminating 30 elements and measuring the mutual coupling between 2 elements at a time so as to get a proper S matrix of the array. This would also help in accurate characterisation of active impedance for very low side lobe (< -35 db) design.

The feed network, which was made on glass epoxy substrate and coaxial cables, due to low cost involved, could be made fully on duroid substrate which has a very low loss factor and can handle high power. This could improve the gain of the array. Cross polar measurement of the radiation has not been performed. The cross polar level is expected to be very small because of the basic radiating element geometry, which is horizontally polarised. Cross polar component arises out of the shielded microstrip structure which introduces some vertical edges. By proper design of the structure one can keep the cross polar level low. There is also scope for development of the linear array into a planar array.

The impedance of a conducting slot in a finitely thick, low dielectric constant, plate was found experimentally and used in the array. However, accurate characterization of a wide and thick conducting slot, on a low dielectric constant plate, could be performed. Theoretical analysis of the notch antenna element has not been done. This could also be taken up for accurate characterization of the notch element and optimise its dimensions

for a given requirement.

References

[1] S.N.Prasad and S.Mahapatra. A new mic slot-line aerial. *IEEE Transactions on Antennas and Propagation.*, vol AP-31, No.3: pp.525–527, May. 1983.

[2] K.Sigfrid Yngvesson et al. Endfire tapered slot antennas on dielectric substrates. *IEEE Transactions on Antennas and Propagation.*, vol AP-33, No.12: pp.1392–1400, December. 1985.

[3] D.H.Schaubert R.Janaswamy and D.M.Pozar. Analysis of the transverse electromagnetic mode linearly tapered slot antenna. *Radio Science*, vol.21 Number 5: pp.797–804, September-October. 1986.

[4] R.Janaswamy and D.H.Schaubert. Analysis of tapered slot antenna. *IEEE Transactions on Antennas and Propagation*, vol. AP-35, No.9: pp.1058–1065, September. 1987.

[5] R.Janaswamy. An accurate moment method model for the tapered slot antenna. *IEEE Transactions on Antennas and Propagation*, vol-37 No. 12: pp.1523–1528, December. 1989.

[6] Young-Sik Kim and K.Sigfrid Yngvesson. Characterization of tapered slot antenna feeds and feed arrays. *IEEE Transactions on Antennas and Propagation.*, vol-38, No.10: pp.1559–1564, October 1990.

[7] Albert K.Y.Lai et al. A novel antenna for ultra-wide-band applications. *IEEE Transactions on Antennas and Propagation.*, vol-40, No.7: pp.755–760, July. 1992.

[8] Eric Thiele and Allen Taflove. Fd-td analysis of vivaldi flared horn antennas and arrays. *IEEE Transactions on Antennas and Propagation.*, vol.-42, No. 5: pp.633–641, May. 1994.

[9] D.H.Schaubert et al. Moment method analysis of infinite stripline-fed tapered slot antenna arrays with a ground plane. *IEEE Transactions on Antennas and Propagation.*, vol-42, No. 8: pp.1161–1166, August. 1994.

[10] Seymour B. Cohn. Slot line on a dielectric substrate. *IEEE Transactions on Microwave Theory and Techniques.*, vol.MTT-17, No.10: pp.768–776, October. 1969.

[11] Elio A. Mariani et al. Slot line characteristics. *IEEE Transactions on Microwave Theory and Techniques.*, vol.MTT-17, No.12: pp.1091–1096, December. 1969.

[12] G.H.Robinson and J.L.Allen. Slot line application to miniature ferrite devices. *IEEE Transactions on Microwave Theory and Techniques.*, vol.MTT-17, No.12: pp.1097–1101, December. 1969.

[13] R.Janaswamy and D.H.Schaubert. Dispersion characteristics for wide slotline on low-permittivity substrate. *IEEE Transactions on Microwave Theory and Techniques.*, vol.MTT-33, No. 8: pp.723–726, August. 1985.

[14] R.Janaswamy and D.H.Schaubert. Characteristic impedance of a wide slotline on low-permittivity substrates. *IEEE Transactions on Microwave Theory and Techniques.*, vol.MTT-34, No. 8: pp.900–902, August. 1986.

[15] B.Bhat and S.K.Kaul. Stripline like transmission lines for microwave integrated circuits. *Wiley Eastern Ltd.*, pages pp.73–75.

[16] Brian C.Wadell. Transmission line design handbook. *Artech House,Boston,London.*